Y 3. At 7:
36-10-1

POWER REACTOR TECHNOLOGY *and* REACTOR FUEL PROCESSING

A Quarterly Technical Progress Review

Prepared for DIVISION OF TECHNICAL INFORMATION, USAEC, by
ARGONNE NATIONAL LABORATORY

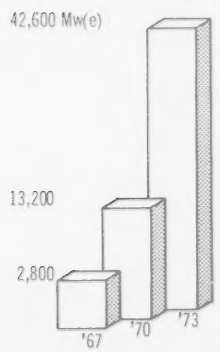

Winter 1966-1967

● VOLUME 10

● NUMBER 1

ILLINOIS STATE LIBRARY
SEP 8 - 1967
U. S. Superintendent of Documents

Power-Reactor Data . . . see page 32

TECHNICAL PROGRESS REVIEWS

The United States Atomic Energy Commission publishes the Technical Progress Reviews to meet the needs of industry and government for concise summaries of current nuclear developments. Issued quarterly, each journal digests and evaluates the latest findings in a specific area of nuclear technology and science.

The journals are:

Isotopes and Radiation Technology
P. S. Baker, A. F. Rupp, and Associates
Oak Ridge National Laboratory

Nuclear Safety
Wm. B. Cottrell, W. H. Jordan, J. P. Blakely, and Associates
Nuclear Safety Information Center, Oak Ridge National Laboratory

Power Reactor Technology
Argonne National Laboratory

Reactor Materials
E. M. Simons and Associates
Battelle Memorial Institute

All are available from the U. S. Government Printing Office. See the back cover for ordering instructions.

The views expressed in this publication do not necessarily represent those of the United States Atomic Energy Commission, its divisions or offices, or of any Commission advisory committee or contractor.

Availability of Reports Cited in This Review

United States Atomic Energy Commission (USAEC) reports are available at USAEC depository libraries and are sold by the Clearinghouse for Federal Scientific and Technical Information (CFSTI), National Bureau of Standards, U. S. Department of Commerce, 5285 Port Royal Road, Springfield, Va. 22151. All reports sold by CFSTI are $3.00 for printed copy and $0.65 for microfiche. Each separately bound part of a report is priced as a separate report. Some reports may not be available because of their preliminary nature; however, the information contained in them will generally be found in later progress or topical reports on the subject.

Other U. S. Government agency reports identified in this journal generally are available from CFSTI.

Private-organization reports should be requested from the originator.

United Kingdom Atomic Energy Authority (UKAEA) and Atomic Energy of Canada Limited (AECL) reports are available at USAEC depository libraries. UKAEA reports are sold by Her Majesty's Stationery Office, London; AECL reports are sold by the Technical Information Officer, Atomic Energy of Canada Limited, Chalk River, Ontario, Canada. UKAEA and AECL reports issued after March 1, 1967, are sold by CFSTI to purchasers in the United States and its territories.

NSAET:
36-10-1

Contents

Power Reactor Technology and Reactor Fuel Processing

Vol. 10, No. 1

COMPONENTS

Letters to the Editor—
Vessel Cladding Failures: Is Oxygen the Culprit? 1

Flow-Induced Vibration in Reactor Internals 2
Martin W. Wambsganss, Jr.

REACTOR TYPES

The Molten Salt Reactor—An Ingredient of Nuclear Progress 6
Fred A. Smith

REACTOR SAFETY

Toward an Understanding of Sodium Fires 17
Paul A. Lottes

ENERGY CONVERSION

Recent Developments in Open-Cycle MHD Power Systems 20
Jerzy Moszynski

FLUID AND THERMAL TECHNOLOGY

Two-Phase Compressibility Phenomena and How They Affect Reactor Safety 27
Hans K. Fauske

OPERATING EXPERIENCE

Operational Data for Power Reactors in the United States 32
Barbara A. Schmeh

REACTOR FUEL PROCESSING

An Introduction to Fuel Processing 59

AQUEOUS PROCESSING

Recent Developments in Aqueous Processing 61
C. E. Stevenson and D. M. Paige

NONAQUEOUS PROCESSING

Volatility Processes 70
J. J. Barghusen

Compact Pyrochemical Processes 79
T. R. Johnson

WASTE DISPOSAL

Progress in Waste-Disposal Research and Development 85
Phillip Fineman

Issued quarterly by the U. S. Atomic Energy Commission. Use of funds for printing this publication approved by the Director of the Bureau of the Budget on July 8, 1966.

Power Reactor Technology and Reactor Fuel Processing

This is the first issue of the consolidated journal that merges the previously separate Technical Progress Reviews *Power Reactor Technology* and *Reactor Fuel Processing.*

Power Reactor Technology and Reactor Fuel Processing is a quarterly review of developments in reactor and reactor fuel technology. As such, this journal reports and interprets progress in the reactor field in terms of its significance to the reactor designer, operator, and fuel-cycle specialist. Articles either summarize and critically evaluate recently reported developments or review the "state of the art" of a particular topic. Both types of articles reference reports and publications that merit study; readers are urged to consult the references for additional information and the judgments of the original authors. If a reader has information that causes his evaluation to reinforce, modify, or contradict the opinions of our reviewers, he is encouraged to write to the Editor.

The scope of the journal encompasses:

CONCEPTS and APPLICATIONS: Progress in evaluating the applicability and economics of various reactor types and systems (including unconventional approaches), as well as of fuel resources and cycles, for utility central-station generation of electricity, auxiliary power, process radiation and heat, desalting, and propulsion—and for terrestrial, undersea, aerospace, and other advanced uses.

ANALYSIS and EXPERIMENTATION: Advancements in the techniques of reactor physics, fluid and thermal technology, energy conversion, fuel elements, materials, mechanics, control and dynamics, and reactor safety.

SYSTEMS and COMPONENTS: Experience as reflected in design and construction practice, components, systems technology, and operating performance of various specific types of reactors—including pressurized- and boiling-water reactors, molten-salt, organic-, gas-, and liquid-metal-cooled reactors, as well as generally applicable aspects of research and test reactors.

FUEL PROCESSING: Recent research and development on fuel aqueous processing, nonaqueous processing, waste disposal, and processing safety.

This journal is prepared by Argonne National Laboratory at the request of the Division of Technical Information of the U. S. Atomic Energy Commission. At Argonne, the Reactor Engineering Division (L. J. Koch, Director) and the Chemical Engineering Division (R. C. Vogel, Director) have the principal responsibility for the preparation of *Power Reactor Technology and Reactor Fuel Processing,* with the regular assistance of the Reactor Physics Division (R. A. Avery, Director) and the Idaho Division (M. Novick, Director) and the occasional assistance of other divisions (Metallurgy, Chemistry, and Reactor Operations). Thus, unless noted otherwise, the reviewers and authors of articles are Laboratory staff members. The editors welcome interpretive review articles contributed by authors outside the Laboratory.

Editor, James J. Dutton
Advisory Editor, David H. Lennox
Managing Editor, Karl K. Brown
Co-Editor (Fuel Processing), Joseph Royal
Associate Editor (Physics), Raymond Gold
Assistant Editor, Barbara A. Schmeh

Argonne National Laboratory

Letters to the Editor

Vessel Cladding Failures: Is Oxygen the Culprit?

In the article entitled "How Serious Are Vessel Cladding Failures?," *Power Reactor Technology*, 9(3): 101-109, by Edward A. Wimunc, the environmental coolant differences of three of the nuclear plant vessels could have been expounded upon for a possible technical contribution to the nuclear industry. Points could have been made as follows:

1. The EBWR vessel shows more clad cracking in the steam phase than in the liquid phase. From an environment viewpoint, oxygen concentrations are higher in the steam phase than in the water phase of a BWR and, similarly, the potential for chloride concentration is also higher.
2. Although parts of the Yankee *reactor* vessel have been extensively investigated by dye-penetrant and Zyglo tests for several years, no cracks have ever been found in Yankee reactor-vessel clad material applied by the same stitch clad process as in the case of the Yankee pressurizer and the EBWR reactor vessel, and by the same manufacturer. The coolant in the Yankee reactor vessel has always been very low in oxygen and chlorides.
3. The Yankee pressurizer-vessel cracking may be the result of oxygen which was found to be present in the pressurizer in substantial concentrations for some as yet not clearly established reason.
4. There appears to be more than coincidence in the cracked cladding of the EBWR (with high coolant oxygen concentrations) and the cracked cladding of the Yankee pressurizer vessel (with high coolant oxygen concentrations).

Glenn A. Reed
Wisconsin Michigan Power Co.

Who Knows What Causes Lurk . . . ?

Mr. Reed's letter suggests that oxygen concentrations in the steam region of the EBWR reactor vessel and in the Yankee pressurizer vessel might be a cause of cladding failures in these vessels. He states that "environmental coolant differences could have been expounded upon for a possible technical contribution." I quite agree. However, such an exposition would become rather speculative. My goal was to summarize the best information available at the time; I believe there is no reason to change the conclusions now.

Each of the three vessels cited by Mr. Reed does have its own unique set of operating conditions. Further, it is also true that conditions varied prior to the start of operations. Cracks in the EBWR vessel—and also in the fourth vessel, for the Elk River reactor—were repaired before they were put into nuclear service; this circumstance makes correlation impossible.

In addition to the possible oxygen concentrations, Mr. Reed has also implied that the potential for chloride concentration is greater in boiling-water reactors than in pressurized-water reactors. Extreme precautions were taken to keep chlorides out of the EBWR system; to the best of my knowledge, chlorides have never been present in more than trace quantities.

Mr. Reed's suggestion for further information and speculation as to relationships is an interesting one, and certainly could be fruitful.

E. A. Wimunc, *Director*
Reactor Operations Division
Argonne National Laboratory

Flow-Induced Vibration in Reactor Internals

By Martin W. Wambsganss, Jr.

Evidence of damage to reactor components by flow-induced vibration has been reported.[1-8] Specifically, the flow-induced vibration of fuel subassemblies, control-rod blades, and a thermal shield has led to such problems as power and neutron-flux oscillation,[1-3] excessive wear of core-component spacer pads,[4] loosening and fracture of bolts,[5] and fretting wear between alignment pins and mating slots.[2] It is possible to extrapolate these effects and to envision more serious consequences that could conceivably lead to catastrophic damage.

Partial explanations for the flow-induced vibrations have been postulated in several cases,[1-5] but these and most other references to flow-induced vibration do not present a theoretical explanation in the form of a mathematical model describing vibration. Recently, however, theoretical analyses of two modes (translational and angular motion) of flow-induced vibration of a suspended blade (Fig. 1) have been made by Miller and Kennison.[9] Their approach to the problem is interesting, and their analysis is instructive.

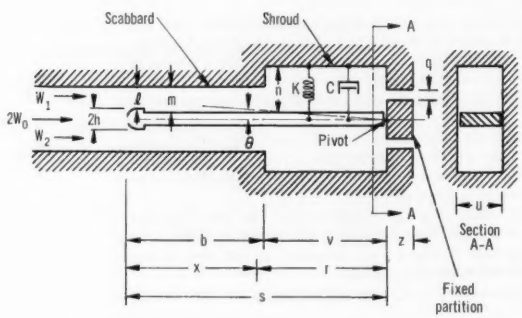

Fig. 1 Model used for analysis of pivoted blade.[9]

Self-Excited Vibrations

The primary objective of their study was to determine under what idealized conditions to fluid flow self-excited vibrations will occur. For linear systems considered, self-excitation occurs when, during a complete vibration cycle, the energy input to the system exceeds the energy dissipated. For the system studied, the energy required to sustain the vibrations is supplied by the flowing fluid.

Miller and Kennison formulate their equations by satisfying two basic requirements:

1. The pressure drop from a point upstream of the blade to a point downstream where the two channels merge is the same whether it is determined by integration of pressure drops along the upper channel or lower channel

$$(\Delta P) = (\Delta P)_L \tag{1}$$

2. The product of angular acceleration and moment of inertia of the blade must be instantaneously equal to the net torque applied to the blade, namely,

$$I\ddot{\theta} = -K\theta - c\dot{\theta} + T_f \tag{2}$$

By assuming the blade is rigid and is vibrating sinusoidally at a constant frequency and constant infinitesimal amplitude, the angular displacement can be represented as

$$\theta = \theta_0 e^{j\omega t} \tag{3}$$

where ω is the angular frequency. Similarly, the per-unit-flow oscillation in the upper channel at the upstream end of the blade can be expressed by

$$w = w_0 e^{j(\omega t - \phi)} \tag{4}$$

Application of the Conservation of Momentum principle (including various losses) and the continuity relation, gives an expression for the pressure gradient in each channel. By integrating over the length to obtain the total pressure drop in each channel and equating these to satisfy Eq. 1, we get, upon substitution of Eqs. 3 and 4 and their derivatives, an equation in complex variables. Then the pressure-gradient

expressions are used to relate the total torque exerted on the blade by the fluid (T_f in Eq. 2). Equation 2 also becomes a complex variable equation when Eqs. 3 and 4 and their derivatives are substituted.

Equations 1 and 2 can, therefore, be written as a sum of real and imaginary terms equal to zero. Four equations in real variables result from recognizing that these equations will be satisfied only if the sum of the real terms and the sum of the imaginary terms are each zero. Elimination of two of the unknowns $[(w_0/\theta_0)$ and $\phi]$ yields two equations that can be solved to give

$$\omega^2 = \omega^2(W_0, \rho, f, \text{system dimensions}) \quad (5)$$

$$c = c(\omega^2, W_0, \rho, f, \text{system dimensions}) \quad (6)$$

Recall that ω is the angular frequency and c is the characteristic coefficient of the external damper. Values of ω and c are determined by Eqs. 5 and 6; if both are real and if ω is also positive, these values correspond to conditions under which infinitesimal-amplitude oscillations would be sustained at a constant amplitude at a particular value of W_0. (Here $2W_0$ equals the total mass flow per unit time.)

CRITICAL INSERTION

A critical amount of blade insertion into the scabbard corresponds to the condition where the theoretical solutions indicate a value of zero for the vibration frequency. With smaller insertions, vibration will occur if sufficient flow is provided. With larger insertions, the solutions diverge, and the blade will strike and lock to the channel wall unless restricted by second-order or higher order effects. However, these effects were neglected in the analysis.

Figures 2 and 3 show the conditions under which fluid flow past the pivoted blade will sustain infinitesimal-amplitude oscillations. The curves correspond to an experimental water-table model with four depths of insertion of the blade.

The curves of Fig. 2 show that for a particular insertion the blade does not vibrate until some critical flow rate is reached. Below the critical flow rate, the fluid exerts a positive damping effect on the blade that must be balanced by an addition of energy to maintain vibrations. At flow rates higher than the critical value, an external damper with a positive characteristic is required to prevent an increase in the intensity of vibration with time. This implies that the fluid is now putting energy into the vibration.

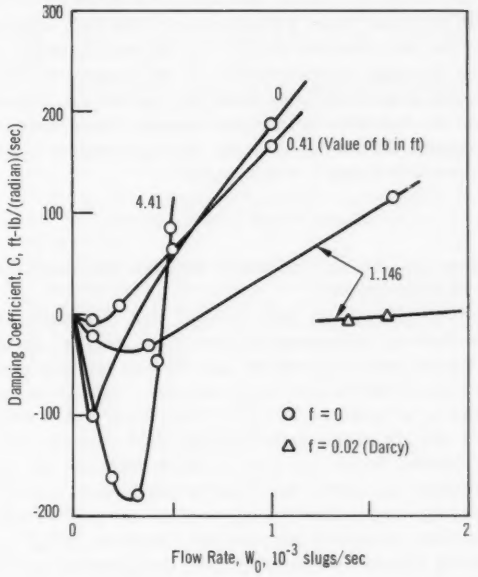

Fig. 2 Damping required for steady-state vibration of pivoted blade varies with distance b that blade is inserted into scabbard.[9]

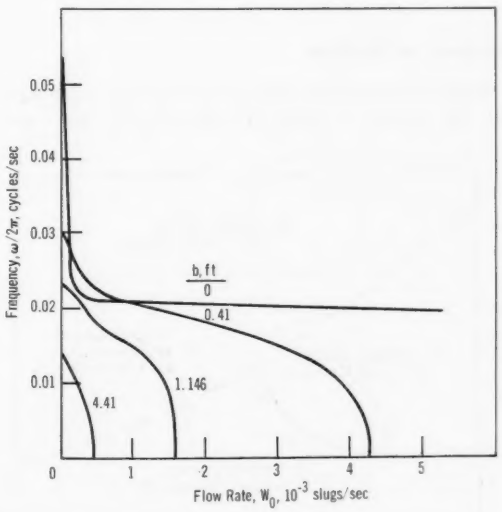

Fig. 3 Frequency of steady-state vibration of pivoted blade.[9]

EFFECT OF FLUID FLOW RATE

Figure 3 shows how the theoretical frequency of sustained infinitesimal-amplitude vibrations varies with flow rate when the characteristic of the external damper is adjusted to satisfy the condition of constant and infinitesimal vibration amplitude. Note that the frequency of vibration decreases with increasing flow rate, then passes through the condition where sustained vibration will occur without an external damper, and finally continues downward until the frequency goes to zero.

The fluid may be treated as inducing a hydraulic spring effect and a hydraulic damping effect. Condi-

tions under which oscillations or divergence occur can be found from a comparison of the fluid-induced spring and damping effects with the elastic restoring and damping characteristics of the suspended blade. To aid in understanding these interpretations, assume that the hydraulic spring and damping characteristics combine additively with the spring constant K and external damping c of the blade,

$$I\ddot{\theta} + (c + c_f)\dot{\theta} + (K + K_f)\theta = 0 \qquad (7)$$

They can be so considered because the model has been made linear.

From Eq. 7 we may reason that, for sustained oscillations at a constant amplitude, the net spring constant must be positive and the net damping must be equal to zero. The values of ω and c, when real and when ω is positive, are calculated from Eqs. 5 and 6 and satisfy these requirements. For example, if c calculated from Eq. 6 is positive (because the net damping is zero) the fluid must induce negative damping, equivalent to $c_f = -c$ or, in other words, supplies energy to support the vibration. If the net spring constant is negative (i.e., the hydraulic spring effect is negative and its equivalence, K_f, is greater in absolute magnitude than K), then the "restoring force" becomes a driving force and the blade will diverge and remain in positive contact with the wall or whatever restrains its deflection.

Regions of Motion

Figure 4 represents the possible motion conditions for the cases in which variables W_0, ω, and c are

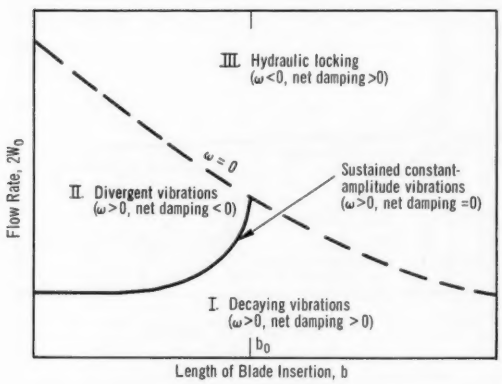

Fig. 4 Physically realizable motions as a function of flow rate and length of blade insertion.

real. The three possible motions include (1) decaying vibrations (Region I), (2) divergent vibrations (Region II), and (3) hydraulic locking or a static type of divergence to the channel wall (Region III). The three regions of motion are given as a function of flow rate and length of insertion of the blade. The dashed line, labeled $\omega = 0$, represents the flow rate that would be required for the net spring constant of Eq. 7 to equal zero, that is, for the negative spring constant induced by the flow to equal, in absolute magnitude, the spring constant of the suspension. The solid line separating Regions I and II corresponds to a net damping of zero in Eq. 7 and gives the flow rate at which infinitesimal-constant-amplitude oscillations are sustained. Note that there is an insertion length b_0 (dimension b in Fig. 1) above which no oscillations can be sustained. The physical interpretation of this phenomenon is that, with increasing flow rate, the net spring constant becomes negative before the net damping becomes negative.

Translating Blade

A similar analysis for the translational motion of a suspended blade has also been performed.[9] The geometrical model is the same as Fig. 1 except translational motion replaces angular motion and an external damper is omitted. The same assumptions were used except for an allowance for stream-contraction energy losses at the blade tip and at its downstream end.

An analysis analogous to that used for the pivoted blade leads to similar results, namely, that with a sufficiently high friction factor there is a critical amount of insertion (corresponding to $\omega = 0$) of the blade into the scabbard. With smaller insertions, vibration will occur.

The results of the theoretical solution for the translating blade are given in a set of curves[9] which show the effect on the critical insertion (zero-frequency position) of various parameters, particularly the friction factor, scabbard flow-channel thickness m, loss coefficients for wear pads and labyrinth at scabbard exit, wear-pad clearance l, and loss coefficient at the downstream end of the blade.

Conclusions

In general, the theoretical results show that, under idealized conditions, fluid flow may cause self-excited vibration of a suspended blade or may cause the blade to deflect statically to one side of its normal, centered position. Quantitatively the results do not correlate well with experiment; the discrepancies have been attributed to a failure to take into account the cross flow or flow around the longitudinal edges of the blade. Qualitatively, however, the results do explain the behavior observed in the experimental water-table model.

The results suggest measures that may be effective in correcting a vibration problem on a suspended blade or other bodies caused to vibrate by the same

phenomenon. However, unless it is clear that only longitudinal flow is significant, testing is still required for a conclusive evaluation of proposed corrective measures.

References

1. R. W. Hyndman et al., EBR-II Self-Excited Oscillations, *Trans. Amer. Nucl. Soc.*, 8(2): 590 (1965).
2. Big Rock Point Nuclear Plant (Docket 50-155), *Nuclear Safety*, 6(2): 222-223 (Winter 1964–1965).
3. Thermal Shield Vibration Eliminated at Big Rock Point, *Nucleonics*, 24(5): 64-65 (May 1966).
4. C. A. Dalke, Elimination of Hydraulically Induced Core Vibrations in the General Electric Test Reactor, *Trans. Amer. Nucl. Soc.*, 8(Suppl.): 2 (1965).
5. J. I. Riesland and E. A. Gustafson, Work Performed on Fuel Channels and the Core Support Plate at Big Rock Point Nuclear Power Plant, *Trans. Amer. Nucl. Soc.*, 8(Suppl.): 5-9 (1965).
6. G. A. Reed, Major Operating and Refueling Problems at the Yankee Atomic Electric Company Rowe Power Plant, *Trans. Amer. Nucl. Soc.*, 8(Suppl.): 28 (1965).
7. R. C. Skaardal, Operational Problems and Solutions, *Power Reactor Technol.*, 8(4): 271-279 (Fall 1965).
8. F. H. Martens, Design Foresight Can Simplify Reactor Modification, *Power Reactor Technol.*, 9(2): 74-79 (Spring 1966).
9. D. R. Miller and R. G. Kennison, Theoretical Analysis of Flow-Induced Vibration of a Blade Suspended in a Flow Channel, presented at the Winter Annual Meeting of the American Society of Mechanical Engineers, New York, Nov. 27–Dec. 1, 1966, P/66-WA/NE-1.

The Molten Salt Reactor— An Ingredient of Nuclear Progress

By Fred A. Smith

The Molten Salt Reactor Experiment (MSRE)[1–3] is unique in that it has a circulating liquid fuel[4] and a new structural alloy.[5] These features permit the 1100 to 1300°F coolant temperatures that can generate steam suitable for modern turbogenerators. In addition to this advantage, the molten-salt-reactor concept holds promise for breeding when applied to larger versions. This article briefly examines the questions:

- What is the MSRE?
- How has the MSRE performed?
- What is the future of the molten-salt reactor?

What Is the MSRE?

The graphite-moderated MSRE is a 7.5- to 10-Mw(t) reactor engineering experiment that is being conducted by Oak Ridge National Laboratory to demonstrate the desirable features of a reactor fuel[6] consisting of a circulating solution of fluorides of U, Li, Be, and Zr. As an experimental facility, MSRE is being used to study the performance of liquid fuel, graphite moderator, structural material, plant equipment, and safety characteristics from an engineering viewpoint. Figure 1 shows the MSRE facility; Fig. 2 shows the arrangement of the components and how the fuel and coolant salts circulate. Figure 3 shows the two fuel drain tanks and a tank for storing flush salt. They are in a sealed and shielded cell in the MSRE building (Fig. 2). A drain tank for the coolant salt, which has only slight induced radioactivity, is in an unsealed cell under the radiator.

MSRE COMPONENT LAYOUT

Figure 4 shows the reactor system installed in its 24-ft-diameter containment cell. The cell is 33 ft

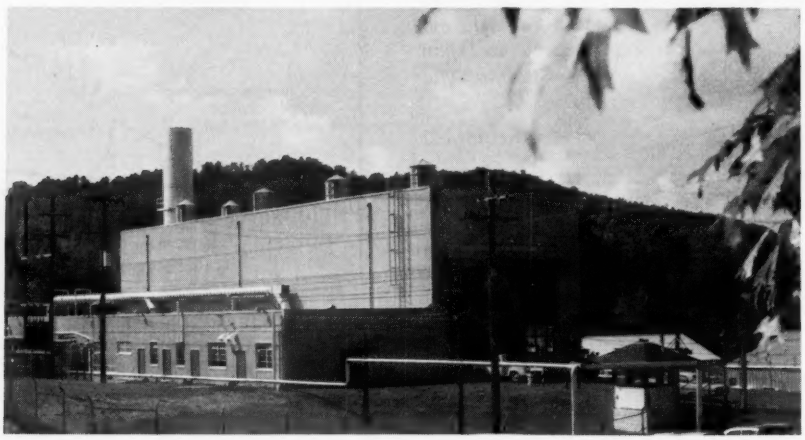

Fig. 1 MSRE building at Oak Ridge National Laboratory.

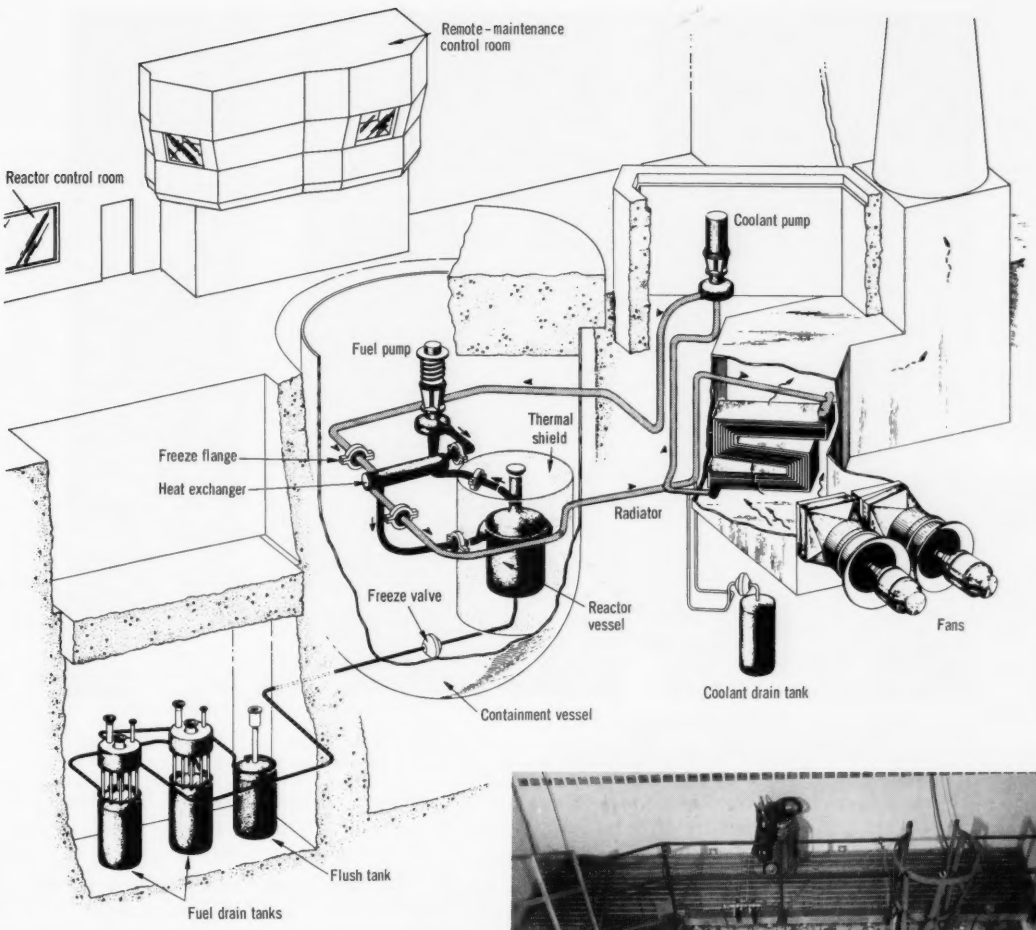

Fig. 2 MSRE system arrangement. Uranium in the fluoride molten fuel fissions and produces heat in reactor vessel, flows through shell side of primary heat exchanger, where it transfers heat to fluoride coolant, then returns to reactor vessel. Secondary loop dissipates heat through air-cooled radiators. The fluoride salt in each loop can be drained by heating freeze plugs.

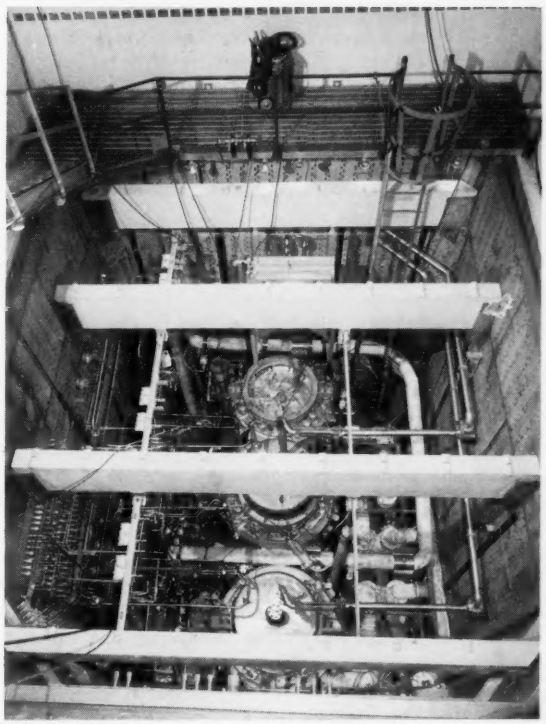

Fig. 3 Cell for two fuel-salt drain tanks and a flush-salt drain tank is shielded by 7.5-ft-thick stack of concrete blocks (which were placed on beams after photo was taken) and is sealed by welding a stainless-steel diaphragm that lines cell and passes between layers of shield blocks. Tanks are in electric furnaces that keep salts molten. Piping, inert-gas, electrical, and thermocouple connections enter cell through sealed penetrations.

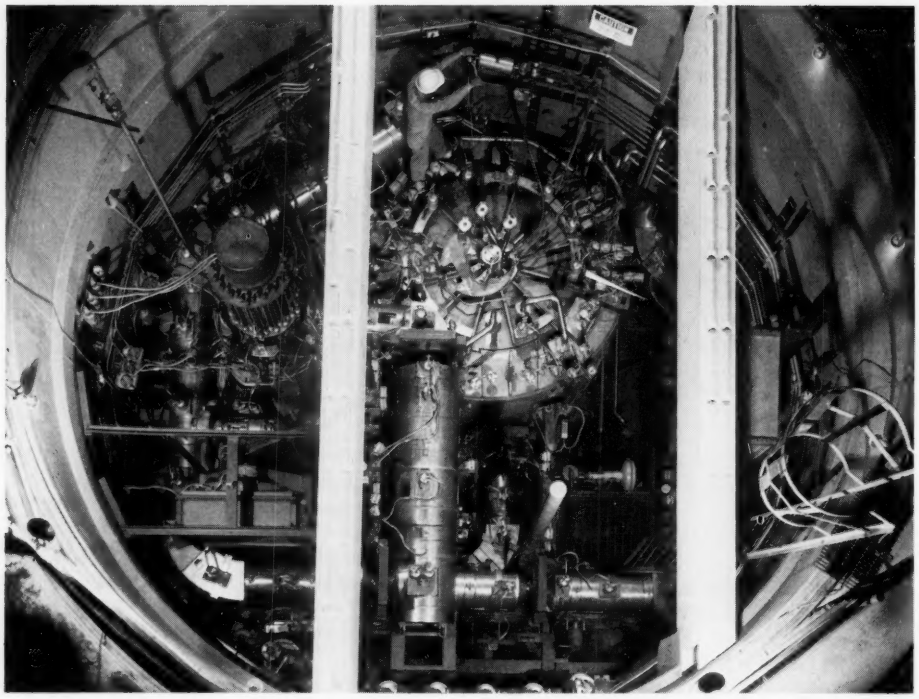

Fig. 4 MSRE containment cell holds reactor (top), its thermal-shield tank, the fuel pump (top left), fuel-to-coolant heat exchanger (bottom), and connecting 5-in. pipes. The other 5-in. pipes, which are covered by heaters and penetrate cell wall above thermal shield over reactor vessel, carry coolant salt between heat exchanger and radiator in a cell south of reactor cell. Clamps shown installed on freeze flanges (connecting components and pipes) hold them tight to form gas seals.

deep. The reactor access nozzle and control-rod thimbles protrude from the thermal shield atop the reactor vessel.

The "thermal" shield around the reactor vessel is a double-wall stainless-steel tank. The 14-in. annulus in the tank is filled with water and carbon-steel balls for primary shielding; the water circulates at 60 gal/min to remove heat generated in the shield. Thermal insulation and heaters line the inner wall of the tank and heat the reactor before startup.

The 5-in. heater-covered pipes that penetrate the cell walls above the thermal shield carry coolant salt between the heat exchanger and the radiator, which is in a separate cell. The coolant-salt pump is also outside the reactor cell.

Remote Maintenance. All equipment in the reactor cell was designed and installed so that major components can be maintained or removed and replaced with remote procedures.[7] The rotary assembly of the pump, the control rods and drives, the pipe heaters, and graphite or metal test samples can be removed most easily. The pump bowl, the reactor vessel, and the heat exchanger and piping sections, which are less subject to failure, also can be replaced, but with some difficulty. Special remote-maintenance tools and techniques are used;[8,9] a remote pipe-cutting and brazing machine is particularly interesting.

A portable maintenance shield that fits over limited-access ports in the top shield plugs is used for some repairs to the fuel loop. If large components must be replaced, the shield blocks over the reactor or drain-tank pits must be removed. Then operators in the shielded maintenance control room can manipulate maintenance equipment to remove the large radioactive components and store them in shielded pits.

The freeze flanges on the fuel loop allow disassembly by remote or semiremote methods. A metal O-ring gasket near the periphery of the 23-in.-OD flat-face freeze flanges forms a gastight seal; fuel salt migrates radially 2.4 in. between the uninsulated flange faces, where at 842°F it freezes to seal in the liquid.

The coolant loop is of all-welded construction. Because the coolant loop is not radioactive, maintenance on it can be performed directly after the coolant salt is drained.

STRUCTURAL ALLOY

A highlight of the MSRE is the new alloy developed to be compatible with the high-temperature fluorides used for the MSRE fuel and coolant. Except for the moderator graphite, all reactor-system and coolant-system components and auxiliaries that contact the fuel or coolant salts are made of this alloy. Called INOR-8, Hastelloy N, or INCO-806, this material is a nickel-base alloy that also contains 15 to 18% molybdenum, 6 to 8% chromium, and 5% iron. It was developed for the ANP (Aircraft Nuclear Propulsion) program for 1500°F design conditions.

Much work has been done toward understanding the bases for the behavior of this alloy in studies of molten-salt corrosion, compatibility with core graphite, air-oxidation resistance, the mechanical properties (such as tensile strength, creep, fatigue, and rupture) and fabrication characteristics, including casting, forming, machining, heat-treatment, welding, and cleaning. The comprehensive development work is summarized in Ref. 10, and further details can be found in Refs. 9 and 11 to 13. In general, INOR-8 appears to be a satisfactory structural material for use with these molten salts and graphite. Although neutron irradiation greatly reduces the ductility and rupture life at high temperature of the INOR-8 that was used in building the MSRE, small changes in the alloy composition are believed to have solved this problem for future reactors.

FUEL AND COOLANT

Table 1 gives the properties of the fuel and coolant fluoride salts. The fuel is a fluoride salt of Li, Be, Zr, and U; it melts at 842°F. When the reactor is operating at its normal power of about 7.5 Mw, the fuel enters the reactor at 1165°F and leaves at 1210°F; reactor design temperature is 1300°F. The coolant is a fluoride salt of lithium and beryllium; it melts at 851°F. The coolant enters the heat-exchanger tubes at 1015°F and is heated there to 1075°F by the fuel flowing outside the tubes. This coolant was selected to be chemically compatible with the radioactive fuel so that there would be no energetic reactions between the fluids if a leak occurs within the heat exchanger. An excellent summary of reactor fuel and coolant considerations is available.[14]

Table 1 CHARACTERISTICS OF MSRE FUEL AND COOLANT

Characteristic	Fuel salt	Coolant salt
Composition, mole %	65 LiF 39.1 BeF_2 5 ZrF_4 0.9 UF_4	66 LiF 34 BeF_2
Volume, cu ft	25 in core 70.5 total	45
Liquidus, °F	842	851
Density, lb/cu ft	141†	120*
Heat capacity, Btu/(lb)(°F)	0.455	0.526
Heat of fusion, Btu/lb	139	160
Viscosity, centipoise	7.64†	8.3*
Σ_a, cm^{-1}	7.0×10^{-3}	
Σ_f, cm^{-1}	5.4×10^{-3}	
Inlet temperature, °F	1165‡	1015§
Outlet temperature, °F	1210	1075
Velocity in core, ft/sec	0.75	

*At 1062°F.
†At 1200°F.
‡To reactor.
§To heat exchanger.

The fuel can be removed to a nearby cell for cleanup or reprocessing.[14] The fuel loop can be flushed and cleaned by circulating a lithium–beryllium fluoride flush salt.

REACTOR VESSEL

The reactor vessel, which is made of INOR-8 alloy, is shown in Fig. 5. Fuel enters the distributor ring at the shoulder of the vessel, flows downward in an annulus (between the vessel wall and an INOR-8 cylinder that surrounds the graphite core region) to the bottom plenum, then streams upward through

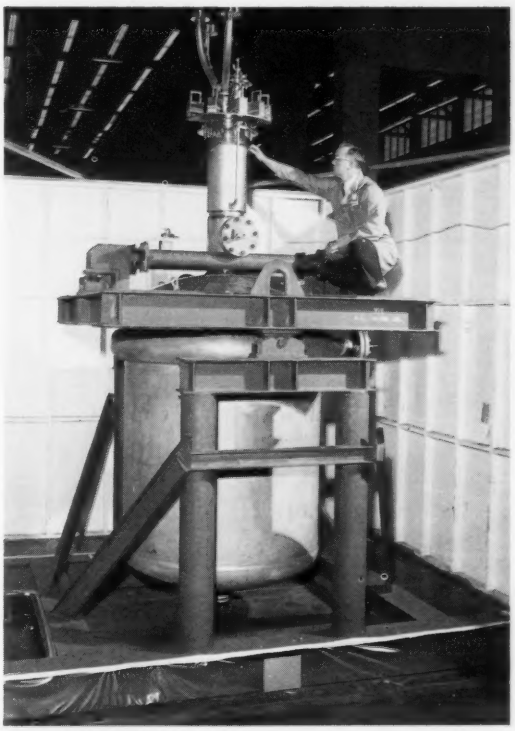

Fig. 5 Reactor vessel is ~60 in. in diameter and has INOR-8 alloy wall 9/16 in. thick; dished heads are 1 in. thick. Height is 100 in. from bottom head to center line of 5-in.-diameter fuel exit nozzle (shown with bolted-flange protective cover). Vessel design conditions are 50 psi and 1300°F.

1140 channels formed by the graphite stringers in the core, converges in the top plenum, flows out through the exit nozzle, and then goes to the pump and heat exchanger before returning to the vessel.

Heaters. Before reactor startup the entire reactor system is heated to about 1200°F. Figure 6 shows how the heater tubes were arranged around the reactor vessel before the >15,000-lb assembly was lowered into the combined thermal shield and furnace.

Figure 6 also shows the freeze flange on the fuel-inlet line (in protective bag at left) and the fuel-drain line (protruding from bottom of vessel) that has a freeze valve which holds the fuel in the reactor during operation.

CORE AND MODERATOR

The 64-in.-high core region consists of 69 cu ft of unclad graphite-moderator stringers in which there are 1140 vertical channels through which the molten fuel salt flows upward (Fig. 7). The graphite is a special material with a density of 1.85 g/cm^3 and with most of the pore openings less than 0.5 μ in diameter. The fuel salt does not wet the graphite and cannot enter the pores at pressures below about 200 psi. There are ~25 cu ft of fuel salt in the core and ~45 cu ft elsewhere in the fuel piping, pump, and heat exchanger. The four faces of each stringer are milled to form flow channels when the stringers are assembled; each channel is 1.2 in. wide and 0.4 in. deep. Points machined on top of stringers prevent fuel or other particles from settling out on top of the core. Clearance is provided in the core center for inserting three control rods and small test samples of graphite or metal.

A $\frac{1}{4}$-in.-thick cylinder made of INOR-8 surrounds the core to direct fuel flow within the reactor vessel and to support the grid from above; the cylinder is 68 in. high, and its outside diameter is 56 in.

Fluxes and Power Density. At 10-Mw(t) power the average thermal-neutron flux in the core is 1.5×10^{13} neutrons/(cm^2)(sec), and the peak flux is 3.4×10^{13} neutrons/(cm^2)(sec). Average power density is 14 watts/cm^3 in the fuel and 0.34 watt/cm^3 in the

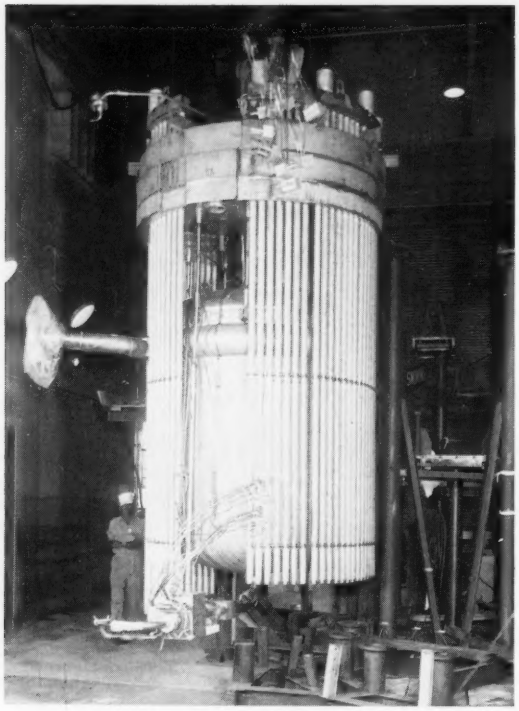

Fig. 6 Heater tubes around reactor vessel penetrate and are suspended from lid of thermal shield. Removable heating elements within the tubes connect to the secondary winding of a low-voltage, high-current transformer to furnish ~70 kw heat.

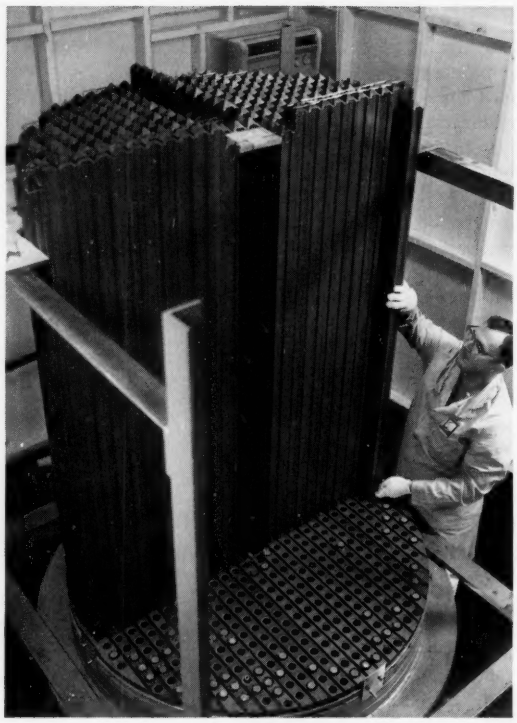

Fig. 7 Graphite core, here shown partly assembled on its INOR-8 support grid, consists of ~55-in.-diameter array of 2- by 2-in. graphite stringers into whose faces are machined flow channels for molten-salt fuel. Between the core array and the grid structure are two horizontal layers of graphite 1- by 2-in. bars drilled to accept the 4-in.-high and 1-in.-diameter spindle on the bottom of each stringer. Stringers are held down by INOR-8 rods that pass through holes in grid and spindles.

graphite; peak power density is 31 watts/cm^3 in the fuel and 0.98 watt/cm^3 in the graphite.

The delayed-neutron fraction is 0.0067 when the fuel is at rest but drops to 0.0036 when the fuel is circulating.[15,16] The total temperature coefficient of reactivity is -6.96×10^{-5} $\Delta k/(k)(°F)$, of which -3.28×10^{-5} is due to the fuel and -3.68×10^{-5} is due to the graphite.

CONTROL RODS

There are three flexible control rods at the center of the core. Each control rod consists of flexible tubes over which are slipped small canned cylindrical segments of $Gd_2O_3-Al_2O_3$ like beads on a string. The segments are 0.83 in. in inside diameter and 1.10 in. in outside diameter and are clad inside and out by 0.02-in.-thick Inconel. Each control rod consists of 1.1 kg of Gd_2O_3 and is attached to its drive motor by a flexible cable and electromagnetic release. Scram time is less than 0.85 sec, and the worth of 1, 2 and 3 rods is 2.3, 4.2 and 5.6% $\Delta k/k$. Up to 2725 watts are generated in a rod.

So that the rods can operate in a gas environment, they move within thimbles that isolate them from the fuel salt. Cooling of the rods is provided by gas (mostly nitrogen) from the reactor containment cell which circulates down through the hollow control-rod tube and returns up between the tube and the thimble wall.

An access nozzle attached to the 10- by 5-in. flanged tee atop the reactor vessel accommodates (Fig. 8) three control-rod thimbles and a sample port. The flexible control rods attach to the drives (not shown) mounted in the three recessed flanges at the top of the assembly. Circulating fuel is prevented from moving up into the access nozzle by a frozen-salt plug in the annulus formed by this assembly and the 10-in.-diameter section of the flanged tee.

The removal of any of five central graphite stringers from the core requires that the entire assembly shown in Fig. 8 be removed from the reactor.

FUEL-TO-COOLANT HEAT EXCHANGER

The components of the primary heat exchanger are shown in Fig. 9. The unit is ~8 ft long, 16 in. in diameter, and has 169 U tubes. The 25% cut cross baffles are 12 in. apart. Each tube is ~14 ft long, ½ in. in diameter, and has a 0.042-in.-thick wall. Tubes are welded and back brazed into the tube sheet, with a 0.775-in.-pitch triangular spacing. The effective heat-transfer area is ~259 sq ft. The active length is 6 ft. The shell is ½ in. thick, has 5-in.-diameter nozzles, and holds 6.1 cu ft of fuel. At 7.5 Mw, fuel enters the shell at 1210°F and leaves at 1165°F; the flow rate is 1200 gal/min. Coolant salt flows through the tubes, entering at 1015°F and leaving at 1075°F; its flow rate is about 850 gal/min.

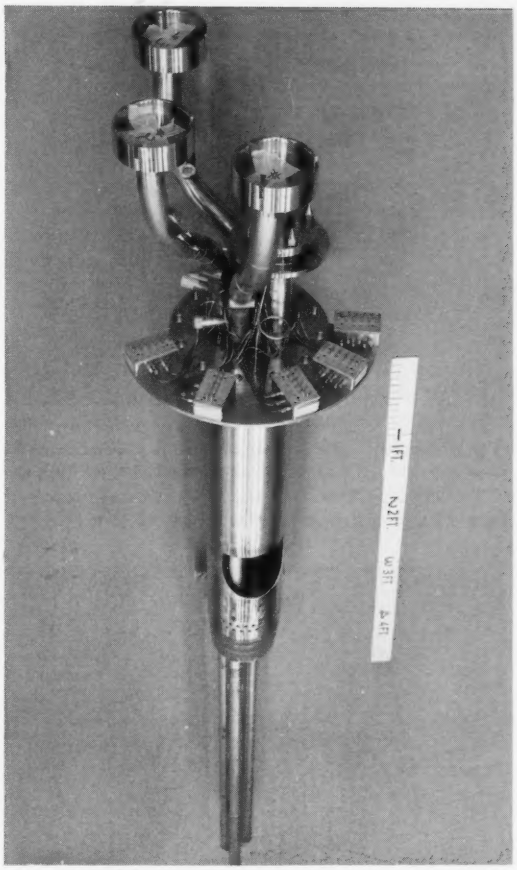

Fig. 8 Reactor-access nozzle and control-rod thimbles attach to flanged tee atop reactor vessel (see Fig. 3). Drives for three flexible control rods mount in recessed flanges at top. Terminal boxes are for thermocouple connections. Fuel from reactor flows through semicircular opening on way to exit nozzle.

PUMPS FOR MOLTEN SALT

Figure 10 illustrates the impeller and 75-hp motor for the 1200 gal/min fuel pump,[17,18] which turns 1160 rpm and develops an ~50-ft head. The fuel-pump bowl is 36 in. in diameter and 15 in. high, normally holds 4.1 to 5.2 cu ft of molten salt and has space for 2 cu ft of gas above the salt. Thus the bowl serves as both sump and expansion volume. An inert-gas blanket over the seals on the shaft flows inward slowly to prevent escape of salt or fission products. The volute built into the bowl bypasses a 65 gal/min spray of fuel so as to remove volatile fission products from the fuel stream; the gases are swept into a charcoal trap where fission products are adsorbed (a continuous helium purge flows through a filter to the off-gas stack). The motor–pump combination,

Fig. 9 Primary heat exchanger is ~8 ft long and 16 in. in diameter, and it has 169 U tubes. Coolant salt flows through the tubes.

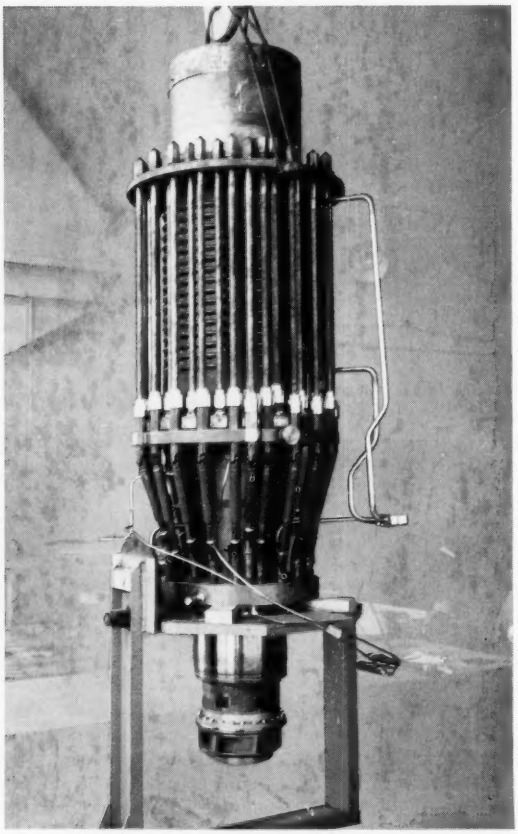

Fig. 10 Impeller and motor for the vertically mounted centrifugal fuel pump can be replaced semiremotely; lengthened flange bolts facilitate manipulation.

which stands 8.6 ft high overall, is hermetically sealed to prevent fission gases escaping to the cell. Conventional ball bearings in the pump are lubricated and cooled by oil. The coolant-salt pump is quite similar to the fuel-salt pump except that it circulates only 850 gal of salt per minute, develops a 78-ft head, has no provision for stripping fission-product gas (because none is generated in the coolant salt), and can be maintained or replaced by direct means.

FUEL STORAGE

Two drain tanks (one is shown in Fig. 11) store the molten-salt fuel when it is not being circulated

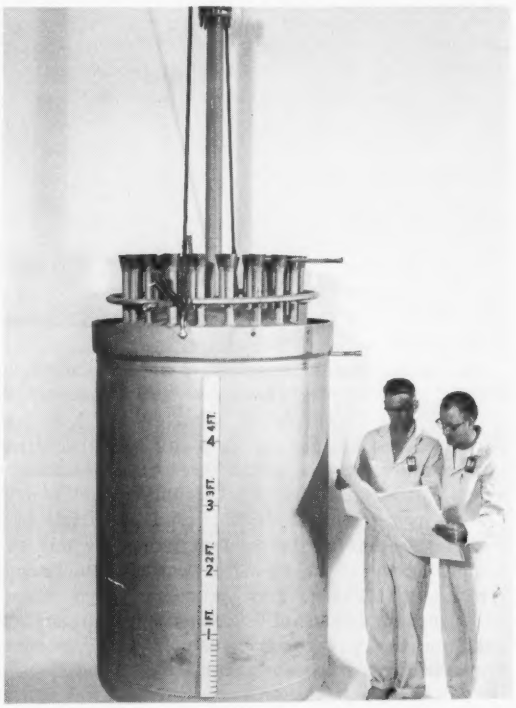

Fig. 11 Fuel-drain tank made of INOR-8 safely stores molten-salt fuel when it is not being circulated through reactor system. Flared thimbles, which extend to tank bottom, accept bayonet-tube coolers that remove fission-product heat from fuel.

through the reactor. Each tank can store all the fuel in a geometrically safe configuration.

The removal of ~100 kw of fission-product decay heat from fuel stored in a drain tank is accomplished with the use of a steam-dome and bayonet-tube cooler assembly. The bayonet tubes extend to the bottom of the 24 thimbles shown in Fig. 11. Demineralized water is fed by gravity into the dome and then down a tube in the center of each bayonet; decay heat from

the fuel salt convects across the annulus between the thimbles and the bayonet tubes and then boils the water. The steam rises through the bayonet tube and is condensed elsewhere.

The two fuel drain tanks and a tank for storing flush salt are in a sealed and shielded cell in the MSRE building (Fig. 3). A drain tank for the coolant salt, which has only slight induced radioactivity, is in an unsealed cell under the radiator (Fig. 2). Except for needing and having no system for removing decay heat, the flush and coolant tanks are similar to the fuel tanks.

How Has MSRE Performed?

The reactor is operating. Performance data through May 10, 1967, are shown in Table 2. Figure 12 summarizes plant operations in 1966.

OVERALL PERFORMANCE

In most respects the performance of the MSRE has been excellent.[19] The plant has been under test for about 2 years. The salts have been kept molten for the entire time and have been circulated for many months. The plant has been through several major and many minor thermal cycles, with no obvious important effect on any major equipment of significance to future molten-salt reactors. According to chemical analyses and reactor nuclear behavior,[20] the fuel has been completely stable. Analyses of fuel and coolant salts confirm that there has been no significant general corrosion of the metal in the system. Specimens of both metal and graphite from the core look new.

Table 2 HIGHLIGHTS OF MSRE OPERATION*

Performance	Fuel circulating system		Coolant circulating system
Time above 1000°F, hr			
Circulating helium†	3,468		2,126
Circulating salt‡	9,031		10,656
Total	12,499		12,782
Time critical, hr		5,788	
Total power, Mw-hr		32,450	
No. of heating cycles (200 to 1200°F)	7		6
No. of fill cycles	28		10
No. of power cycles	48		45

*Through May 10, 1067.
†Pumps circulate helium when reactor systems are at high temperature and salts are in drain tanks.
‡Fuel-salt temperature usually has been 1100 to 1230°F.

The only major difficulties have been with the off-gas system on the reactor primary system and with the radiator and blowers in the heat-dump system. The off-gas system of future molten-salt reactors probably must be equipped to handle aerosols. The problems with the blowers and the radiator and its housing have caused delays. However, these pieces of equipment are peculiar to the MSRE and would not be part of future large molten-salt power breeder reactors.

CONSTRUCTION AND TESTING

The MSRE design began in mid-1960; construction began in late 1961 and was sufficiently complete by September 1964 to allow in-plant training and checking of certain systems. The reactor fuel and coolant systems were pressure- and helium-leak tested in October 1964; they were heated to 1200°F, purged with helium to remove air and moisture and cooled for inspection in November. Everything went through the first thermal cycle properly except for the housing for the heat-dump radiator (Fig. 13). Temperature gradients bowed the housing doors in their tracks so they could not be raised. The housing around the radiator tubes is subject to severe temperature cycling when the reactor is operating and, although

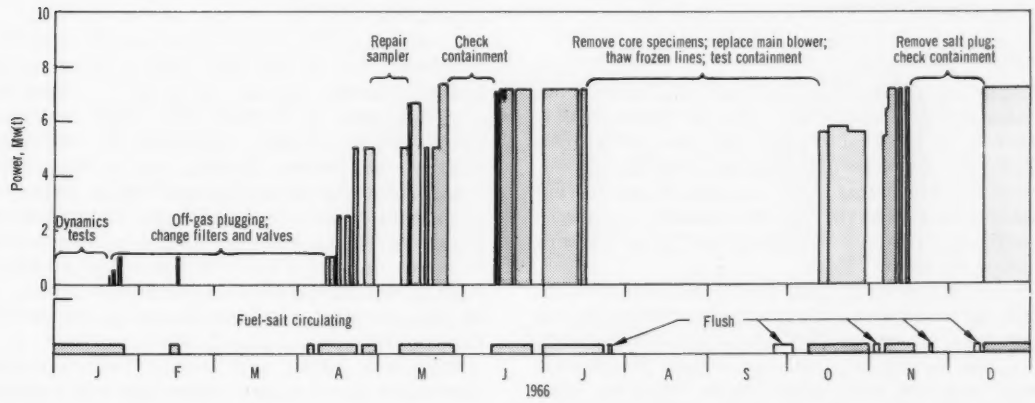

Fig. 12 Summary of MSRE operations in 1966.

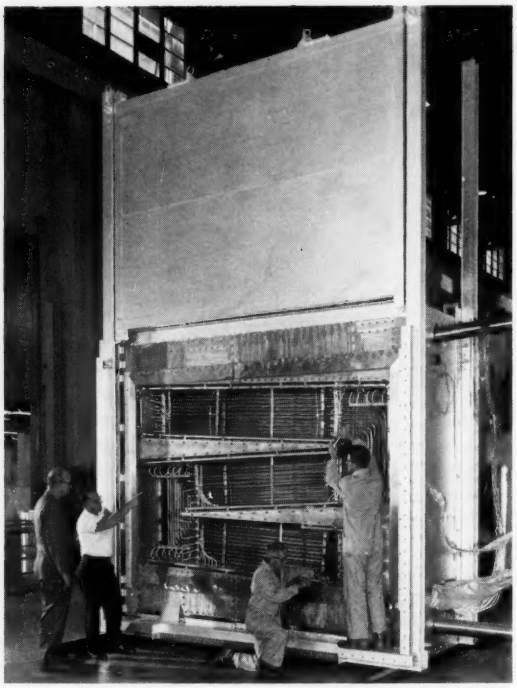

Fig. 13 Radiator transfers heat from MSRE coolant salt to air. Salt flows (830 gal/min) through S-formed tubes, which have a 0.060-in.-thick wall, a $^3/_4$-in. diameter, and a 30-ft length and are arranged in 10 banks with 12 tubes per bank. Two axial-vane blowers having 200,000 cu ft/min combined-capacity blast air over tubes and up metal stack. Thermocouples monitor temperature of each 0.072-in.-wall tube; electric heaters in radiator preheat the equipment for startup and keep salt molten when reactor is not generating heat. Doors on each side of radiator automatically drop quickly if coolant or fuel salts stop flowing—thus preventing coolant from freezing in coils.

numerous improvements have been made, is not yet completely satisfactory.

SALT FILLING

About 45 cu ft of coolant salt was added to the coolant-system drain tank late in October 1964. Another 80 cu ft of coolant salt was added to the flush-salt tank in the fuel-drain-tank system early in December 1964. Next came a period of transferring salt between tanks in the fuel system to calibrate weigh cells and level indicators and to learn how to operate the freeze valves.

Fuel and coolant systems were reheated to 1200°F, salts were charged, and circulation began for the first time in January 1965. Draining and filling tests and long periods of circulation without interruption were continued until early March. Then the salts were returned to the drain tanks, and the other equipment was cooled for inspection and maintenance.

While equipment inspection and maintenance were under way, about 75 cu ft of 65 $LiF-30\ BeF_2-5\ ZrF_4$ fuel-carrier salt was added to a fuel drain tank. For the precritical tests ^{238}U tetrafluoride was added to the carrier salt in the drain tank, and the fuel salt was circulated for 2 weeks to ensure that all systems were working properly and to investigate chemical behavior before enriched uranium was added.

Beginning in April 1965 ^{235}U was added in a number of steps. (For chemistry reasons it was decided to operate MSRE for the first few years with salt containing ~0.8 mole% uranium, which meant that uranium enriched only 30% could be used.) First, the carrier salt was returned to a drain tank, and 45 kg of ^{235}U (in a UF_4-LiF eutectic mixture) was added to it. Then the fuel salt was brought into the circulating system, and the reactor multiplication factor was measured with the pump operating and at rest. The procedure was repeated on addition of 15, 5, and then 4.3 kg of ^{235}U, by which time the reactor was within 1 kg of criticality. Subsequent additions were made to the fuel-pump bowl in capsules containing 85 g of ^{235}U.

CRITICALITY

The reactor was first critical on June 1, 1965, at 1200°F, with the three control rods fully withdrawn.[21] Low-power experiments were continued through June.

The plant was shut down early in July to prepare for power operation. Major modifications were made to the coolant-line penetrations through the containment vessel and to the radiator doors to reduce thermal stresses. Other parts of the reactor systems and auxiliaries required minor attention. Samples of graphite and metal were removed from the core for examination; the pump rotary element was removed and inspected. Then the reactor containment was completed and sealed.

APPROACH TO POWER

Containment tests started in October and were completed early in December 1965. Then the reactor fuel and coolant systems were heated, filled, and pressure-tested at temperature. Tests at powers below ~50 kw continued until Jan. 20, 1966, when work on the radiator housing was completed. The power was raised gradually to 1 Mw by January 24 and was held there for about 1 day. At this time the helium cover-gas pressure in the fuel-pump bowl, required to force 4 liters of purge gas per minute through the off-gas system, increased from 5 to 10 psi. Remedial measures failed, so the reactor was drained to permit investigation.

Study and testing and a brief 1-Mw operation showed that small control valves and other orifices in the off-gas system were accumulating small amounts of organic compounds in the form of very

viscous liquids and varnishlike solids. Apparently a very small amount of oil leaked through a gasketed seal between the bearing housing and the shield block in the fuel-circulating pump, seeped down through the crevice between the shield block and the neck of the pump tank, and, when it reached the high-temperature pump bowl, vaporized and was carried into the off-gas system with the helium purge gas. The vapors should have condensed on the cool off-gas piping, but some droplets were carried as aerosols all the way to the control valves.

Although the small amounts of oil caused no problems at low power, at 1 Mw the beta radiation from krypton and xenon fission products in the off-gas system polymerized some of the oil. The trouble was reduced by replacing some of the piping and valves in the off-gas system and by installing an absolute filter and a small carbon trap ahead of the control valves. Future pumps will have welded, not gasketed, seals.

FULL-POWER OPERATION

Beginning early in April, power was raised in steps. The ~7.5 Mw full operational power under design conditions was reached late in May 1966. Radiator and heat-exchanger performance prevented attainment of the 10 Mw design power. The effective air-side heat-transfer coefficient was less than had been calculated. Also, the primary heat exchanger did not perform up to expectations; this was attributed to the actual value of the thermal conductivity being lower by a factor of 3 than had been used in the design calculations. Operation was continued at high power with only minor interruptions until mid-July, when the rotary element disintegrated on one of the main air blowers. Inspection revealed a large crack in the hub of the second blower, so the plant was shut down to obtain replacements, to change samples of graphite and INOR-8 in the core, and to service other equipment. The reactor was back in operation again at 5.3 Mw, with one blower, beginning the second week in October. The second blower was installed early in November, and reactor power was raised again to 7.5 Mw.

Operations in October and early November were not entirely smooth. Flush salt had been raised into the off-gas line during tests that were made as the reactor was being shut down in July, and some salt had frozen in the line near the pump bowl. Although there was no indication of difficulty when the plant was started again in October, the off-gas line began to plug at the pump bowl after only a day or two at power. Reactor operation was continued by discharging the gas via an alternative path through the pump overflow tank; but that procedure was inconvenient, so the fuel was drained in the middle of November to unplug the off-gas line and to make some tests on the reactor containment. These tests were completed by the middle of December, and the reactor was operated continuously until the middle of January. The particle trap in the fuel-system off-gas line and disconnects in air lines to valves in the reactor cell were replaced during a shutdown the last 2 weeks in January. Reactor operation was resumed at the end of January and was continuous through May 10, 1967, when the plant was shut down to remove metal and graphite specimens from the core.

The Future of Molten-Salt Reactors

The future of the MSR's, which has been discussed in some detail,[10,22] depends on projections that, in a larger two-region reactor, breeding with Th–U fuel is feasible and offers economic promise. Certainly the simplicity of core design for a thermal molten-salt-fuel reactor,[23] the prospect of low-cost continuous fuel reprocessing, and the possibility of low capital cost merit careful consideration. Whether molten-salt-fuel reactors can develop sufficiently high breeding ratios and can demonstrate reliability sufficient to compete with heterogeneous fast reactors are still questions. They can be answered only after the MSRE accumulates more operating experience and studies of its fuel, structure, and moderator demonstrate performance. Then design projections based on these sound data can define the promise of molten-salt reactors. Thus MSRE, a single-region reactor not capable of breeding, is demonstrating a technological base from which to draw judgments as to whether a larger plant to demonstrate breeding is worthwhile.

• • •

I want to express my appreciation to R. B. Briggs and his associates at Oak Ridge National Laboratory for their assistance in reviewing the manuscript and for suggesting appropriate photographs.

References

1. James A. Lane, H. G. MacPherson, and Frank Maslan (Eds.), *Fluid Fuel Reactors*, Addison-Wesley Publishing Company, Inc., Reading, Mass., 1958.
2. H. G. MacPherson, Molten Salt Reactors Will Produce Low-Cost Power, *Power Eng.*, 71(1): 28-31 (January 1967).
3. A. L. Boch, E. S. Bettis, and W. B. McDonald, The Molten Salt Reactor Experiment, in *Power Reactor Experiments*, Symposium Proceedings, Vienna, 1961, Vol. 1, pp. 247-315, International Atomic Energy Agency, Vienna, 1961 (STI/PUB/51).
4. W. R. Grimes, E. G. Bohlmann, and L. O. Kirkbride, Irradiation Behavior of Fluid Fuels, in *Proceedings of the Third International Conference on the Peaceful Uses of Atomic Energy, Geneva, 1964*, Vol. 11, p. 256, United Nations, New York, 1965.
5. W. R. Grimes, Materials Problems in Molten Salt Reactors, in *Materials and Fuels for High Temperature Nuclear Applications*, Chap. 7, M. T. Simnad and L. R. Zumwalt (Eds.), The M.I.T. Press, Cambridge, Mass., 1964.
6. R. B. Briggs, Molten Salt Reactor Systems, presented

at the Sixth Nuclear Congress Symposium on Uranium Thorium Cycle, Rome, Italy, June 13–15, 1961.
7. R. Blumberg, Maintenance of Radioactive Systems and Components of the MSRE, *Trans. Amer. Nucl. Soc.*, 9(2): 530 (October–November 1966).
8. R. Blumberg, Remote Maintenance of the MSRE, in Molten Salt Reactor Program Semiannual Progress Report for Period Ending July 31, 1964, pp. 190-200, USAEC Report ORNL-3708, Oak Ridge National Laboratory, November 1964.
9. Molten-Salt Reactor Program Semiannual Progress Report for Period Ending February 28, 1965, USAEC Report ORNL-3812, pp. 190-200, Oak Ridge National Laboratory, June 1965.
10. Molten-Salt Reactor Program Semiannual Progress Report for Period Ending July 31, 1964, USAEC Report ORNL-3708, pp. 330-372, Oak Ridge National Laboratory, November 1964.
11. Molten-Salt Reactor Program Semiannual Progress Report for Period Ending August 31, 1965, USAEC Report ORNL-3872, Oak Ridge National Laboratory, December 1965.
12. Molten-Salt Reactor Program Semiannual Progress Report for Period Ending February 28, 1966, USAEC Report ORNL-3936, Oak Ridge National Laboratory, June 1966.
13. Molten-Salt Reactor Program Semiannual Progress Report for Period Ending August 31, 1966, USAEC Report ORNL-4037, Oak Ridge National Laboratory, January 1967.
14. C. D. Scott and W. L. Carter, Preliminary Design Study of a Continuous Fluorination–Vacuum-Distillation System for Regenerating Fuel and Fertile Streams in a Molten Salt Breeder Reactor, USAEC Report ORNL-3791, January 1966.
15. S. J. Ball and T. W. Kerlin, Theoretical and Experimental Dynamic Analysis of the Molten Salt Reactor Experiment, *Trans. Amer. Nucl. Soc.*, 9(2): 464 (October–November 1966).
16. S. J. Ball and T. W. Kerlin, Stability Analysis of the Molten-Salt Reactor Experiment, USAEC Report ORNL-TM-1070, Oak Ridge National Laboratory, December 1965.
17. A. G. Grindell, W. F. Boudreau, and H. W. Savage, Development of Centrifugal Pumps for Operation with Liquid Metals and Molten Salts at 1100–1500°F, *Nucl. Sci. Eng.*, 7(1): 83-91 (January 1960).
18. P. G. Smith and L. V. Wilson, Development of an Elevated Temperature Centrifugal Pump for a Molten Salt Nuclear Reactor, presented at American Society of Mechanical Engineers Winter Annual Meeting, November 1965, Paper 65-WA/FE-27.
19. P. N. Haubenreich, Operation of the Molten Salt Reactor Experiment, USAEC Report ORNL-P-2397 (CONF-660524-18), Oak Ridge National Laboratory, 1965.
20. J. R. Engel, P. N. Haubenreich, and B. E. Prince, Predicted and Observed Nuclear Characteristics of the Molten Salt Reactor Experiment, *Trans. Amer. Nucl. Soc.*, 8(2): 530 (November 1965).
21. J. R. Engel, Application of an On-Line Digital Computer to a Reactor Experiment, *Trans. Amer. Nucl. Soc.*, 8(2): 585-586 (November 1965).
22. Paul R. Kasten, E. S. Bettis, and Roy C. Robertson, Design Studies of 1000-Mw(e) Molten-Salt Breeder Reactors, USAEC Report ORNL-3996, Oak Ridge National Laboratory, August 1966.
23. L. G. Alexander, W. L. Carter, C. W. Craven, D. B. Janney, T. W. Kerlin, and R. Van Winkle, Molten Salt Converter Reactor Design Study and Power Cost Estimates for a 1000 Mw(e) Station, USAEC Report ORNL-TM-1060, Oak Ridge National Laboratory, September 1965.

Toward an Understanding of Sodium Fires

By Paul A. Lottes

In safeguards analyses of sodium-cooled reactors, sodium fires are quite important; the particular concern is the possibility of dispersion of radioactivity as a result of a large fire that involves primary-system sodium coolant. Atomics International (AI) has reported early results of investigations designed to characterize such fires.[1]

Fire and Dispersion

To study dispersion effects, AI feels it is necessary to determine the effects of time, initial condition variables, and system parameters of (1) the spatial distribution of energy, (2) the amount of sodium released (presumably sodium oxide), and (3) the amount of selected fission products released. Their study includes three phases:

Phase I is the study of sodium fires with relatively unrestricted access to air. Various theoretical models have been postulated and tested by experiment. One large fire (LF-1) has been staged to date[1] in Phase I.

Phase II will cover experimental variations in sodium geometry, container geometry, and air flow rate.

Phase III will be full-scale demonstration tests to verify the developed models.

Results

Work done in Phase I is covered in Ref. 1, which describes the large fire and also excellently summarizes previous experiments[2–16] that include burning in shallow pools, burning in deep pools, and injection-type experiments. The injection experiments reviewed were related to determinations of minimum concentrations of oxygen required for reaction, minimum reaction temperature, etc. Shallow-pool tests (< 9 in. deep) were made to determine burning rates. The deep-pool tests were concerned with burning and release rates.

The large fire test apparatus used by AI is shown in Fig. 1. One gram of NaI containing 6.5 mc of ^{131}I was added to 615 lb of sodium, producing an initial concentration of ~3 ppm iodine in sodium (simulating fission-product retention by sodium). The sodium was initially 4 ft deep in a 2-ft-diameter burn pot and was heated to 350° F in an inert atmosphere.

After ignition, the fire (LF-1) burned for 32 hr (Fig. 2) at an average rate of ~2 lb/(hr)(sq ft) for 26 hr. At about the 26th hour, the oxide had built up from the bottom of the pot to the surface; it formed a hard crust that cut off smoke generation and, as Fig. 2 shows, initiated the decline of oxidation.

A material balance on the system (see Table 1) accounted for 94% of the sodium and 77% of the iodine. About 67% of the sodium remained as residue in the pot and 27% was released. Approximately 8% of the iodine was released and 69% remained in the residue.

Table 1 MATERIAL BALANCE FOR SODIUM FIRE LF-1

Material	Sodium		^{131}I		Iodine in sodium, μc/lb
	lb	%	μc	%	
Residue in burn-pot batch No. 1	338	55	2848	45	8.33
Residue in burn-pot batch No. 2	35	6	1039	16	29.7
Burn-pot leakage (soluble)	37	6	76	1	2.05
Burn-pot leakage (insoluble)	0	0	460	7	
Total residue	410	67	4423	69	10.8
Cleaning solution	132	21	465	7	3.52
Cleaning-solution precipitate	0	0	34	1	
Deposition and fallout	35	6	26	0	0.75
Total released	167	27	525	8	3.14
Total accounted for	577	94	4948	77*	8.57
Initial total	615	100	6400	100	10.4
Unaccounted for	38	6	1452	23	

*An unspecified amount of iodine was lost during the dissolution process.

The thermal analysis of the fire included analysis of the diffusion of sodium through the nitrogen layer at the sodium liquid–vapor interface, the calculation

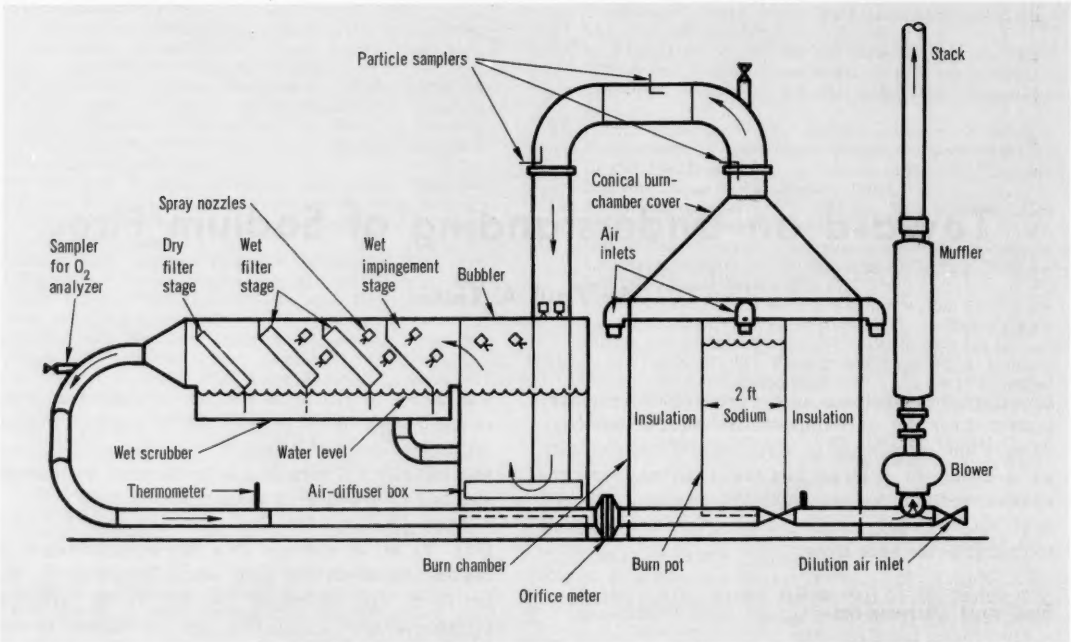

Fig. 1 Test apparatus for large sodium fires. Iodine-131 was added to the sodium to simulate fission-product retention.

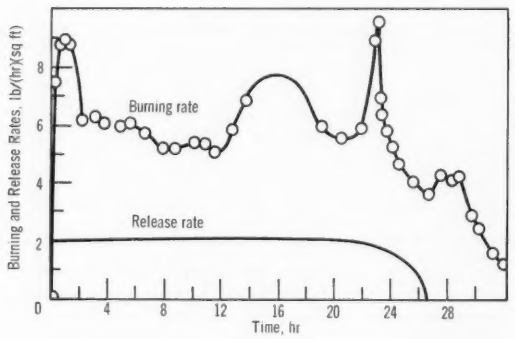

Fig. 2 Results of large sodium fire LF-1. Burning rate was determined from oxygen depletion of the effluent. Release rate of sodium oxide was derived from analysis of scrubber water.

of heat-transfer coefficients for flame to sodium, and the calculation of energy transfer for flame to cloud.

The diffusion coefficient was calculated to be 4.43 sq ft/hr at 1550°F. Total energy release at the flame front next to the surface was 34,200 Btu/(hr)(sq ft) of surface, of which 13,200 Btu/(hr)(sq ft) was transmitted by conduction, radiation, and convection to the sodium liquid.

References

1. G. N. Lauben, Initial Experience with Large Sodium Fires Experiments (LF-1), USAEC Report NAA-SR-12041, Atomics International, Aug. 1, 1966.
2. J. J. Droher and J. D. Gracie, A Study of Sodium Fires, USAEC Report NAA-SR-4383, Atomics International, Oct. 15, 1960.
3. Edward Hines and J. K. Kelly, Determination of Maximum Pressures Attained During the Reaction of Sodium with Air in Closed Systems, Detroit Edison Company, Report NP-7320, Feb. 15, 1956.
4. C. O. Nelson and D. B. Nelson, Sodium-Air Reaction Experiments, USAEC Report KAPL-639, Knolls Atomic Power Laboratory, Jan. 1, 1952.
5. H. C. Cowen and H. Vickers, The Oxidation of Sodium — A Review of Progress from April 1, 1954, to December 31, 1954, British Report RDB(C)/TN-121(FRDC/P-105), Apr. 15, 1955.
6. F. L. Mangold and R. A. Tidball, Sodium Fire Studies, Report NP-3812, Mine Safety Appliances Company, Apr. 23, 1952.
7. J. R. Humphreys, Jr., Sodium-Air Reactions as They Pertain to Reactor Safety and Containment, in *Proceedings of the Second United Nations International Conference on the Peaceful Uses of Atomic Energy Geneva, 1958*, Vol. 15, p. 1893, United Nations, New York, 1958.
8. G. N. Lauben, Fission Product Release from Sodium Fires, in AEC Unclassified Program, Quarterly Technical Progress Report, January–March 1964, USAEC Report NAA-SR-9700, p. 1-C-23, Atomics International, May 19, 1964.
9. E. Garelis, Sodium-Air Accident Study for a Sodium Cooled Reactor, USAEC Report AECU-4161, Atomic Power Development Associates, Inc., Apr. 6, 1959.

10. Atomics International, unpublished, Oct. 16, 1963.
11. G. N. Lauben, Atomics International, unpublished, Apr. 15, 1961.
12. N. A. Bredig, W. J. Johnson, and Wm. T. Smith, Jr., Equilibrium Concentrations in Sodium Halide–Sodium Systems, *J. Amer. Chem. Soc.*, 77: 307 (1955).
13. R. J. Begley, Fission Product Release from Sodium Fires, in Annual Technical Progress Report, AEC Unclassified Programs, Fiscal Year 1963, USAEC Report NAA-SR-8888, Atomics International, Apr. 1, 1964.
14. S. J. Stachura, Atomics International, unpublished, Aug. 25, 1964.
15. J. H. Perry, *Chemical Engineering Handbook*, 3rd ed., p. 404, McGraw-Hill Book Company, Inc., New York, 1950.
16. R. J. Begley, Liquid Sodium Absorbs Gaseous Iodine, *Nucleonics*, 20(10): 100 (October 1962).

Recent Developments in Open-Cycle MHD Power Systems

By Jerzy Moszynski, University of Delaware

Developments in magnetohydrodynamic (MHD) power generation—the direct conversion of heat to electricity when an electrically conductive fluid moves in an electromagnetic field—are of practical interest because (1) of the improvements in high-temperature-materials technology and (2) when and if fuel costs start to rise, MHD topping cycles may be incorporated in steam power plants to raise efficiencies[1] to 50 to 55%.

Currently the most advanced MHD devices are the open-cycle generators. Several of these facilities, in which the electrically conducting fluid is usually a coal- or oil-fired combustion plasma, have operated successfully, and others are being completed in at least five countries. Gas temperatures in the plasmas (often seeded with potassium or its salts to improve conductivity) have usually been <2500°K; however, isolated experiments have reached 3000°K.

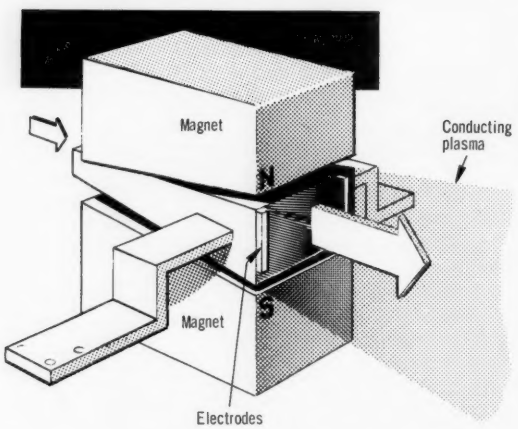

Fig. 1 Basic principle of MHD: ions in an electrically conductive fluid driven through a magnetic field induce a flow of electricity. The conducting fluid may be a liquid metal or a combustion plasma.

This article, a sequel to the *Power Reactor Technology* review of liquid-metal MHD power systems,[2] summarizes open-cycle MHD technology (Fig. 1) as it emerges from papers presented at the recent third International Symposium on Magnetohydrodynamic Electric Power Generation.[3–5] Topics reviewed include operating experience; high-temperature-materials developments; component design problems; basic combustion plasma physics; and the direction of future progress as indicated by developing programs, analytical studies, and novel ideas.

Operating Experience

The largest operational open-cycle MHD generator[6] is the AVCO Mark V. Designed to provide large amounts of power for limited durations, it uses the products of a rocket-engine-like combustion of a liquid hydrocarbon fuel and gaseous oxygen, seeded with potassium hydroxide. The generator provides its own excitation current to the air-core magnets and has been operated as a single electrode-pair machine (magnet windings in series with the external load) and as a multielectrode machine (magnet windings in parallel with 50 pairs of segmented electrodes). Figure 2 shows a schematic of the generator wherein a net power output of 23,000 kw was achieved at ~1000 volts. Although the overall efficiency has not been given, we may estimate it from the available data to 5% or less. The electrical performance of the machine substantially exceeds design specifications, allegedly because high supersonic gas velocities were used.

HALL-MODE OPERATION

Another generator, tested in the same laboratory,[7] uses similar seeded combustion gases generated in a

rocket-type combustion chamber. Operating in the Hall mode, it developed 1000 kw at 5510 volts using a rectangular channel and 930 kw at 2800 volts using a circular channel with a volume 75% of the rectangular one. The rectangular channel, operated in the Faraday mode, was previously reported to deliver 1480 kw with a conductivity 3.3 to 10 times higher than in the Hall mode. The operating time of this generator was ~10 to 15 sec, the magnetic field ~3 tesla; maximum value of the Hall parameter reached was 4.

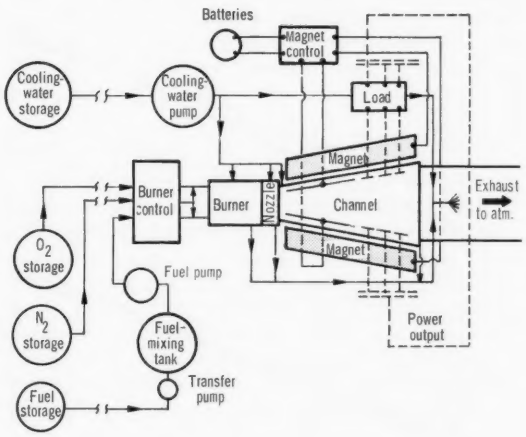

Fig. 2 Typical open-cycle MHD generator uses products of rocket-engine-like combustion of liquid hydrocarbon fuel and gaseous oxygen, seeded with KOH to improve conductivity, to produce net power output[6] of 23,000 kw at ~1000 volts.

SMALLER GENERATORS

Operating experience and extensive experimental results with several smaller generators[8–12] were reported. These range from a 7-Mw(t) input Japanese unit[8] to 0.3-Mw(t) Polish installation.[12] In particular, one paper[11] reported extensive experimental comparisons of the various modes of generator operation; these are shown in Fig. 3.

Experiments concerned with cathode characteristics[13–15] indicated relatively stable voltage threshold values, below which no current was observed and above which the current rose rapidly with voltage. This effect was attributed to the formation of an arc in the cold boundary layer near the electrode.

Materials Developments

High-resistance insulating materials for duct walls and high-conductivity electrode materials—both for service at >2500°K—are the major materials needs.

INSULATING MATERIALS

The behavior of insulating materials in a high-temperature environment and under conditions of thermal shock caused by cycling was investigated extensively.[16–20] Silicone carbide and aluminum oxide-based materials and chromium–aluminum oxide cermet laminated walls were studied in the range 1500 to 1700°C and again during rapid cycling at these temperatures.[16] Above 1800°K, ceramic insulators such as strontium and calcium zirconates were found[17] to become too highly conductive ($\sigma > 1.0$ mho/m). High purity increased resistance at higher temperatures. High-purity magnesia, zirconia, and thoria were tested[18] up to 15 hr and 2400°C. Thermal and electrical properties were measured up to 1600°C and again confirmed severe decrease in resistivity above 1500°C. Insulating walls of $SrZrO_3$ were exposed successfully[19] to seeded gases at 2300°K; the indicated wall temperature was ~1500°K.

ELECTRODES

Even more interest was directed at suitable electrode materials.[16–27] The most frequently considered ceramic electrode materials[16–25] were zirconia (wholly or partially stabilized by calcium), yttrium or lanthanum oxide, zircon boride, and certain chromites, particularly that of lanthanum. These materials were tested for durability under exposure to seeded gases at high velocities and up to 2300°C, as well as to thermal cycling. Electrical- and thermal-conductivity measurements were performed up to 2000°C.

Erosion Tests. Metallic peg walls and cooled electrodes of copper, stainless steel, and Monel were exposed to 2700°K gases at a velocity[26] of

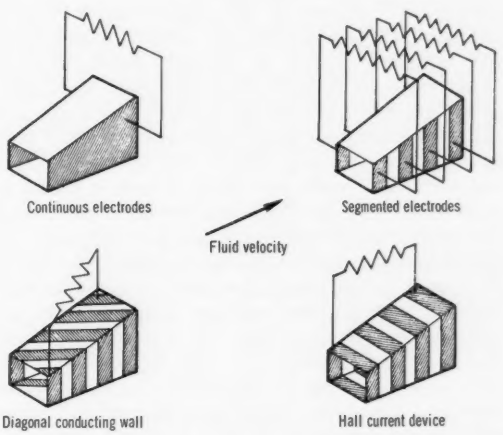

Fig. 3 Various MHD generator designs have been compared.[11]

650 m/sec for 1 to 1.5 hr. The electrode temperatures were maintained at ~1200°K. Monel exhibited the lowest erosion during these tests. Unusually large potential losses near the electrodes were observed.

Electron emission of refractory metallic electrodes of Nb, Mo, Ta, and W was investigated in argon and in mercury vapor seeded with cesium.[27] The electrodes were maintained at 1200°K, whereas the gases reached 2000°K. Current densities were ~10 amp/cm^2.

The electrical and thermal conductivities and the hemispheric emissivity of niobium, molybdenum, and tantalum were measured[28] in the range 1300 to 3000°K. The total hemispheric and monochromatic emissivities of niobium and zirconium carbides as well as their electric conductivities were measured[29] up to 3500°K.

Component Design

Major design problems include high-intensity magnets and the development of preheaters that will raise air temperatures to ~1200°C prior to combustion.

Magnets. Successful MHD power-generation systems require high-intensity magnets of reasonable weight and cost. Developments in cryogenic and superconducting magnets hold considerable promise; in fact, the feasibility of superconducting magnets for MHD applications has been amply demonstrated by the construction of a magnet that produces a field of 4 tesla in a 12-in.-diameter bore.[30] Total weight of the 128-in.-long magnet is 16,000 lb, and it is maintained at 4.2°K. The superconducting material is Nb–Zr wire. Some aspects of transition in superconducting magnets were also investigated.[31]

Optimum Design. Optimization studies of magnet design were concerned with applications of cooled and uncooled resistive magnets, as well as permanent and cryogenic types[32] or, in more detail, with the design of ferritic core electromagnets for larger power plants.[33] In the first study, Faraday- and Hall-type generators were considered separately over wide ranges of power outputs (100 kw to 1000 Mw) and duration (1 msec to 1 year). A field of 8 tesla is considered to be the upper limit for MHD generators and, from the strength viewpoint, for aluminum and superconductor materials in the windings. The major conclusion is that liquid-hydrogen-cooled aluminum magnets offer greatest cost and weight savings, except for very large power and very long duration. The aluminum magnets can compete with superconductors while cooled to only 20°K by pool boiling of hydrogen. Representative system costs for Faraday generators[32] are shown in Fig. 4. In the study concerned with ferritic core magnets, it is found that, in the range of 2 to 3.5 tesla intensity in the gap, minimum costs dictate a current density of 3.2 to 4×10^6 amp/m^2, which compares with present practice in electrical machines.

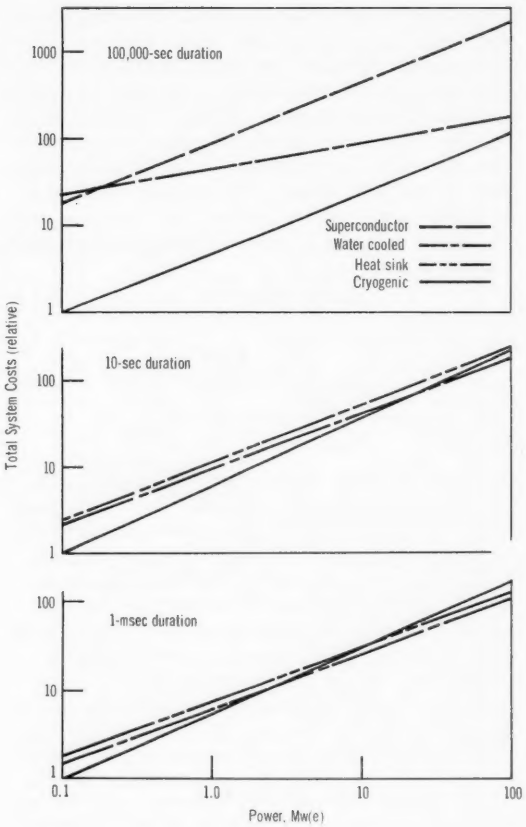

Fig. 4 Faraday generator system costs increase with power level and duration.[32]

AIR PREHEATERS AND HEAT EXCHANGERS

Air used in MHD combustion chambers should be preheated to at least 1200°C to eliminate the need for oxygen enrichment, particularly if the fuel is a heavy (residual) oil or coal. Exhaust gases leave the MHD generator typically at 2500°K; the regenerative enthalpy recovery is further complicated by the extremely corrosive nature of the seed materials, which may be expected to leave the generator as carbonates or sulfates (depending on the nature of the fuel). These salts of alkali metals condense at ~1900°K and solidify at ~1200°K.

In a discussion of the design of heat exchangers and seed-recovery systems,[34] the need has been stressed for very complete seed recovery, a problem common to both open- and closed-cycle installations. The enormous requirements for air at high

temperature and pressure are without precedent. Other heat-exchanger design problems and operating experiences were described,[12,35,36] as was the development of a combustion chamber with convection-cooled walls.[37]

Basic Studies of Combustion Plasma

The equilibrium thermodynamic properties of potassium-seeded plasmas generated by the combustion of methane or fuel oil in air were calculated[38] in the range 1000 to 4000°K. The results are summarized in the form of an enthalpy–entropy diagram and another that gives the composition of the seeded combustion products. The composition and thermodynamic properties of oxides and carbonates of potassium and cesium were also investigated.[39]

RADIANT HEAT

Thermal radiation of the combustion products of kerosene with enriched air was studied[40] over a range of 2100 to 2700°K that resulted from various degrees of oxygen enrichment. At pressures of 1 and 10 atm and a gas velocity of 800 m/sec in channels of up to 8 cm in diameter, the radiant heat loss represents a small fraction of the convective heat loss from the plasma. Another paper[41] reports an experimental determination of radiant heat losses from a potassium carbonate-seeded plasma at ~3000°K.

ELECTRICAL CONDUCTIVITY

The electrical conductivities of seeded, thermally ionized plasma and of nonequilibrium ionized plasma have been investigated[42] with a radio-frequency technique intended to minimize electrode boundary-layer losses. Of considerable interest is the high degree of electrically induced nonthermal ionization in the combustion chamber, which results in a high electrical conductivity of the combustion products. This conductivity is actually reduced by the addition of seeding materials. These measurements were confined to temperatures below 2400°K. These results, particularly concerning the effect of seed addition, were confirmed and enlarged by an extensive study of chemically induced ionization in combustion chambers.[43] Electron concentrations of $10^{13}/cm^3$ have been attained, whereas $10^{14}/cm^3$ appears necessary for MHD power-generation applications.

The effect of adding barium and calcium oxides to methane and coal flames was studied[44] at temperatures up to 2500°K. Significant increases in conductivity were observed with low additive concentrations.

Prospects for Open-Cycle MHD

In surveying the papers discussing the future of open-cycle MHD and the statements of the panelists, one would conclude that development proceeds in the direction of MHD–steam power plants of combined output in excess of 1000 Mw and overall thermal efficiency of 50 to 55%. Oil firing, or possibly coal firing, and air preheating in preference to oxygen enrichment are generally indicated. Numerous economic optimization and design studies[45–53] support this conclusion.

Near-term developments include the completion of various experimental installations, the continuation of analytical studies, and the development of novel ideas proposed at the symposium.

NEW EXPERIMENTAL INSTALLATIONS

Among the planned experimental installations is a 300-Mw(t)-input plant in Great Britain[54] with water-cooled duct walls and magnet; the magnet provides a field of up to 4 tesla. The generator will be fired by fuel oil with up to 25% potassium sulfate addition (combustion takes place in oxygen). Periods of operation up to 20 min are envisaged initially.

In final stages of construction is a 24-Mw(t)-input generator in Japan.[55] The generator is designed for basic studies of MHD characteristics; the magnet is the iron-core type and provides a field of 3 to 5 tesla with a peak power consumption of 1.2 Mw. The generator uses the products of combustion of light fuel oil and oxygen with potassium hydroxide solution as the seed material. Short periods of operation are contemplated.

A 2-Mw(t)-input experimental generator is starting operation in Poland.[56] Its salient features are a low-temperature heat exchanger and a high-temperature separately fired pebble-bed air preheater. It will provide experimental data to be used in the design of larger power-station experiments.

In final construction stages in the United States is a Hall generator designed to operate[57] at values of the Hall parameter as high as 6. The generator has an iron-core magnet that will provide a field of up to 2.7 tesla. It is planned to replace this later by a superconducting magnet that will provide a field of up to 5 tesla. The combustion of a liquid fuel in oxygen, with some nitrogen dilution, provides a working fluid at a maximum temperature of 2900°K.

ANALYTICAL STUDIES

A proposal to produce in the working fluid alternating zones of low and high conductivity (low and high temperature) has prompted three analytical studies of striated flow and its application to MHD power generation. Apart from providing a fluctuating output, the scheme offers some advantages from the viewpoint of thermal demands on the construction materials. The studies were concerned with the overall performance of a cycle of 1000-Mw output[58] and maximum temperatures up to 3200°K, with the general study of an induction generator using striated

flow[59] and with the effects of turbulent diffusion and Rayleigh–Taylor instability on the performance of striated-flow generators.[60] In addition, a study of the stability of the interface between the hot and cold zones is presented;[59] it indicates that there exists a region in which stable operation is possible. An experimental study of the Rayleigh–Taylor instability is also presented.[60]

The effects of the electrical conductivity varying sinusoidally in time were studied analytically,[61] as was the operation of a pulsating-flow MHD generator in which the working fluid is alternately compressed by a driver shock and then expanded.[62] To generate a-c power, it is proposed[63] to direct slugs of alternately hot and cold fluid into one of two series-connected channels (Fig. 5) by using the Coanda effect. Developments with fluid amplifiers have demonstrated the feasibility of high-frequency oscillation of a fluid jet between two alternative passages.

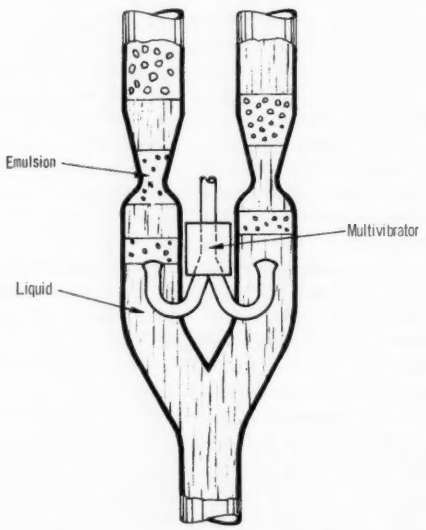

Fig. 5 High-frequency oscillation of a fluid jet between two alternative passages may lead to a-c power generation.[63]

An extensive analytical and experimental study of linear and vortex generators, using pressure pulsations to modulate the combustion of fuel and thereby the conductivity of the plasma, was presented.[64] An improvement was noted in power density owing to an increase in mean conductivity and particle velocity over those permissible in a continuous mode of operation.

NOVEL IDEAS

Two apparently novel ideas proposed at the symposium may lead to significant MHD developments. One of these deals with a vortex generator in which the main flow is continuously recycled through the generator.[65] Only a small fraction of this flow is discharged into the atmosphere and made up by supersonic injection of very hot gas from the heat source into the generator stream. Such a generator removes the need for electrode segmentation by short-circuiting the Hall electromotive force.

The other idea concerns the regeneration of the enthalpy from the exhaust of the MHD generator.[66] It is suggested that this enthalpy be stored in the form of chemical energy in the fuel by subjecting the latter to an endothermic reaction, possibly involving the oxidizer. In this manner the need for handling air or fuel at very high temperatures prior to entry into the combustion chamber may be removed, facilitating separation of seed material at the lower regeneration temperature.

* * *

The help of several members of the Staff at Argonne National Laboratory, and in particular of Michael Petrick, with the preparation of the manuscript of this paper and with the final editing is gratefully acknowledged.

References

All references except 1 to 5 are papers presented at the Symposium on Magnetohydrodynamic Electrical Power Generation, jointly organized by the International Atomic Energy Agency and the European Nuclear Energy Agency of the OECD and held in Salzburg, Austria, July 4–8, 1966. Volume I of the proceedings of this symposium, *Electricity from MHD*, is now available in the United States through the National Agency for International Publications, Inc., 319 E. 34th St., New York, N. Y. 10016.

1. Michael Petrick, Liquid-Metal MHD Topping Cycles, *Power Reactor Technol.*, 8(4): 199-209 (Fall 1965).
2. Michael Petrick, Recent Developments in Liquid-Metal MHD Systems, *Power Reactor Technol.*, 9(4): 187-193 (Fall 1966).
3. Proceedings of the Symposium on Magnetohydrodynamic Electrical Power Generation, Salzburg, Austria, July 4–8, 1966.
4. *Magnetohydrodynamic Electrical Power Generation*, Symposium Proceedings, Paris, July 1964, Vols. 1–4, European Nuclear Energy Agency, Organization for Economic Cooperation and Development, 1964.
5. *Magnetoplasmadynamic Electrical Power Generation*, Symposium Proceedings, Newcastle upon Tyne, England, September 1962, The Institution of Electrical Engineers, London, 1963.
6. A. C. Mattsson and T. R. Brogan, Self-Excited MHD Generators, Paper No. SM-74/168.
7. J. Teno, T. R. Brogan, and L. R. DiNanno, Hall Configuration MHD Generator Studies, Paper No. SM-74/50.
8. M. Yamamoto, T. Tamaoki, and Y. Saito, Experimental Studies of Oil-Fired MHD Power Generation, Paper No. SM-74/135.
9. K. G. Reseck, R. H. Eustic, and C. H. Kruger, MHD Generator Performance Prediction Including Two-Dimensional Effects and Wall Leakage, Paper No. SM-74/175.
10. P. Dubois, A. Dubois, and D. Parizot, Magnetoaero-

dynamic Conversion Test Rig with Subatmospheric Operating Conditions, Paper No. SM-74/145.
11. J. B. Dicks et al., An Experimental and Theoretical Comparison of the Performance of Diagonal Wall Generators, Faraday Generators and Hall Current Generators, Paper No. SM-74/169.
12. W. S. Brzozowski, Z. N. Celinski, and T. Kozlowski, Operating Experience of an Open Cycle MHD Test Facility, Paper No. SM-74/53.
13. E. P. Strashinin, N. I. Mazur, and V. V. Shtefan, Experimental Determination of Volt-Ampere Characteristics of an MHD Duct with Various Electrodes, Paper No. SM-74/209.
14. E. I. Yantovsky, Experimental Investigation of Ionized Gas Flows in Ducts, Paper No. SM-74/253.
15. E. P. Strashinin et al., Experiments with an MHD Generator, Paper No. SM-74/206.
16. W. S. Brzozowski, J. Fiszdon, and W. Gauk, Study of Electrodes in an MHD Generator, Paper No. SM-74/62.
17. A. M. Anthony and M. Foex, Insulators and Conductors for MHD Flow, Paper No. SM-74/67.
18. A. Nagahiro et al., Preparation and Test of MHD Duct Wall and Electrode Materials, Paper No. SM-74/130.
19. D. Yerouchalmi, Testing of Materials and Structures Forming a 200 kw Experimental Duct for Open-Cycle MHD Conversion, Paper No. SM-74/144.
20. A. I. Rekov, A. I. Romanov, and A. B. Ivanov, Processes of Interaction Between Refractory Materials and Gas Flows in the Duct of an MHD Generator, Paper No. SM-74/228.
21. J. Péricart and D. Yerouchalmi, Behaviour of Electrodes with Electrically-Conducting Ceramic Frontal Faces on the Renardières 8 Mw Test Rig, Paper No. SM-74/63.
22. A. Dubois and J. Péricart, Design and Testing of Electrodes for MHD Converters, Paper No. SM-74/65.
23. M. Guillou and J. Millet, Electrochemical Criteria for Selecting MHD Electrode Materials: Research on Electronically-Conducting Zirconium Oxide, Paper No. SM-74/77.
24. A. Dubois et al., Investigation and Tests on Ceramic Materials for Magnetoaerodynamic Conversion Duct Electrodes, Paper No. SM-74/150.
25. J. Elston, Z. Mihailovic, and M. Roux, Study of the Electrical Properties of Sintered Zirconium Products and Lanthanum Chromite at High Temperatures, with a View to Their Utilization as MHD Electrodes, Paper No. SM-74/152.
26. J. Heurtin and A. deMontardy, Behaviour of Metal Electrodes in an Open-Cycle MHD Duct, Paper No. SM-74/79.
27. V. T. Karpukhin and A. D. Muzychenko, Investigation of High-Melting Metal Electrodes for MHD Generators with Non-Equilibrium Conductivity, Paper No. SM-74/92.
28. D. L. Timrot, V. E. Peletsky, and V. Yu. Voskresensky, Experimental Investigation of the Integral 2π Emissivity, Electrical Conductivity and Thermal Conductivity Coefficient for a Number of High-Melting Metals in the Temperature Range, 1300–3000°K, Paper No. SM-74/224.
29. V. A. Petrov, V. Ya. Chekhovskoy, and A. E. Sheindlin, Experimental Determination of the Electrical Resistance, and the Integral 2π and Monochromatic Emissivity ($\lambda = 0.65\ \mu m$) of Niobium and Zirconium Carbides, Paper No. SM-74/230.
30. A. Kantrowitz, Z. J. Stekly, and A. M. Hatch, A Model MHD Type Superconducting Magnet, Paper No. SM-74/256.
31. V. V. Sychev, V. B. Zenkevich, and V. V. Andrianov, Transient Processes in Superconducting Magnetic Systems, Paper No. SM-74/229.
32. R. R. Barthelemy and C. E. Oberly, Optimum Magnets for MHD Generators, Paper No. SM-74/167.
33. J. Senk, A Method of Optimizing the Electromagnet of a D.C. MHD Generator, Paper No. SM-74/83.
34. British MHD Collaborative Research Committee, Some Mechanical Engineering Aspects of MHD Power Generation, Paper No. SM-74/43.
35. J. Aptel, Recovery of Residual Enthalpy of Gases at the Outlet of an MHD Duct, Paper No. SM-74/117.
36. F. Hals and L. Keefe, A High Temperature Regenerative Air Preheated for MHD Power Plants, Paper No. SM-74/68.
37. J. Schneller and J. Vampola, Some Problems Concerning High Temperature Equipment for Open-Circuit MHD Generators, Paper No. SM-74/82.
38. V. S. Yungman, L. V. Gurvich, and N. P. Rtishcheva, Composition and Thermodynamic Properties of the Seeded Combustion Products of Natural Fuels, Paper No. SM-74/217.
39. A. V. Gusarov and L. N. Gorokhov, Mass-Spectrometric Investigation of Gaseous Compounds of Alkali Metals, Paper No. SM-74/233.
40. X. Nguyen Duc and A. Lemarquand, Radiation of Flames Used in MHD, Paper No. SM-74/84.
41. H. Wittel, Wall Losses by Radiation in an Oil-Fired MHD Generator, Paper No. SM-74/109.
42. H. Milde and H. Gallant, Electrodeless Conductivity Measurements Within the Reaction Zone of a Combustion Chamber, Paper No. SM-74/21.
43. J. Poncelet, G. Harris, and L. Lozano, Prospects for the Utilization of Chemical Ionization Phenomena in MHD, Paper No. SM-74/122.
44. V. A. Popov, E. P. Zimin, and Z. G. Mikhnevich, Investigation of Ionization and Conductivity of Combustion Products in the Presence of Solid Particles with a Low Electron Work Function, Paper No. SM-74/243.
45. M. Rosner, The Oil-Fired MHD Power Plant, Paper No. SM-74/28.
46. Z. Jedrzejowski and S. Andrezejewski, Study of Cycle Diagrams of Power Plants with MHD Generators, Paper No. SM-74/54.
47. R. Gebel, Optimization of Open Cycle MHD Power Plants, Paper No. SM-74/112.
48. T. C. Tsu, W. E. Young, and S. Way, Optimization Studies of MHD-Steam Plants, Paper No. SM-74/179.
49. V. A. Kirillin and A. E. Sheindlin, Some Problems of the Operation of MHD Generator Plants, Paper No. SM-74/221.
50. G. Dinelli and M. Massé, Effect of Various Parameters on the Efficiency of the MHD Power Stations, Paper No. SM-74/75.
51. G. I. Rossievsky et al., Effectiveness of Oxygen Enrichment of Air in MHD Generator Facilities, Paper No. SM-74/201.
52. G. I. Rossievsky, B. Ya. Shumyatsky, and E. K. Vinokurov, Effect of the Size of Electric Power Stations with MHD Generators on Their Thermal Efficiency, Paper No. SM-74/204.
53. G. M. Shchegolev, Thermodynamic Features of High-Temperature Open Cycles, Paper No. SM-74/235.
54. British MHD Collaborative Research Committee, A Large Experimental Combustion-Fired Generator, Paper No. SM-74/44.
55. F. Mori, K. Fushimi, and M. Yamamoto, An MHD Power Generator—E.T.L. Mark II, Paper No. SM-74/133.
56. W. S. Brzozowski et al., An Open-Cycle Power Generation Experiment with High Preheat Temperature for the Air, Paper No. SM-74/57.
57. R. R. Barthelemy, B. G. Stephan, and R. F. Cooper, Experimental Evaluation of MHD Generators Operating at High Hall Coefficients, Paper No. SM-74/166.
58. C. Karr, M. LaPorte, and R. Porte, Estimation of the Efficiency of an Inhomogeneous-Flow MHD Generator, Paper No. SM-74/114.
59. J. Milewski, Striated Flow in the Induction Synchronous Magnetogasdynamic Generator, Paper No. SM-74/58.
60. R. Devime et al., Evaluation of Rayleigh-Taylor In-

stability and Turbulent Diffusion Effects in Inhomogeneous Flow Conversion, Paper No. SM-74/80.
61. L. G. Bezusy, Electrical Parameters of the Synchronous MHD Generator with Pulsating Electrical Conductivity of the Medium, Paper No. SM-74/210.
62. E. Brocher and J. L. Chevalley, An A.C. MHD Generator with Pulsating Flow in a Preheated Gas, Paper No. SM-74/118.
63. C. Pavlin and L. Pascual, Application of Fluid Switching to MHD Energy Conversion, Paper No. SM-74/66.
64. V. J. Ibberson and D. Harris, Non-Steady Modulated MHD Systems, Paper No. SM-74/73.
65. J. C. de Simone, G. Klein, and P. Dubois, "Carrousel" Magnetoaerodynamic Generator, Paper No. SM-74/147.
66. J. Carasse, Chemical Recovery of Energy in a Combined MHD/Steam Power Station, Paper No. SM-74/156.

Two-Phase Compressibility Phenomena and How They Affect Reactor Safety

By Hans K. Fauske

How rapidly can two-phase coolant flow from a channel? And how fast can pressure disturbances propagate in flowing liquid–vapor mixtures? Answers to these fundamental questions about compressible fluids are important to reactor safety design. This article examines the relations between compressible fluids and reactor safety, reviews our knowledge of critical flow and acoustic velocity in liquid–vapor mixtures, and then summarizes the spotty (Table 1) state of the art.

Table 1 STATUS OF DATA ON CRITICAL FLOW AND ACOUSTIC VELOCITY IN TWO-PHASE COMPRESSIBLE MIXTURES

Two-phase fluid	Critical flow		Acoustic velocity	
	Nonmetallic	Metallic	Nonmetallic	Metallic
Low quality, <50%	Few data	No data	Few data; none for rarefaction waves	No data
High quality, 50 to 100%	Fair data; correlation is conceivable	No data	Few data	No data

Relation to Safety

The design of containment and emergency cooling systems that can withstand the transient and maximum pressure buildups arising from loss-of-coolant accidents requires an understanding of two-phase flow.[1] For example, if a break in the primary coolant system of a pressurized- or boiling-water reactor occurs, pressures and temperatures throughout the reactor and containment will change, and the barriers and emergency cooling systems must operate properly.

The maximum escape rate of reactor coolant affects the maximum pressure buildup in the containment building and determines the time in which emergency cooling systems must begin operation to prevent fuel melting. Blowdown rate is further related to liquid–vapor action in the reactor vessel which determines the core heat-transfer environment and the transient forces on vessel internals. Furthermore, the high-pressure water system (reactor vessel) may experience a rapid decompression following a break in the primary loop.[2] To describe the possible serious effects of this decompression on reactor internals, one must have an understanding of the propagation of pressure disturbances in single-phase and two-phase mixtures.

Critical-flow and acoustic effects must also be accounted for in analyses that attempt to describe accurately liquid-metal-coolant flow behavior in a fast reactor during a power excursion or loss-of-cooling accident.[3–5] Occurrence of critical flow in the core will lead to detrimental effects, such as voidage of the coolant channel, shocks, and pressure buildup. Because shocks will cause subsonic velocities, the critical or maximum flow rate will dictate the expulsion velocity and hence the void distribution in the coolant channel. Void distribution is most important in sodium-cooled fast reactors because of its effect on the rate of insertion of reactivity.[5] The possible sequence of events in accidents that may occur in a fast reactor and how coolant dynamics affect fast reactor safety have been summarized.[6]

Critical Flow

The phenomena of gas–liquid flow have received special study in recent years; included in these studies is critical flow, which is also sometimes referred to as maximum, choking, or sonic flow.[7] Most of these efforts have concerned one- and two-component nonmetallic fluids; recent data sources are summarized in Table 2. No experimental data exist for critical flow of liquid metals.

CRITICAL-FLOW MODELS

Several models have been proposed. The first analytical model to appear in the literature was the

Table 2 RECENT CRITICAL-FLOW INVESTIGATIONS

References	Critical pressure, psia	Exit quality or stagnation enthalpy, Btu/lb	Test fluid	Flow system and diameter, in.
Isbin et al.[8]	4 to 43	0.01 to 1.0	Water	Annuli and pipes, 0.37 to 1.0
Faletti and Moulton[10]	26 to 106	0.001 to 1.0	Water	Annuli, 0.2 and 0.39
Fauske[21]	40 to 360	0.01 to 0.7	Water	Pipes, 0.27 and 0.125
Zaloudek[11]	40 to 110	0.004 to 0.99	Water	Pipes, 0.52
James[22]	14 to 64	230 to 1200	Water	Pipes, 3, 6, and 8
Fauske[23]	100 to 1100	300 to 670	Water	Pipes, 0.249
Zaloudek[24]	23 to 87	500 to 1000	Water	Pipe elbow and tee, 0.625
Klingebiel[13]	25 to 60	140 to 1000	Water	0.504
Fauske[14]	17	0.0006 to 1.0	Air–Water	0.25 to 0.5

homogeneous thermal-equilibrium model HEM[8] that implied equal velocities and thermal equilibrium between the liquid and vapor phases. The critical flow rate was obtained from the same equation as in single-phase flow[9]

$$G^2 = -\frac{g_c}{(dv/dp)_s} \tag{1}$$

where the specific volume for homogeneous flow is

$$v_H = v_g x + v_l (1 - x) \tag{2}$$

Although predicted values of G_{HEM} are generally much lower than the measured flow rates, $G_{\mathrm{exp.}}$, they have been used frequently to correlate the data.[8,10,11] Failure of the homogeneous equilibrium model to predict the data resulted initially in an introduction into the literature of such terms as slip and metastability. The effects of these phenomena increased the predicted flow rates and brought them into closer agreement with experimental values.

More recently, several empirical and analytical models have appeared in the literature. All these analyses assure thermal equilibrium and separated flow (annular flow pattern); each phase is represented by a single average velocity. The combination of a momentum balance (negligible friction and head losses),

$$G^2 = -\frac{g_c}{(dv^*/dp)_s} \tag{3}$$

where

$$v^* = \frac{v_g x^2}{\alpha} + \frac{v_l (1 - x)^2}{1 - \alpha} \tag{4}$$

a total energy balance,

$$G^2 = -\frac{2 g_c J}{(dv'^2/dh)_s} \tag{5}$$

where

$$v'^2 = \frac{x^3 v_g^2}{\alpha^2} + \frac{v_l^2 (1 - x)^3}{(1 - \alpha)^2} \tag{6}$$

or a mechanical energy balance,

$$G^2 = -\frac{2 g_c v_H}{dv'^2/dp} \tag{7}$$

with an empirical or analytical relation for void fraction (α) or velocity ratio ($k = u_g/u_l$) results in several flow models, as summarized in Table 3.

Table 3 RECENT CRITICAL-FLOW MODELS

References	Equations used	Void or velocity ratio relation used
Isbin et al.[8]	3, 4	Modified Martinelli–Nelson
Massena[25]	3, 4	Modified Armand
Fauske[21]	3, 4	$k = (v_g/v_l)^{1/2}$
Levy[26]	3, 4	Momentum exchange model
Ryley,[27] Moody,[28] Zivi[29]	5, 6	$k = (v_g/v_l)^{1/3}$
Cruver and Moulton[30]	3, 4, 6, 7	$k = (v_g/v_l)^{1/3}$

The models referenced in Table 3 predict experimental data listed in Table 2 to within 20% for qualities above 1%. Data below 1% quality are few and indicate larger deviations from predicted values. The 1% quality range is particularly important in fast reactor safety analyses where the initial formation of void and its behavior must be predicted. One of the models listed in Table 3 has been used to evaluate liquid-metal flow rates.[12]

APPLICATION TO LIQUID-METAL SYSTEMS

Despite relatively good agreement between models and data, the models are open to serious criticism: (1) they are unable to explain clearly why two-phase choking occurs, and (2) their physical formulism deviates significantly from recent experimental observations.[13,14] Measured velocity ratios are considerably smaller than those used in the analytical models, and the assumption of thermal equilibrium applied in the models appears to be invalid. Use of high velocity ratios apparently compensates for metastability effects that have been neglected in the models. Consequently application of these models to liquid-metal systems could give erroneous results and therefore must await experimental verification.

Extrapolating Steam–Water Data. In the high-quality region (50 to 100%), a considerably better basic understanding of the two-phase critical-flow phenomenon has become available for steam–water mixtures,[15] and a more realistic extrapolation to other fluids is believed possible. Considerations include the rate of momentum, mass, and heat transfer between the vapor and liquid in the approach region to critical flow. Figure 1 illustrates the ability of this method to predict steam–water data in the high-quality region. Also depicted in Fig. 1 is the range of predicted values from the models listed in Table 3.

Experiments Under Way. Critical-flow experiments with water, and others with sodium, are in progress at Argonne National Laboratory.[16] The water experiment concentrates primarily on measuring local conditions (void and quality) in the approach region to critical flow using low-quality mixtures; to test existing steam–water correlations, the sodium test measures overall quantities such as flow rate, pressure profile, and stagnation conditions.

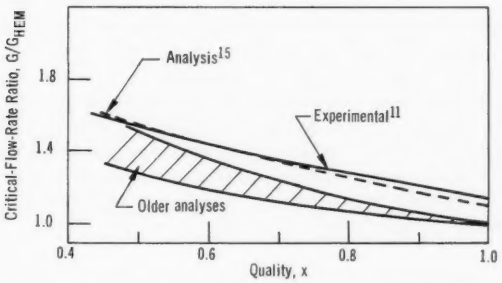

Fig. 1 Comparison between calculated and experimental critical-flow rates at 40 psia shows improved ability to predict steam–water performance.[15] Older predictions were obtained with models listed in Table 3.

Velocity of Sound

Considerably less effort has been devoted to pressure-wave propagation, i.e., to sonic velocities, in two-phase mixtures. Only three experimental studies on the velocity of sound are available for steam–water mixtures,[17–19] and no data exist for liquid-metal systems. Further, for low-quality one-component mixtures, only the propagation velocity of compression waves has been measured.[17,18] No information exists for rarefaction waves, which are particularly interesting in connection with propagation of depressurization waves caused by a vessel fracture or pipe failure.

The experimental data in Fig. 2 illustrate the low sonic velocity that occurs in a steam–water mixture and its dependence on void fraction.[18] (Note that models predict lower-than-actual velocities.) However, in the high-quality region (10 to 100%), the velocity of sound appears to be independent of quality and equal to that in pure vapor.[19]

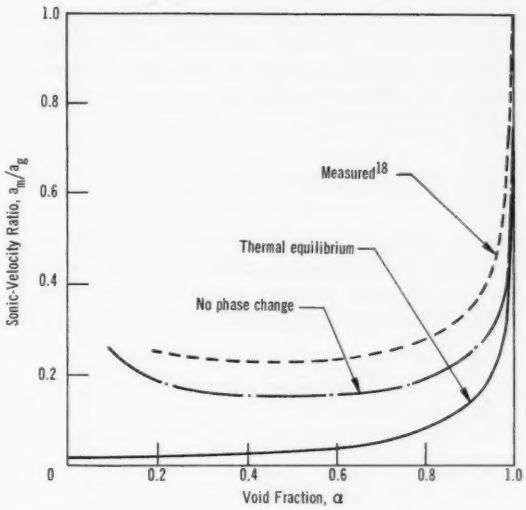

Fig. 2 Comparison of measured and calculated sonic velocity[18] in steam–water mixtures at 142 psia.

VELOCITY-OF-SOUND MODELS

Analytical derivations of the velocity of sound have been limited to the case where the two-phase fluid is assumed to behave as a homogeneous mixture with no slip between the phases.[6,17,18,20] This assumption leads to an expression for the sonic speed in a two-phase mixture similar to single-phase flow,[3]

$$a^2 = \frac{v^2}{(dv/dp)_s} \tag{8}$$

where v is given by Eq. 2.

Two limiting cases in which the mixture of liquid and its vapor may respond to a pressure disturbance have been calculated from Eq. 8: (1) no transfer of mass between phases (no phase change, constant quality), liquid and vapor behaving independently isentropic, leading to

$$\left(\frac{dv}{dp}\right)_s = (1-x)\left(\frac{dv_l}{dp}\right)_s + x\left(\frac{dv_g}{dp}\right)_s \tag{9}$$

and (2) mass transfer between the phases according to thermal equilibrium, liquid and vapor on the saturation line, leading to

$$\left(\frac{dv}{dp}\right)_s = (1-x)\left(\frac{dv_l}{dp}\right)_{\text{sat.}} + x\left(\frac{dv_g}{dp}\right)_{\text{sat.}} + (V_g - v_l)\left(\frac{dx}{dp}\right)_s \tag{10}$$

Equations 8 to 10 result in two widely different values for the velocity of sound, as is illustrated in Fig. 3. The sonic velocity is plotted as a function of the void fraction α, which is related to the quality x, according to

$$\alpha = \frac{x v_g}{v_g x + v_l (1-x)} \tag{11}$$

Figure 2 shows the same two solutions displayed to illustrate the deviations from measured steam–water data when thermal equilibrium is assumed during the passage of the pressure wave. Reemphasis

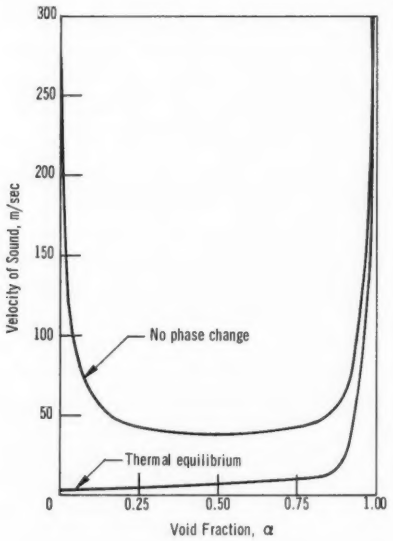

Fig. 3 Sound velocity in sodium two-phase mixture at 1000°C as a function of void fraction is predicted to have different values, depending on how mixture is assumed to respond to pressure disturbance.[5]

that the data in Fig. 2 represent the speed of propagation to compression waves seems important. Thermodynamic considerations indicate that a compression wave may travel without phase change (i.e., without evaporation or condensation) to agree with experimental observation (Fig. 2); however, a rarefaction wave may follow closer to an equilibrium cycle.[20] If we assume no phase change in Fig. 2 data, the observed differences between measured and calculated values appear to be caused by slip between the phases. Further, the magnitude of the slip and the degree of phase change seen by the pressure wave are probably related to the frequency of the pressure disturbance because mass, heat, and momentum transfer between phases require finite equilibration times. Therefore sonic velocity is normally a thermodynamic property in single-phase flow but becomes transport-process dependent in a two-phase mixture. Consequently the behavior of nonmetallic fluids may differ significantly from that of metallic fluids. Thus a basic understanding is required before extrapolations can be made from one fluid to another.

Conclusions

Spotty data and a rather primitive understanding of the behavior of two-phase mixtures limit the precision of analyses of thermal and fast reactors. We need more knowledge of critical flow and the velocity of sound. In particular:

There are few detailed data for two-phase critical flow of nonmetallic fluids in the low-quality region, especially with respect to metastability and the occurrence of slip between the phases.

Only the high-quality region (50 to 100%) of nonmetallic fluids appears fairly well understood, at least for steam–water mixtures at $p < 100$ psia. Data for higher pressures are not available. However, existing data may lead to safe predictions in metallic fluids.

Data are not available for critical flow of metallic fluids. However, these data are required in tests of existing correlations of steam–water mixtures.

Data are few on the velocity of sound and pressure-wave propagation in two-phase nonmetallic fluids; for the low-quality region, only compression-wave data are available, and none are available for the speed of propagation of rarefaction waves.

No data exist for the velocity of sound in two-phase metallic fluids.

Symbols

a = sonic velocity
g_c = Newton's constant
G = mass flow rate
h = specific enthalpy
J = mechanical equivalent of heat
k = velocity ratio, u_g/u_l
p = pressure
u = velocity
v, v^*, or v' = specific volume
x = quality, weight fraction of vapor or gas
α = void fraction of vapor or gas

Subscripts

c = critical
exp. = experimentally measured
g = gas or vapor
H = homogeneous
HEM = homogeneous thermal-equilibrium model
l = liquid
m = mixture
s = isentropic
sat. = saturation line

References

1. H. S. Isbin et al., Critical Flow Phenomena in Two-Phase Mixtures and Their Relationships to Nuclear Safety, in *Proceedings of the Third International Conference on the Peaceful Uses of Atomic Energy, Geneva, 1964*, Vol. 8, pp. 286-293, United Nations, New York, 1965.
2. R. P. Rose, Studies of Acoustic Effects in Reactor System Blowdown, *Trans. Amer. Nucl. Soc.*, 9(2): 558 (October–November 1966).
3. Argonne National Laboratory, Reactor Development Program Progress Report, October 1965, USAEC Report ANL-7115, p. 78, Nov. 23, 1965.
4. G. Friz, Coolant-Ejection Studies with Analogy Experiments, in Safety, Fuels, and Core Design in Large Fast Power Reactors, Conference Proceedings, Argonne, Ill., 1965, USAEC Report ANL-7120, p. 890, Argonne National Laboratory, 1966.
5. M. Fischer and W. Häfele, Shock Front Condition in Two-Phase Flow Including the Case of Desuperheat, in Safety, Fuels, and Core Design in Large Fast Power Reactors, Conference Proceedings, Argonne, Ill., 1965, USAEC Report ANL-7120, p. 895, Argonne National Laboratory, 1966.
6. R. M. Singer, How Coolant Dynamics Affect Fast Reactor Safety, *Power Reactor Technol.*, 9(1): 46-50 (Winter 1965–1966).
7. H. K. Fauske, What's New in Two-Phase Flow, *Power Reactor Technol.*, 9(1): 35 (Winter 1965–1966).
8. H. S. Isbin, J. E. Moy, and A. J. DaCruz, Two-Phase, Steam-Water Critical Flow, *A.I.Ch.E. (Amer. Inst. Chem. Eng.) J.*, 3(3): 361 (September 1957).
9. A. H. Shapiro, *The Dynamics and Thermodynamics of Compressible Fluid Flow*, Vol. II, The Ronald Press Company, New York, 1953.
10. D. W. Faletti and R. W. Moulton, Two-Phase Critical Flow of Steam-Water Mixtures, *A.I.Ch.E. (Amer. Inst. Chem. Eng.) J.*, 9(2): 247 (March 1963).
11. F. R. Zaloudek, The Low Pressure Critical Discharge of Steam-Water Mixtures from Pipes, USAEC Report HW-68934(Rev.), Hanford Atomic Products Operations, March 1961.
12. H. K. Fauske, Two-Phase Critical Flow with Applications to Liquid-Metal Systems (Mercury, Cesium, Rubidium, Potassium, Sodium, and Lithium), USAEC Report ANL-6779, Argonne National Laboratory, October 1963.
13. W. J. Klingebiel, Critical Flow Slip Ratios of Steam-Water Mixtures, Ph. D. Thesis, University of Washington, Seattle, Wash., 1964.
14. H. K. Fauske, Two-Phase Two- and One-Component Critical Flow, in *Proceedings of Symposion on Two-Phase Flow*, University of Exeter, Devon, England, Vol. 3, p. SG101, 1965.
15. H. K. Fauske, Critical Flow and the Velocity of Sound in Two-Phase One-Component Droplet Flow, presented at the 16th Canadian Chemical Engineering Conference of the Chemical Institute of Canada, Windsor, Ont., October 1966.
16. Argonne National Laboratory, Reactor Development Program Progress Report, December 1966, USAEC Report ANL-7286, p. 66, Jan. 26, 1967.
17. H. B. Karplus, Propagation of Pressure Waves in a Mixture of Water and Steam, USAEC Report ARF-4132-12, Armour Research Foundation, January 1961.
18. N. I. Semonov and S. I. Kosterin, Results of Studying the Speed of Sound in Moving Gas-Liquid Systems, *Teploenergetika*, 11(6): 59 (1964).
19. R. E. Collingham and J. C. Firey, Velocity of Sound Measurements in Wet Steam, *Ind. Eng. Chem., Process Design Develop.*, 2(3): 197-202 (July 1963).
20. A. L. Davies, The Speed of Sound in Mixtures of Water and Steam, British Report AEEW-M-452, October 1965.
21. H. K. Fauske, Critical Two-Phase, Steam-Water Flows, in *Proceedings of Heat Transfer and Fluid Mechanics Institute*, pp. 79-89, Stanford University Press, Stanford, Calif., 1961.
22. R. James, Steam-Water Critical Flow Through Pipes, *Proc. Inst. Mech. Eng.(London)*, 176: 741 (1962).
23. H. K. Fauske, The Discharge of Saturated Water Through Tubes, in *Heat Transfer*, Chemical Engineering Progress Symposium Series, No. 61, pp. 210-216, American Institute of Chemical Engineers, New York, 1965.
24. R. F. Zaloudek, The Low-Pressure Critical Discharge of Steam-Water Mixtures from Pipe Elbows and Tees, USAEC Report BNWL-34, Battelle–Northwest, March 1965.
25. W. A. Massena, Steam-Water Critical Flow Using the "Separated Flow Model," USAEC Report HW-65739, Hanford Atomic Products Operation, June 20, 1960.
26. S. Levy, Prediction of Two-Phase Critical Flow Rate, *J. Heat Transfer*, 87: 53 (1965).
27. D. J. Ryley, The Flow of Wet Steam, *Engineer*, 193: 363 (March 1952).
28. F. J. Moody, Maximum Flow Rate of a Single Component, Two-Phase Mixture, *J. Heat Transfer*, 87: 134 (1965).
29. S. M. Zivi, Estimation of Steady-State Steam Void Fraction by Means of the Principle of Minimum Entropy Production, *J. Heat Transfer*, 86: 247 (1964).
30. J. E. Cruver and R. W. Moulton, Critical Flow of Liquid-Vapor Mixtures, Preprint 29*e*, American Institute of Chemical Engineers 55th National Meeting, Houston, Tex., 1965.

Operational Data for Power Reactors in the United States

By Barbara A. Schmeh

Thermal and electrical generating statistics for U. S. power reactors through 1966 are summarized[1,2] in Tables 1 to 3 and in Figs. 1 to 39. Included are essentially all reactor facilities that have directly affected development programs concerned with central-station power.

Table 1 provides data on annual and total electrical generation, reactor availability, and plant capacity factor (the latter is defined as percent of power the plant did produce as compared with what it would have produced if it operated full time at full power). Table 2 summarizes the principal milestones achieved by central-station plants, and Table 3 lists past and projected nuclear electrical generating capacities.[3]

The charts show cumulative thermal power generated by 15 utility central-station reactors (Figs. 1 to 15), 9 experimental reactors (Figs. 16 to 24), 10 reactor experiments (Figs. 25 to 32), and 7 military remote-station power reactors (Figs. 33 to 39). The causes of shutdowns of 5 days or more, which are indicated by numbers on the curves, are explained in the captions. Although the figures do not provide detailed operating information, they do summarize plant operations for a wide variety of reactors.

The data themselves are of interest to reactor designers and operators. However, as a previous article[4] pointed out, interpretation and application of these data to predict improvements or trends for other plants require an understanding of the design and operational goals of the particular plants involved.

Utility Reactors: 1966 Highlights

More than 57 reactors figured prominently in U. S. utility plans during 1966. Noteworthy highlights of activities on these major central-station nuclear power plants have been summarized.[5]

15 PLANTS OPERABLE

During 1966, 15 utility reactors were considered to be operable. Activities with each of these during the year are described here.

Shippingport, which continued to operate on the second core, is providing data on long-life fuel elements, a new physics concept, and new control-rod concepts.

Indian Point Unit 1 achieved criticality March 27 with the low-enrichment uranium oxide core of modified design, which replaced the original highly enriched uranium oxide and thorium oxide core. The plant reached full power, including oil-fired superheating of steam, in May and then operated on a normal load-following basis.

Dresden Unit 1 operated normally, except that some cracks were detected in small-diameter piping early in the year; the cause is unknown. The cracked pipe sections were removed, tested, and replaced. Refueling was scheduled for January 1967.

Yankee (Rowe) achieved 6 billion kw-hr net cumulative electrical generation on August 27. Refueling started October 4 with Core 6. The plant returned to power operation on November 7.

Hallam, which shut down on Sept. 27, 1964, because of moderator-can failures, remained shut down. On May 24, 1966, the Atomic Energy Commission (AEC) was notified that Consumers would not exercise its option to purchase the AEC-owned portion of the sodium–graphite reactor facility. Then work began to dismantle the plant and render the premises radiation safe by the end of 1967.

Fermi began a stepwise approach to full power, which proceeded satisfactorily until October 5, when the reactor was shut down following a malfunction presumed to involve fuel damage. Fuel-pin warping is evident in at least one assembly. Investigations are in progress to determine the extent of damage and the remedial action required to put the facility back in operation.

Elk River shut down on April 15 for refueling, maintenance, and thorough inspection to determine status and future serviceability of the control rods and the pressure vessel. Minor repairs were made to the control rods. The reactor was started up on July 9 with one-third of Core 2 in place; by July 13 the reactor was at full power. The reactor was shut down from August 27 until September 14 so that leaking evaporator tubes could be plugged. Then operation continued at or near full power.

Piqua operation was adversely affected when extensive deposits of carbonaceous material in the moderator regions of the core were encountered in mid-January. The entire core was unloaded and examined. The carbonaceous deposits, which caused fuel-element control-rod binding, were removed and the reactor vessel and systems were being flushed at year end. New slightly modified fuel elements will be loaded into the core, and the plant will be returned to service in 1967.

Pathfinder began a stepwise approach to power early in June; the plant produced its first electricity on July 25. Full-power operation is scheduled to be reached in 1967.

Carolinas–Virginia Tube Reactor operated satisfactorily at full power from May 1964 to Mar. 8, 1966, when stress–corrosion cracks were found in the stainless-steel pipes and vessels of an auxiliary system. The first refueling was carried out in April concurrently with repair work. The reactor resumed power operation May 13. It was shut down from August 26 to October 3 for partial refueling. The reactor was shut down October 27 for removal of a defective fuel assembly; subsequent operation was intermittent and a second defective element was found and removed. Power operation resumed in mid-December.

Humboldt Bay operated satisfactorily at reduced power to extend life of the core until late November, when the reactor was shut down, as scheduled, to refuel half of the core with Zircaloy-clad fuel. Power operation was scheduled to be resumed in early 1967.

BONUS began a 6-month extended load test at full power on January 13. The testing had passed the 50% mark when buildup of hydrogen was discovered in the housings for the control-rod-drive mechanism. Thus the reactor was shut down April 10 so that a vent system could be installed to purge the accumulated gases and prevent their future buildup. Operating responsibility for the reactor was transferred to the Puerto Rico Water Resources Authority on July 8, and full-term operating authorization was issued. The reactor again achieved full 50-Mw(t) power on October 14.

Peach Bottom Unit 1 achieved initial criticality on March 3. After the reactor completed low-power tests, it was shut down in May to await the full-power operating permit and so that the steam generators and other equipment could be repaired and modified. That work and plant check-out prior to rise-to-power were completed. Authorization was granted for power operation of the reactor to begin in January 1967.

Big Rock Point reactor power was reduced in mid-February to minimize radioactivity in the off-gas system. The reactor operated satisfactorily at less than full power until April 9, when it was shut down for the first partial refueling (30%). Beginning May 8, the facility began production of ^{60}Co in addition to power. The cobalt production is a joint venture of Consumers Power Co. and Neutron Products, Inc. The reactor was shut down from September 17 until October 20 for the second partial refueling with Zircaloy-clad vibratorily compacted UO_2 fuel. Power operation was delayed until November 9 because of control-rod-drive problems.

N-Reactor (New Production Reactor) began initial electric-power production on April 8, and full gross power of 800 Mw(e) was achieved on December 10. A high-voltage transformer failed on December 10, and at year end the output was being held to 400 Mw(e).

10 PLANTS UNDER CONSTRUCTION

At the end of 1966, nine utility reactors were under construction and one was on the verge of operation. Startup plans are reported.

San Onofre construction was completed in November. Initial criticality was scheduled to be achieved early in 1967. The delay from the originally scheduled December 1966 criticality is attributed to deliberateness in the startup program and nonnuclear operational problems.

La Crosse construction completion and start of fuel loading were scheduled for early 1967. The additional delay is occasioned by the need to repair leaking seal welds on control-rod-drive nozzle flanges.

Connecticut Yankee construction is more than 80% complete and is proceeding essentially on schedule. Fuel loading was scheduled to start about mid-1967.

Oyster Creek construction is more than 40% complete. Initial criticality is expected by early 1968, with start of commercial operation scheduled for several months later.

Nine Mile Point construction is about 50% complete. The reactor is scheduled to go critical by mid-1968 and to reach full power by late 1968.

Dresden Unit 2 construction is scheduled to be completed by the fall of 1968. Criticality is scheduled to be attained by the end of 1968.

Millstone construction is scheduled to be essentially completed by early 1969. Initial criticality is scheduled for April 1969, with start of commercial operation in August 1969. A public hearing was held by the Atomic Safety and Licensing Board on April 21 and 22; a provisional construction permit was issued on May 19, 1966.

(Text continues on page 39.)

Table 1 OPERATIONAL DATA FOR U. S. NUCLEAR POWER PLANTS[1,2]

Plant, power, dates		Electricity generated, Mw-hr (gross)	Reactor availability, hr	Plant capacity factor, %
Utility Stations				
Shippingport Atomic	1957–1959	388,536	11,650	
Power Station,	1960	268,096	5,900	
Shippingport, Pa.	1961	351,902	7,000	
90 Mw(e) net	1962	369,266	7,700	
critical 12/2/57	1963	395,400	7,800	
electricity 12/18/57	1964	25,400	900	
	1965	363,100	4,256	
	1966	587,270	8,400	67.0
		2,748,970 (9,726,401 thermal)	53,606	
Dresden 1 Nuclear	1959–1960	275,611	3,872.8	22.9
Power Station,	1961	555,141	3,520.2	33
Morris, Ill.	1962	1,249,602	7,061.5	74.3
200 Mw(e) net	1963	989,721	7,070.8	53.8
critical 10/15/57	1964	1,037,511	7,264.9	56.2
electricity 4/15/60	1965	1,018,344	7,268.9	55.4
	1966	1,474,832	8,513.0	80.2
		6,600,762 (21,311,788 thermal)	44,572.1	
Yankee Atomic Power	1960	38,885	1,198	25
Station,	1961	922,463	7,627	76
Rowe, Mass.	1962	740,124	5,923	55
175 Mw(e) net	1963	1,004,088	6,913	69
critical 8/19/60	1964	1,257,556	7,973	79.8
electricity 11/10/60	1965	1,027,725	6,635	64.6
	1966	1,371,620	7,847	85.8
		6,362,461 (20,844,039 thermal)	44,116	
Indian Point 1 Nuclear	1962	78,790	2,179	27.7
Power Station,	1963	953,900	6,258	38
Indian Point, N. Y.	1964	625,560	4,246	24.6
265* Mw(e) net	1965	1,145,510	5,611	46.4
critical 8/2/62	1966	1,227,785	5,912	50.3
electricity 9/16/62		4,031,545 (8,820,598 thermal)	24,206	
Big Rock Point Nuclear	1962	43		
Power Plant,	1963	130,351	4,201	35.3
Big Rock Point, Mich.	1964	203,633	3,758	42.2
72.8 Mw(e) net	1965	190,722	2,661	29.03
critical 9/27/62		363,306	6,567	55.3
electricity 12/8/62		888,055 (2,767,241 thermal)	17,187	
Enrico Fermi Atomic	1963–1965			
Power Plant,	1966	1,000	5,800	
Lagoona Beach, Mich.		(20,354 thermal)		
60.9 Mw(e) net				
critical 8/23/63				
electricity 8/5/66				
Peach Bottom Atomic	1966		5,152	
Power Station,		(7.49 thermal)		
Peach Bottom, Pa.				
40 Mw(e) net				
critical 3/3/66				
electricity 1/27/67				
Experimental Reactors				
EBWR,	1956–1959	35,006		
Argonne, Ill.	1960	197		
4000 kw(e) net	1961	355		
critical 12/1/56	1962	4,138		
electricity 12/29/56	1963–1965			
	1966	5,519		
		45,215 (344,782 thermal)		
VBWR,	1957–1959	25,183	9,170	
Pleasanton, Calif.	1960	204	840	
5000 kw(e) net	1961	6,519	3,700	
critical 8/3/57	1962	8,264	3,400	
electricity 10/20/57	1963	14,259	4,400	
		54,429 (389,852 thermal)	21,510	
SRE,	1957–1959	15,311	4,080	
Santa Susana, Calif.	1960			
7500 kw(e) net	1961	864	1,944	
critical 4/25/57	1962	2,217	2,064	
electricity 7/12/57	1963	16,737	6,264	
	1964	2,045	1,053	
		37,174 (162,800 thermal)	15,405	
OMRE,	1957–1963			
NRTS, Idaho		(71,208 thermal)		
12 Mw(t) net				
critical 9/17/57				

Humboldt Bay Power	1963	176,025	2,982	77.8
Plant, Humboldt Bay,	1964	380,222	7,811	83.3
Calif.	1965	272,064	7,005	59.9
68.5 Mw(e) net	1966	166,404	7,784	36.5
critical 2/16/63		994,715	25,582	
electricity 4/18/63		(3,318,758 thermal)		
Hallam Nuclear Power	1962			
Facility,	1963	85,939	2,327	26.5
Hallam, Nebr.	1964	106,519	3,943	45.0
75 Mw(e) net	1965			
critical 8/25/62	1966			
electricity 5/29/63		192,458	6,270	
terminated 5/24/66		(638,712 thermal)		
Elk River Reactor,	1962–1963	757		
Elk River, Minn.	1964	59,354	3,428	33
22* Mw(e) net	1965	151,010	6,885	75
critical 11/19/62	1966	135,367	6,127	66.1
electricity 8/24/63		(867,739 thermal)	16,440	
Piqua Nuclear Power	1963	1,163	1,132	
Facility,†	1964	39,626	6,139	36
Piqua, Ohio	1965	27,917	5,940	25.5
11.4 Mw(e) net		1,895	302	1.7
critical 6/10/63		70,601	13,513	
electricity 11/4/63		(256,729 thermal)		
CVTR,	1963	12		
Parr, S. C.	1964	43,985	5,092	66.2
17* Mw(e) net	1965	80,852	7,340	70.7
critical 3/30/63	1966	78,631	6,216	51.3
electricity 12/18/63		203,480	18,648	
		(826,172 thermal)		
BONUS, Punta Higuera,	1964	1		
Puerto Rico	1965	18,065	1,530	20.5
17 Mw(e) net	1966	37,799	3,164	26.0
critical 4/13/64		55,865	4,694	
electricity 8/14/64		(219,348 thermal)		
N-Reactor,	1963–1965			
Richland, Wash.	1966	1,012,000	4,880	41.0
786 Mw(e) net		(11,970,000 thermal)		
critical 12/31/63				
electricity 4/8/66				
Pathfinder Atomic Power	1964–1965			
Plant,	1966	15,500		
Sioux Falls, S. D.		(108,900 thermal)		
58.5 Mw(e) net				
critical 3/24/64				
electricity 7/25/66				
PRTR,	1960–1966			
Richland, Wash.		(999,622 thermal)		
70 Mw(t)				
critical 11/20/60				
Saxton,	1962	205	258	
Saxton, Pa.	1963	16,613	6,389	
3000 Kw(e) net	1964	12,828	4,709	
critical 1/13/62	1965	4,636	1,938	
electricity 11/16/62	1966	23,193	5,981	58.8
		57,475	19,275	
		(340,085 thermal)		
HWCTR,	1962–1964			
Savannah River,		(333,190 thermal)	(9,262 total critical)	
Aiken, S. C.				
61 Mw(t) net				
critical 3/3/62				
EBR-2,	1963			
NRTS, Idaho	1964	3,459	1,227	
16,500 kw(e) net	1965	29,553	1,530	
critical 11/11/63	1966	44,311	4,578	
electricity 8/7/64		77,323	7,335	
		(293,892 thermal)		
EVESR,	1963–1964		3,884	
Pleasanton, Calif.	1965	15,505	5,200	
5 Mw(e) net	1966	9,694	6,764	58
critical 11/25/63		25,199	15,848	
electricity 1/27/65		(159,643 thermal)		

Reactor Experiments

EBR-1,	1951–1959	465	
NRTS, Idaho	1960	70	
500 kw(e) net	1961		
critical 12/1/56	1962	18	
electricity 12/29/56	1963	26	
		579	
		(7,705 thermal)	
HRE-1,	1952–1959	81	
Oak Ridge, Tenn.			
140 kw(e) net			
critical, 1952			
BORAX-2, 3	1954–1959	1,600	
NRTS, Idaho			
2400 kw(e) net			
critical (No. 3)			
6/9/55			

*Includes power generated with aid of thermal energy from oil-fired superheater—equivalent of 104 Mw(e) in the case of Indian Point 1, 6 Mw(e) for Elk River, and 2.5 Mw(e) for Carolinas–Virginia.

†Estimate based on 27.5% conversion factor—steam produced by reactor is sent to header to be used as process steam or for electrical generation.

(Table continues on the next page.)

Table 1 (Continued)

Plant, power, dates		Electricity generated, Mw-hr (gross)	Reactor availability, hr	Plant capacity factor, %
Reactor Experiments (Continued)				
BORAX-4,	1957–1959	800		
NRTS, Idaho				
2400 kw(e) net				
critical 12/56				
LAPRE-1,2,	1956–1959			
Los Alamos, N. Mex.		(52.8		
1–2 Mw(t)		thermal)		
critical 2/56				
and 2/59				
HRE-2,	1959	680		
Oak Ridge, Tenn.	1960	100		
140 kw(e) net	1961	120		
critical, 1957		900		
		(16,122		
		thermal)		
GCRE,	1960–1961			
NRTS, Idaho		(2,989		
2.2 Mw(t)		thermal)		
critical 2/23/60				
LAMPRE,	1961–1964			
Los Alamos, N. Mex.		(2,370		
1 Mw(t)		thermal)		
critical 4/3/61				
BORAX-5,	1962			
NRTS, Idaho	1963	100		
2500 kw(e) net	1964	463		
critical 9/12/62		563		
electricity 10/9/63		(7,799		
		thermal)		
MSRE,	1965–1966			
Oak Ridge, Tenn.		(14,033		
10 Mw(t) net		thermal)		
critical 6/1/65				
Military Stations				
SM-1,	1957–1959	23,180		
Ft. Belvoir, Va.	1960	6,359		
1750 kw(e) net	1961	4,167		
critical 4/8/57	1962	2,743		
electricity 4/15/57	1963	3,331		
	1964	1,869		
	1965	3,809		
	1966	3,513	4,545	20.1
		48,971		
		(263,791		
		thermal)		
SL-1,	1958–1959	806		
NRTS, Idaho	1960	1,131		
300 kw(e) net		1,937		
critical 8/12/58		(22,342		
electricity 10/9/58		thermal)		
PM-2A,	1960			
Camp Century, Greenland	1961	2,704		
1560 kw(e) net	1962	5,397		
critical 12/2/60	1963	3,361		
electricity 11/12/60		11,462		
		(83,500		
		thermal)		
PM-1	1962	1,662		
Sundance, Wyo.	1963	2,840		
1000 kw(e) net	1964	3,730		
critical 2/25/62	1965	5,823		
electricity 4/19/62	1966	5,719		65.3
		19,774		
		(172,338		
		thermal)		
SM-1A,	1962	6,220		
Ft. Greely, Alaska	1963	8,423		
1640 kw(e) net	1964	7,270		
critical 3/13/62	1965	6,858		
electricity 5/16/62	1966	9,226	7,002	52.7
		37,997		
		(324,436		
		thermal)		
PM-3A,	1962	2,336		
McMurdo, Antarctica	1963	4,667		
1500 kw(e) net	1964	3,240		
critical 3/3/62	1965	6,903		
electricity 7/9/62	1966	8,690	6,782	59.0
		25,836		
		(161,106		
		thermal)		
ML-1,	1961–1965			
NRTS, Idaho		(7,674		
300 kw(e) net		thermal)		
critical 3/30/61				

Table 2 SIGNIFICANT MILESTONES: U. S. CENTRAL-STATION NUCLEAR POWER PLANTS[3]

Station	Owner	Capacity, Mw(e) net	Reactor Type	Reactor Designer	Announcement	Contract awarded	Construction permit Applied	Construction permit Awarded	Initially critical	Electricity First	Electricity IDP*
Shippingport Atomic Power Station	Duquesne Light Co. and AEC	90	PWR	West.	10/53	7/53			12/2/57	12/18/57	12/57
Indian Point Nuclear Power Station, Unit 1	Consolidated Edison Co.	265†	PWR	B&W	2/55	2/55	3/55	5/56	8/2/62	9/16/62	1/63
Dresden Nuclear Power Station, Unit 1	Commonwealth Edison Co.	200	BWR	GE	4/55	7/55	3/55	5/56	10/15/59	4/15/60	6/60
Yankee Nuclear Power Station	Yankee Atomic Electric Co.	175	PWR	West.	4/55	6/56	7/56	11/57	8/19/60	11/10/60	1/61
Hallam Nuclear Power Facility	Consumers Public Power District and AEC	75	SGR	AI	4/55	9/57	9/57	7/60	8/25/62	5/29/63	7/63 [shut down 9/64]
Enrico Fermi Atomic Power Plant	Power Reactor Development Co.	60.9	FBR	PRDC	4/55	3/57	1/56	8/56	8/23/63	8/5/66	
Elk River Nuclear Plant	Rural Cooperative Power Association and AEC	22†	BWR	AC	2/56	6/58	6/58	12/59	11/19/62	8/24/63	2/64
Piqua Nuclear Power Facility	City of Piqua, Ohio, and AEC	11.4	OMR	AI	2/56	6/59	6/59	1/60	6/10/63	11/4/63	1/64
Pathfinder Atomic Power Plant	Northern States Power Co.	58.5	BWR	AC	2/57	5/57	3/59	5/60	3/24/64	7/25/66	1967
Carolinas–Virginia Tube Reactor	Carolinas–Virginia Nuclear Power Association, Inc.	17†	HWR	West.	8/57	1/59	7/59	5/60	3/30/63	12/18/63	9/65
Humboldt Bay Power Plant, Unit 3	Pacific Gas & Electric Co.	68.5	BWR	GE	2/58	2/58	4/59	11/60	2/16/63	4/18/63	5/63
Boiling Nuclear Superheat Power Station	Puerto Rico Water Resources Authority and AEC	16.5	BWR	Comb.	6/58	1/60	12/59	7/60	4/13/64	8/14/64	9/65
Peach Bottom Atomic Power Station, Unit 1	Philadelphia Electric Co.	40	HTGR	GA	11/58	11/58	7/60	2/62	3/3/66	1/27/67	5/67
Big Rock Point Nuclear Plant	Consumers Public Power Co. of Michigan	70.4	BWR	GE	12/59	12/59	1/60	5/60	9/27/62	12/8/62	3/63
San Onofre Nuclear Generating Station	Southern California Edison and San Diego Gas & Electric Co.	430	PWR	West.	4/60	1/63	2/63	3/64	(1967)‡		
La Crosse Boiling Water Reactor	Dairyland Power Cooperative and AEC	50	BWR	AC	4/61	6/62	11/62	3/63	(1967)		
N-Reactor	Washington Public Power Supply System and AEC	786	PWR	B&R	4/62	4/63			12/31/63	4/8/66	7/66
Malibu Nuclear Plant, Unit 1	Los Angeles Department of Water & Power	462	PWR	West.	11/62	1/63	11/63		(1972)		
Connecticut Yankee Atomic Power Plant	Connecticut Yankee Atomic Power Co.	462	PWR	West.	12/62	12/62	9/63	5/64	(1967)		
Oyster Creek Nuclear Power Plant, Unit 1	Jersey Central Power & Light Co.	515	BWR	GE	5/63	12/63	3/64	12/64	(1968)		
Nine Mile Point Nuclear Station	Niagara Mohawk Power Corp.	500	BWR	GE	7/63	10/63	3/64	4/65	(1968)		
Dresden Nuclear Power Station, Unit 2	Commonwealth Edison Co.	715	BWR	GE	2/65	2/65	4/65	1/66	(1968)		
Fort St. Vrain Power Station	Public Service Co. of Colorado	330	HTGR	GA	3/65	3/65	10/66		(1971)		
Millstone Nuclear Power Station	Millstone Point Co.	549.2	BWR	GE	4/65	9/65	11/65	5/66	(1969)		
Shoreham Atomic Power Station	Long Island Lighting Co.	500	BWR	GE	4/65	2/67			(1973)		
Pilgrim Station	Boston Edison Co.	620.6	BWR	GE	8/65	8/65			(1971)		
R. E. Ginna Nuclear Power Plant, Unit 1	Rochester Gas & Electric Co.	420	PWR	West.	8/65	8/65	10/65	4/66	(1969)		
Turkey Point Station, Unit 3	Florida Power & Light Co.	721.5	PWR	West.	11/65	11/65	3/66	4/67	(1970)		
Turkey Point Station, Unit 4	Florida Power & Light Co.	721.5	PWR	West.	11/65	11/65	3/66	4/67	(1971)		
Indian Point Nuclear Power Station, Unit 2	Consolidated Edison Co.	873	PWR	West.	11/65	11/65	12/65	10/66	(1969)		
Vermont Yankee Generating Station	Vermont Yankee Nuclear Power Corp.	513.9	BWR	GE	12/65	8/66	11/66		(1970)		
Bailey Point Station	Maine Yankee Atomic Power Corp.	800	PWR	Comb.	1/66	2/67			(1972)		
H. B. Robinson S. E. Plant, Unit 2	Carolina Power & Light Co.	663	PWR	West.	1/66	1/66	7/66	4/67	(1970)		
Dresden Nuclear Power Station, Unit 3	Commonwealth Edison Co.	715	BWR	GE	1/66	1/66	2/66	10/66	(1969)		
Palisades Nuclear Power Station	Consumers Power Co. of Michigan	700	PWR	Comb.	1/66	1/66	6/66	3/67	(1970)		
Point Beach Nuclear Plant, Unit 1	Wisconsin Michigan Power Co.	454.6	PWR	West.	2/66	2/66	9/66		(1970)		
Quad-Cities Station, Unit 1	Commonwealth Edison Co. and Iowa–Illinois Gas & Electric Co.	715	BWR	GE	4/66	4/66	5/66	2/67	(1970)		
Monticello Nuclear Generating Plant	Northern States Power Co.	471.7	BWR	GE	4/66	4/66	8/66		(1970)		

*Initial design power.

†Includes power generated with additional thermal energy from oil-fired superheaters— equivalent of 104 Mw(e) in the case of Indian Point 1, 6 Mw(e) for Elk River, and 2.5 Mw(e) for Carolinas–Virginia.

‡Dates in parentheses are the estimated dates of initial operation.

(Table continues on the next page.)

Table 2 (Continued)

Station	Owner	Capacity, Mw(e) net	Reactor		Announcement	Contract awarded	Construction permit		Initially critical	Electricity	
			Type	Designer			Applied	Awarded		First	IDP
Peach Bottom Atomic Power Station, Unit 2	Philadelphia Electric Co., PSE&GC, ACEC, and DP&LC	1065	BWR	GE	5/66	8/66	2/67		(1971)		
Peach Bottom Atomic Power Station, Unit 3	Philadelphia Electric Co., PSE&GC, ACEC, and DP&LC	1065	BWR	GE	5/66	8/66	2/67		(1972)		
Burlington Nuclear Generating Station, Unit 1	Public Service Electric & Gas Co., PEC, ACEC, and DP&LC	993	PWR	West.	5/66	8/66	12/66		(1971)		
Unit 2 (?)	Public Service Electric & Gas Co., PEC, ACEC, and DP&LC	993			5/66				(1974)		
Browns Ferry Nuclear Power Plant, Unit 1	Tennessee Valley Authority	1064.5	BWR	GE	6/66	6/66	7/66	5/67	(1970)		
Browns Ferry Nuclear Power Plant, Unit 2	Tennessee Valley Authority	1064.5	BWR	GE	6/66	6/66	7/66	5/67	(1971)		
Surry Power Station, Unit 1	Virginia Electric & Power Co.	783	PWR	West.	6/66	10/66	3/67		(1970)		
(Nebraska)	Consumers Public Power District and Iowa Power & Light Co.	800	BWR	GE	6/66	4/67			(1972)		
Fort Calhoun Station, Unit 1	Omaha Public Power District	450	PWR	Comb.	6/66	10/66	4/67		(1971)		
Oconee Nuclear Station, Unit 1	Duke Power Co.	874	PWR	B&W	7/66	7/66	11/66		(1971)		
Oconee Nuclear Station, Unit 2	Duke Power Co.	874	PWR	B&W	7/66	7/66	11/66		(1972)		
Quad-Cities Station, Unit 2	Commonwealth Edison Co. and Iowa–Illinois Gas & Electric Co.	715	BWR	GE	7/66	7/66	8/66	2/67	(1971)		
Bolsa Island Nuclear Power and Desalting Plant, Unit 1	MWD, LADWP, SCE, SDG&EC	800§			8/66				(1972)		
Bolsa Island Nuclear Power and Desalting Plant, Unit 2	MWD, LADWP, SCE, SDG&EC	800§			8/66				(1972)		
Diablo Canyon	Pacific Gas & Electric Co.	1060	PWR	West.	9/66	11/66	1/67		(1971)		
Surry Power Station, Unit 2	Virginia Electric & Power Co.	783	PWR	West.	10/66	10/66	3/67		(1972)		
Easton Nuclear Station	Niagara Mohawk Power Corp.	755	BWR	GE	10/66	10/66			(1971)		
Three Mile Island Nuclear Station	Metropolitan Edison Co.	831	PWR	B&W	11/66	11/66	5/67		(1971)		
Rancho Seco Nuclear Power Plant	Sacremento Municipal Utility District	700–800			11/66				(1973)		
(Michigan)	Indiana & Michigan Elec. Co. (Sub. of American Elec. Power Co.)	1100			12/66				(1972)		
(?)	New England Elec. Systems	800			12/66				(1973)		
Bailly Generating Station	Northern Indiana Public Service Co.	515	BWR	GE	1/67	1/67			(1972)		
Prairie Island Nuclear Plant	Northern States Power Co.	550	PWR	West.	2/67	2/67	4/67		(1972)		
(New Jersey)	Jersey Central Power & Light Co.	800	PWR	B&W	2/67	2/67			(1973)		
Trojan Station	Portland General Electric Co.	1000			2/67				(1975)		
(Illinois)	Commonwealth Edison Co.	1100	PWR	West.	2/67	2/67			(1972)		
(Illinois; option)	Commonwealth Edison Co.	1100	PWR	West.	2/67				(1973)		
Kewaunee Nuclear Station	Wisconsin Group (WPSC, WP&LC, MG&EC)	527	PWR	West.	2/67	2/67			(1972)		
Crystal River Plant, Unit 3	Florida Power Corp.	825	PWR	B&W	2/67	2/67			(1972)		
Point Beach Nuclear Plant, Unit 2	Wisconsin Michigan Power Co.	454.6	PWR	West.	2/67	2/67			(1971)		
(Washington)	Washington Public Power Supply System	1000			2/67				(1973)		
(New York)	New York State Electric & Gas Co.	750			3/67				(1973)		
(New Hampshire)	Public Service Co. of New Hampshire	800			3/67				(1975)		
(Arkansas)	Middle South Utilities Inc.	800–1000	PWR	B&W	4/67	4/67			(1972)		
Indian Point Nuclear Power Station, Unit 3	Consolidated Edison Co.	965	PWR	West.	4/67	4/67	4/67		(1971)		
Oconee Nuclear Station, Unit 3	Duke Power Co.	874	PWR	B&W	5/67	5/67	5/67		(1973)		
Susquehanna Nuclear Electric Station, Unit 1	Pennsylvania Power & Light Co.	800–1000			5/67				(1974)		

§Excluding desalting plant and related use amounting to ~160 Mw(e) for both units together.

Table 3 INSTALLED CAPACITY OF U. S. CENTRAL-STATION NUCLEAR POWER PLANTS[3]

Year of first electricity	Capacity, Mw(e) net	
	Added	Cumulative
1957	60	60
1958	0	60
1959	0	60
1960	321	381
1961	0	381
1962	322.8*	703.8
1963	209.4†	913.2
1964	39.1‡	952.3
1965	−45§	907.3
1966	933.9¶	1,841.2
1967	(982)	(2,823.2)
1968	(1,730)	(4,553.2)
1969	(2,557.2)	(7,110.4)
1970	(6,087.2)	(13,197.6)
1971	(10,899.2)	(24,096.8)
1972	(11,901)	(35,997.8)
1973	(6,574)	(42,571.8)
1974	(1,893)	(44,464.8)
1975	(1,800)	(46,264.8)

*Includes 20-Mw(e) uprating of Yankee [from 141 to 161 Mw(e)].

†Includes 20-Mw(e) uprating of Dresden 1 [from 180 to 200 Mw(e)] and 14-Mw(e) uprating of Yankee [from 161 to 175 Mw(e)].

‡Includes 22.6 Mw(e) uprating of Big Rock Point [from 47.8 to 70.4 Mw(e)].

§Includes shutdown of 75-Mw(e) Hallam reactor and 30-Mw(e) uprating of Shippingport [from 60 to 90 Mw(e); reactor also produces steam equivalent to 37 Mw(e)].

¶Includes 18.5-Mw(e) uprating of Humboldt Bay [from 50 to 68.5 Mw(e)] and 10-Mw(e) uprating of Indian Point 1 [from 255 to 265 Mw(e)].

Robert Emmett Ginna Unit 1 (formerly called Brookwood) construction is about 10% complete and on schedule. Initial criticality is scheduled for early 1969. A public hearing was held by the Atomic Safety and Licensing Board on April 5; the provisional construction permit was issued on Apr. 25, 1966.

Indian Point Unit 2 construction is about 15% complete. Construction completion and criticality are scheduled for the spring of 1969. A public hearing was held on September 14 and 15, and a provisional construction permit was issued on October 14.

Dresden Unit 3 reactor is scheduled to achieve initial criticality in late 1969. This unit is expected to be the last reactor addition at the Morris, Ill., site. A public hearing was held September 27 and 28; the provisional construction permit was issued on October 14.

16 PLANTS AWAITING CONSTRUCTION PERMITS

As of the end of 1966, applications for construction permits for 16 utility reactors were under review by AEC. Status of the plans for each plant are reported.

Malibu Unit 1 schedule calls for construction to be completed and full power to be attained early in 1972 and for commercial operation to begin in mid-1972. Issuance of the construction permit was awaiting formal Commission review at year end.

Fort St. Vrain proposed plant site is about 35 miles north of Denver. The preliminary design is nearing completion. Construction is scheduled to begin in early 1968. The plant is expected to be in service in late 1971 or early 1972.

Turkey Point Units 3 and 4 are to be located 25 miles south of Miami. The first nuclear unit is scheduled to go into operation during 1970; the second, about a year later.

Vermont Yankee plant is to be located on the Connecticut River at Vernon, Vt. It is expected to be ready for service in late 1970.

Palisades plant site is about 35 miles west of Kalamazoo on Lake Michigan. The plant is scheduled for operation by the spring of 1970.

(Text continues on page 57.)

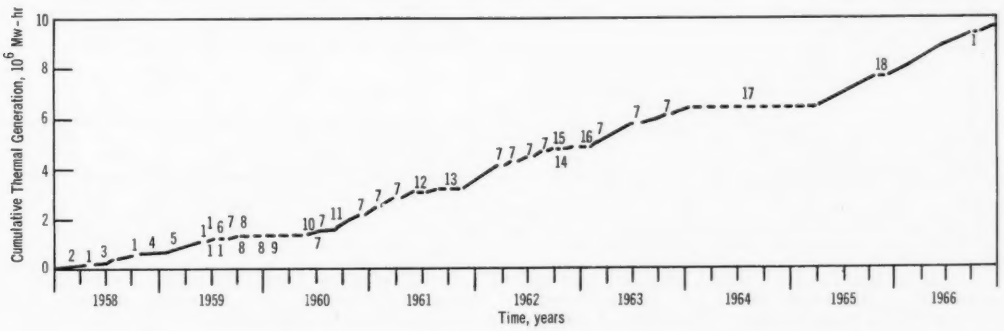

Fig. 1 Shippingport, a 505-Mw(t) uprated PWR, has produced ~2.7 million Mw-hr of electricity since December 1957. Major shutdowns had the following causes: 1, testing and training; routine maintenance. 2, steam-generator leak. 3, coolant-pump failure. 4, repair moisture separator. 5, repair turbine governor. 6, final reactivity-lifetime test; full-power run for Core 1, Seed 1. 7, low-power physics testing. 8, end of Seed 1 life; low-power runs and tests. 9, testing, training, and refueling; Core 1, Seed 1 replaced by Seed 2. 10, replace E-12 control drive mechanism. 11, return 1-B loop to service. 12, end Seed 2 life tests. 13, replace Seed 2 with Seed 3. 14, repair 1-B pilot valve. 15, end Seed 3 life; low-power runs and tests. 16, replace Seed 3 with Seed 4. 17, refueling; plant modifications. 18, periodic tests and minor modifications to control-rod-drive mechanisms.

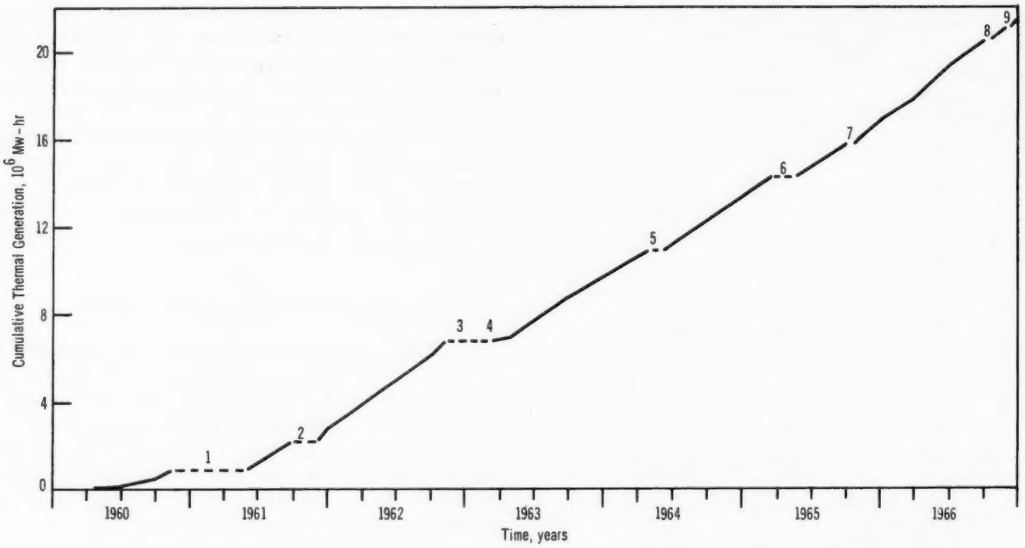

Fig. 2 Dresden, a 700-Mw(t) BWR, has produced ~6.6 million Mw-hr of electricity since April 1960. Major shutdowns had the following causes: 1, modify rod drive. 2, inspect 6 drives, 6 blades, and core support grid. 3, partial refueling; inspect 6 drives, 6 blades, core support grid, and turbine generator. 4, remove turbine test equipment; modify No. 3 gland drain piping on turbine. 5, refueling; maintenance; test reactor-enclosure leak rate. 6, partial refueling; overhaul turbine; test containment sphere. 7, repair high-pressure drain line. 8, locate primary-system leak; AEC operator licensing examinations. 9, repair throttle valve; test primary-containment overpressure for Dresden 2.

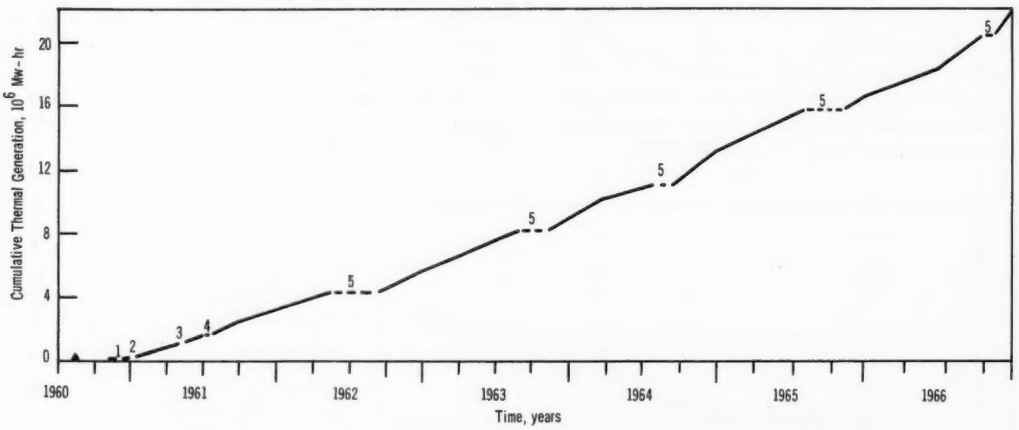

Fig. 3 Yankee, a 600-Mw(t) PWR, has produced ~6.3 million Mw-hr of electricity since November 1960. Major shutdowns had the following causes: 1, turbine shaft vibration. 2, modify turbine throttle valves. 3, repair turbine control valve. 4, license-required physics tests. 5, refueling.

H. B. Robinson Unit 2 construction is scheduled to be essentially completed early in 1970, with commercial operation to start about mid-1970.

Point Beach Unit 1 construction was scheduled to begin in early 1967 near Green Bay, 90 miles northeast of Milwaukee, and to be completed by the end of 1969. Initial criticality and commercial operation are expected by mid-1970.

Quad-Cities Unit 1 reactor is scheduled for initial criticality very late in 1969 or early in 1970.

Monticello plant, planned to be the first in the United States with a field-fabricated reactor pressure

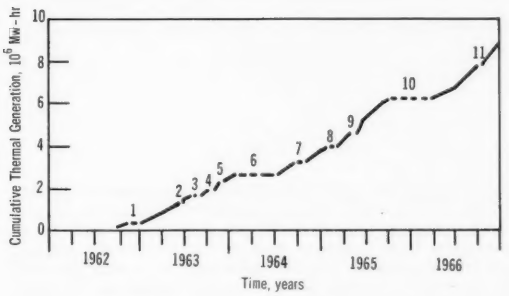

Fig. 4 Indian Point, a 615-Mw(t) PWR, has produced ~4.0 million Mw-hr of electricity since September 1962. Major shutdowns had the following causes: 1, modify conventional system and control-rod drive. 2, modify control-rod N_2 purge system. 3, repair primary-coolant pumps; replace microswitches in control-rod-drive assemblies. 4, install lining in transfer pool; repair primary-coolant pump; repair leak in No. 14 nuclear boiler. 5, repair steam-line crack. 6, complete stainless-steel lining of sphere fuel-transfer canal; gamma scan for power-distribution analysis of core. 7, repair tube leaks in 2 nuclear boilers; replace thermal barrier gaskets in 3 primary-coolant pumps. 8, repair No. 4 control-rod-drive line; repair tube leak in No. 11 nuclear boiler. 9, replace Nos. 14 and 16 control-rod-drive seal shaft pins; replace primary-loop relief valves in Nos. 11 and 12 loops. 10, refuel; maintenance on control-rod-drive mechanisms. 11, license-required tests; repair tube leaks in Nos. 12 and 14 nuclear boilers.

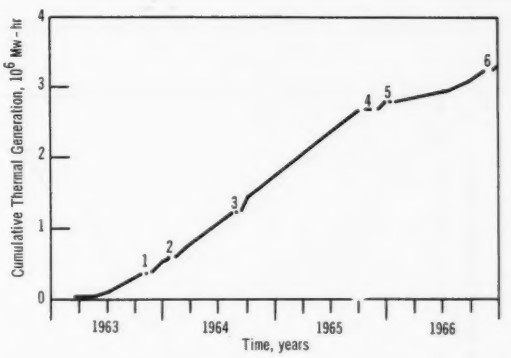

Fig. 6 Humboldt Bay, a 240-Mw(t) BWR, has produced 994,715 Mw-hr of electricity since December 1963. Major shutdowns had the following causes: 1, remachine reactor-vessel head to correct leakage. 2, correct turbine system leak; perform reactor protection system tests. 3, remove poison curtains and add new fuel to core; minor modifications; maintenance and routine operational tests. 4, refuel; modify containment systems for higher pressure capability; install additional emergency core cooling system; perform required maintenance and tests. 5, repair leakage from reactor emergency vent valves. 6, refuel; replace metal feedwater tube bundles; routine maintenance and tests.

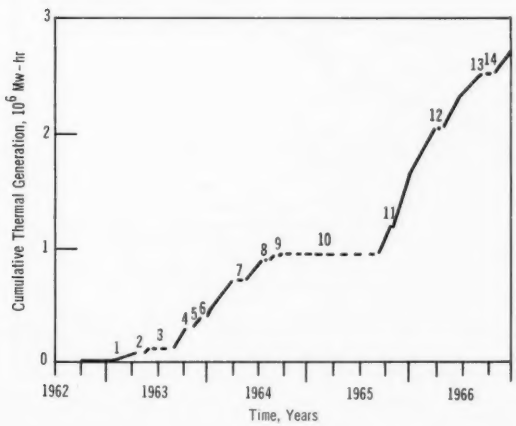

Fig. 5 Big Rock Point, a 240-Mw(t) BWR, has produced 888,055 Mw-hr of electricity since December 1962. Major shutdowns had the following causes: 1, modify control rod and fuel channel. 2, install equipment and fuel for R&D program. 3, modify core support system. 4, change from 800- to 1500-psia operation. 5, replace vessel O-ring. 6, increase core size from 56 to 74 bundles. 7, load reactor to 84 fuel bundles. 8, reload to 44 bundle core. 9, inspect core and reactor-vessel internals. 10, modify thermal-shield hold-down assembly and install new thermal-shield annular seal. 11, repair steam leaks under turbine; install modification kits in control-rod drives. 12, refuel; replace 14 fuel bundles; test containment leak rate. 13, refuel; replace 46 fuel bundles; install bypass for high-pressure feedwater heater and remove heater. 14, replace 78 bolts associated with grid-bar locking mechanism.

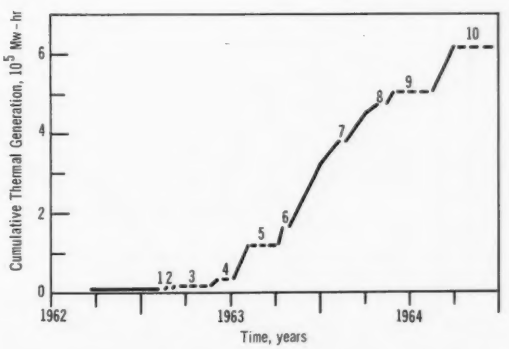

Fig. 7 Hallam, a 240-Mw(t) SGR, produced 192,458 Mw-hr of electricity. Major shutdowns had the following causes: 1, operator licensing; repair leak in steam dump facility. 2, scram tests; secondary sodium throttle valve maintenance. 3, regulatory checks and modifications to sodium pumps, throttle valve actuators, and intermediate heat exchanger. 4, replace 2 control-rod thimbles; repair secondary sodium pumps; install level probes in steam generator. 5, replace Zircaloy-2 thimbles with stainless steel; insert 10 UC elements; relocate 10 U–Mo elements. 6, repair primary sodium block valve drive train. 7, evaluate flux depression; repair leak in steam-generator superheater relief valve. 8, repair bellows seal valve. 9, verify core integrity following moderator-can failure; modify throttle valves and plant protective system. 10, replace failed moderator cans; operation terminated.

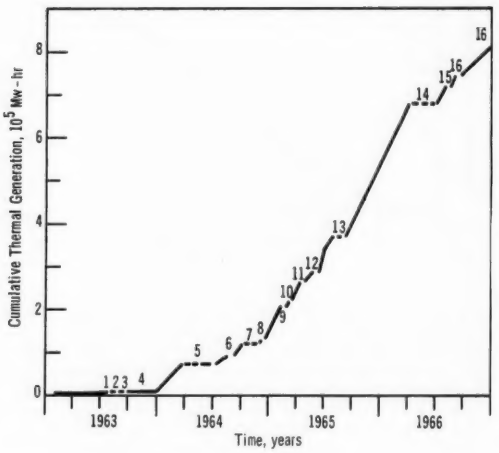

Fig. 8 Elk River, a 58.2-Mw(t) BWR, has produced 346,488 Mw-hr of electricity since August 1963. Major shutdowns had the following causes: 1, routine maintenance. 2, revise boric acid to pentaborate system. 3, investigate off-gas activity. 4, evaluate reactor problems. 5, revise primary piping; other modifications. 6, install additional air conditioning. 7, complete punch-list items; inspect control rods. 8, revise instrumentation. 9, replace center control rod. 10, repair turbine governor. 11, precautionary shutdown (plant-area flood conditions). 12, overhaul turbine generator; leak-test containment shell. 13, correct tube leaks in No. 1 evaporator. 14, refuel; inspect equipment; repair control rod and modify to four-rod scram system; convert superheater to burn multiple fossil-fuel combinations. 15, primary-system water quality problems. 16, repair evaporators; plug defective tubes.

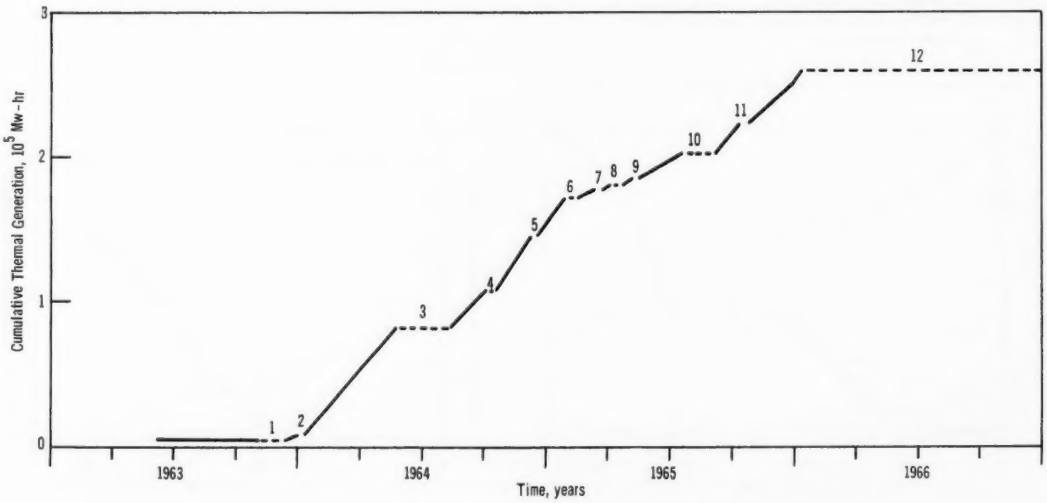

Fig. 9 Piqua, a 45.5-Mw(t) OMR, has produced 70,601 Mw-hr of electricity since November 1963. Major shutdowns had the following causes: 1, repair superheater leaks. 2, replace main pump impeller to reduce flow rates. 3, routine maintenance; fuel shuffling; repair superheater leak. 4, repair superheater leak. 5, remove and examine fuel element. 6, replace in-vessel filters; relocate an instrumented fuel element to core position of lower relative power. 7, test and evaluate anomalous reactivity behavior; calibrate control rods. 8, repair control-rod drives; modify core loading. 9, remove 3 instrumented fuel elements which had shown abnormal temperature rise. 10, modify control-rod drives; replace in-vessel filters; relocate fuel element; remove Charpy impact specimens for analysis; maintenance; 11, repair leaks in superheater; remove 3 elements which had shown abnormal temperature rise. 12, cleanup decomposed organic (coke) from core; modify to prevent future buildup of coke; extensive modification of control-rod electrical drive assemblies.

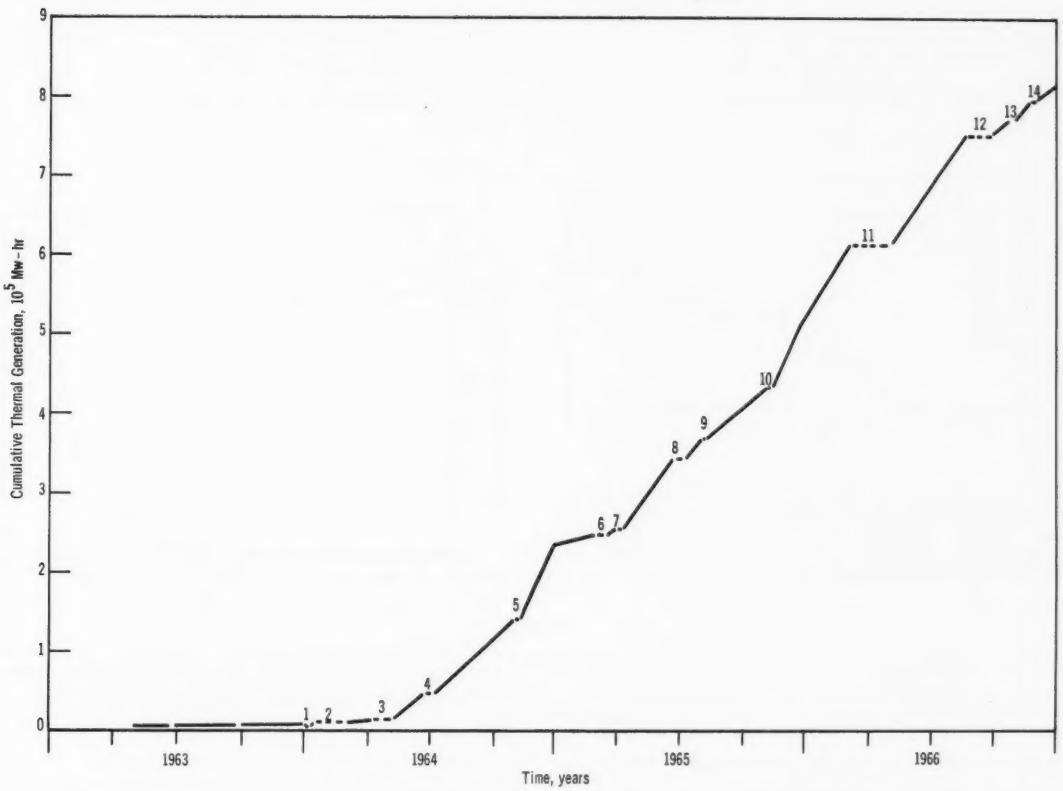

Fig. 10 CVTR, A 64-Mw(t) HWR, has produced 203,480 Mw-hr of electricity since December 1963. Major shutdowns had the following causes: 1, remove insulation from reactor-header cavity. 2, check refueling equipment; replace reactor-header insulation; check control-rod-drive systems. 3, test vapor container leak rate. 4, routine maintenance; prepare additional physics test work. 5, inspect control rods. 6, modify U-tube drying station; final refueling machine check; install radiation capsule. 7, replace rotating shield seal; modify rod-drive amplifiers; install TV in header cavity. 8, remove set of stationary control rods; physics testing. 9, modify control-rod drive. 10, physics testing. 11, first refueling; stress corrosion in sweep-gas system. 12, second refueling; test vapor container leak rate. 13, remove first leaking R&D fuel element. 14, remove second leaking R&D fuel element.

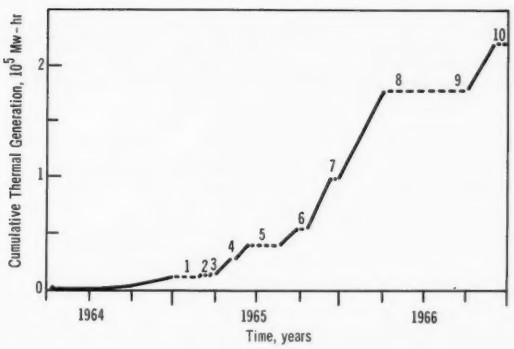

Fig. 11 BONUS, a 50-Mw(t) BWR, has produced 55,865 Mw-hr of electricity since August 1964. Major shutdowns had the following causes: 1, locate and remove failed fuel element. 2, water purification after admission of 3100 gal of nondemineralized water during scram recovery operation. 3, high total solids in reactor water. 4, disassemble minimum flow valve and activator to eliminate vibration. 5, load 8 superheater fuel elements to bring core to full 32 superheater-element capacity; repair cracks in preheater piping. 6, change control-rod actuator graphite bushings; fabricate and install new poppet guide on MFEV. 7, maintenance and modification before starting 6-month power-demonstration run. 8, modify control-rods rack housing; maintenance. 9, checks, maintenance, and modifications after reshimmed core criticality experiments. 10, remove vessel head; strong-back modification; routine plant maintenance.

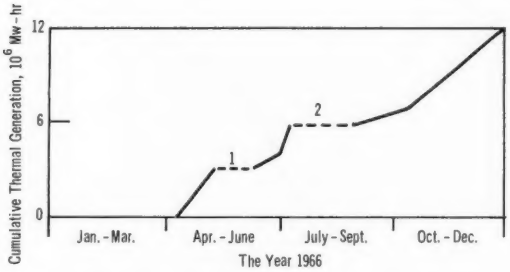

Fig. 12 N-Reactor, a 4000-Mw(t) PWR, has produced 1.0 million Mw-hr of electricity since April 1966. Major shutdowns had the following causes: 1, tie in sixth heat exchanger cell; preventive maintenance. 2, side effect of trades council strike at Richland.

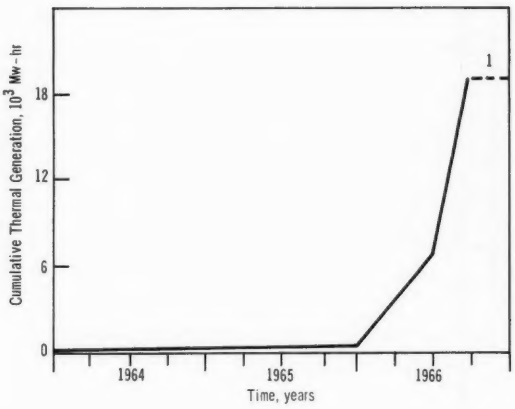

Fig. 14 Enrico Fermi, a 200-Mw(t) FBR, produced ~1000 Mw-hr of electricity during 1966, after 27 months of low-power testing. A fuel failure terminated operations.

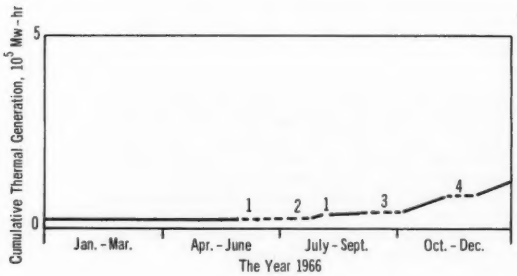

Fig. 13 Pathfinder, a 190-Mw(t) BWR, has produced ~15,500 Mw-hr of electricity since July 1966. Major shutdowns had the following causes: 1, routine maintenance. 2, measure steam-line isolation valve leakage; prepare for initial turbine operation. 3, investigate pressure-control-system problems; control-rod-drive maintenance; replace reactor source. 4, safety analysis of pressure-control system, protection against related potential loss of steam flow.

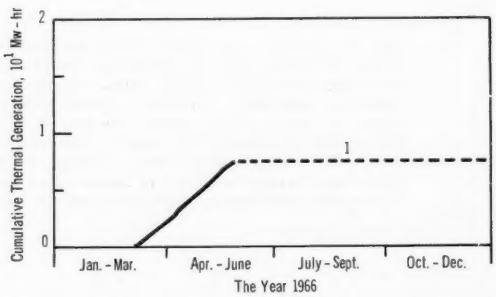

Fig. 15 Peach Bottom, a 115-Mw(t) HTGR, has produced ~7.49 thermal Mw-hr since March 1966. No electricity was generated in 1966. The major delay has been caused by the need for modification of steam generators and control-rod drives.

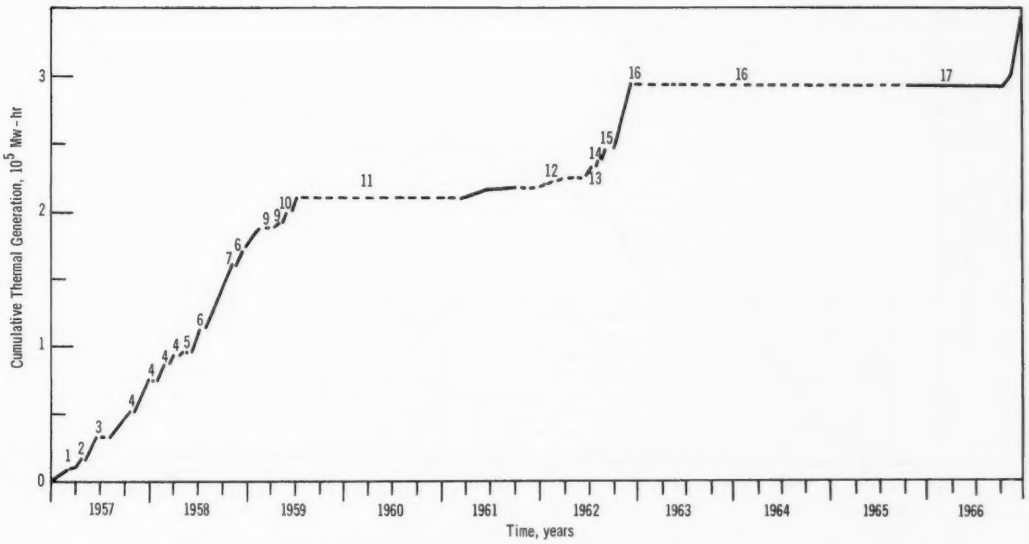

Fig. 16 EBWR, a 100-Mw(t) BWR, has produced 45,215 Mw-hr of electricity since December 1956. Major shutdowns had the following causes: 1, operator training. 2, routine maintenance. 3, modify for reactor-stability tests. 4, reactor stability tests. 5, turbine blade failure. 6, insert defective fuel sample for tests. 7, remove defective fuel sample. 8, routine maintenance; modify pressure vessel. 9, remove and examine fuel element. 10, install core shroud. 11, modify to 100-Mw(t) capacity. 12, modification before 100-Mw(t) tests. 13, test primary reboiler and containment. 14, high pressure in intermediate reboiler. 15, remove boron strips to increase reactivity. 16, program completion; modify for plutonium-recycle program. 17, critical studies for plutonium zone and fully loaded core.

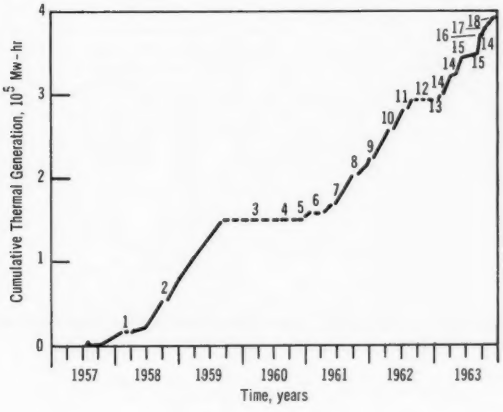

Fig. 17 VBWR, a 33-Mw(t) BWR, produced 54,429 Mw-hr of electricity. Major shutdowns had the following causes: 1, install recirculation pump; replace control rods. 2, inspect main turbine. 3, test control-rod drive; modify plant; load Core 2. 4, repair control rod and core channel. 5, install orifices and zinc channels. 6, replace 17-4 PH parts in vessel. 7, repair steam generator. 8, modify to provide superheat loop penetration of reactor. 9, install superheat loop and rod block system. 10, install and check ESADA. 11, replace pump motor. 12, repair recirculation piping. 13, locate failed fuel; install turbine driver for recirculation pump. 14, locate failed fuel. 15, routine maintenance. 16, rearrange core. 17, routine shutdown. 18, deactivation.

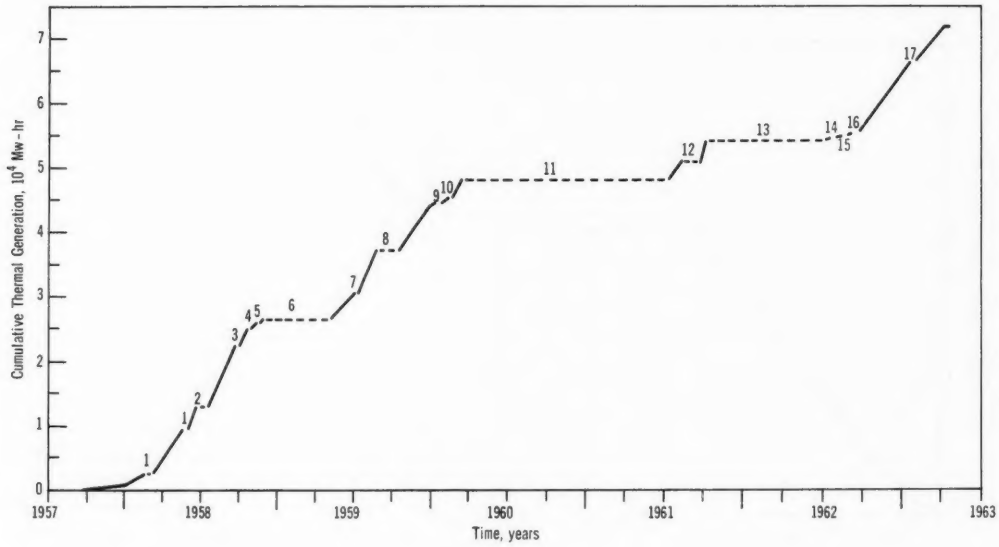

Figure 18

See legends ⟶

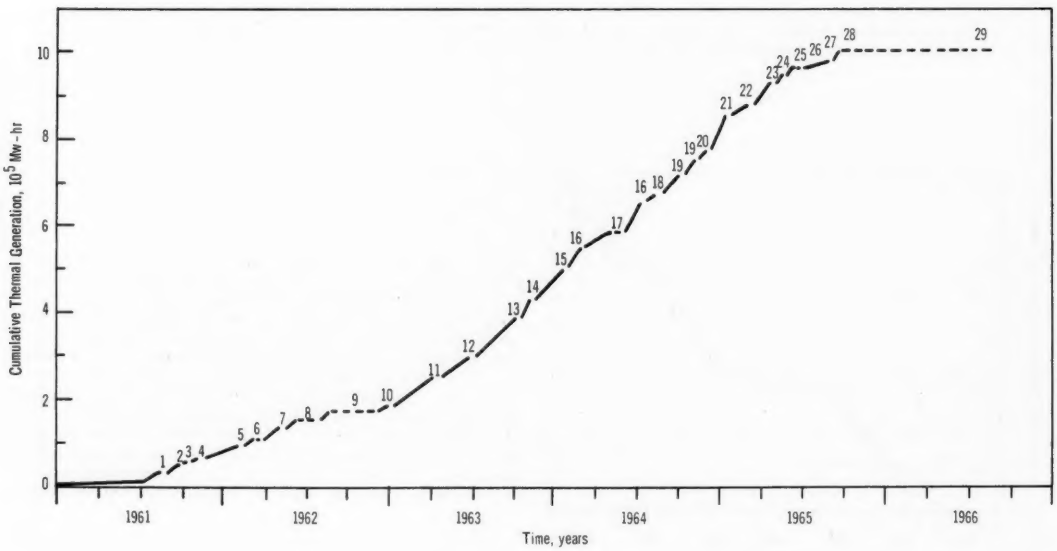

Figure 19

Fig. 18 OMRE, a 12-Mw(t) organic-moderated reactor, produced 71,208 thermal Mw-hr. Major shutdowns had the following causes: 1, routine maintenance. 2, install test fuel elements and new reactor equipment. 3, replace primary-coolant-pump seals. 4, remove failed test fuel element. 5, remove second test fuel element. 6, purify coolant and insert new core. 7, install OMR prototype test elements. 8, examine fuel elements. 9, examine and relocate fuel elements. 10, special physics tests. 11, remove and examine fuel elements; install new coolant purification equipment; load third core. 12, repair fuel thermocouple circuits. 13, end of Core 3 A; install Core 3 B and C. 14, clean and replace 40-μ full-flow filters. 15, replace faulty control-rod magnets and full-flow filter. 16, install new sleeves in water-cooled instrument thimbles; replace full-flow filter with 250-μ strainer. 17, remove experimental fuel elements.

Fig. 19 PRTR, a 70-Mw(t) D_2O-moderated and -cooled reactor, has produced ~1 million thermal Mw-hr since November 1960. Major shutdowns had the following causes: 1, remove foreign materials from primary system. 2, remove additional foreign materials from primary system; repair to reduce heavy-water and helium losses. 3, prepare for power test. 4, repair primary pump seal and other components. 5, repair and modify components. 6, repair and modify equipment. 7, primary-coolant-system instability and fuel substitution tests; equipment maintenance. 8, replace main flow straightening vane in primary coolant system. 9, primary-system decontamination after fuel-element rupture. 10, repair primary pump seal. 11, replace steam export line expansion bellows. 12, replace light-water injection supply valve; leak-test containment. 13, test automatic controller. 14, install fuel-element rupture test facility test section. 15, routine repairs; modify design. 16, refueling and maintenance. 17, containment leak-rate test. 18, repair loop and pump; design changes. 19, routine repair. 20, regeneration of ruptured loop IX units. 21, adjust experimental fuel loading; remove leaker. 22, adjust fuel loading; repair helium compressor. 23, adjust experimental fuel; install creep experiment; relocate test facility. 24, adjust experimental fuel; remove leaker. 25, remove fuel; pressure-test containment; test chemical shim system; find H_2O leak in bottom shield. 26, adjust experimental fuel. 27, adjust experimental elements in Fuel Element Rupture Test Facility (FERTF); repair primary-coolant-system pumps. 28, decontamination after experimental fuel failure in FERTF. 29, complete critical testing for new loading; awaiting safeguards approval for power operation.

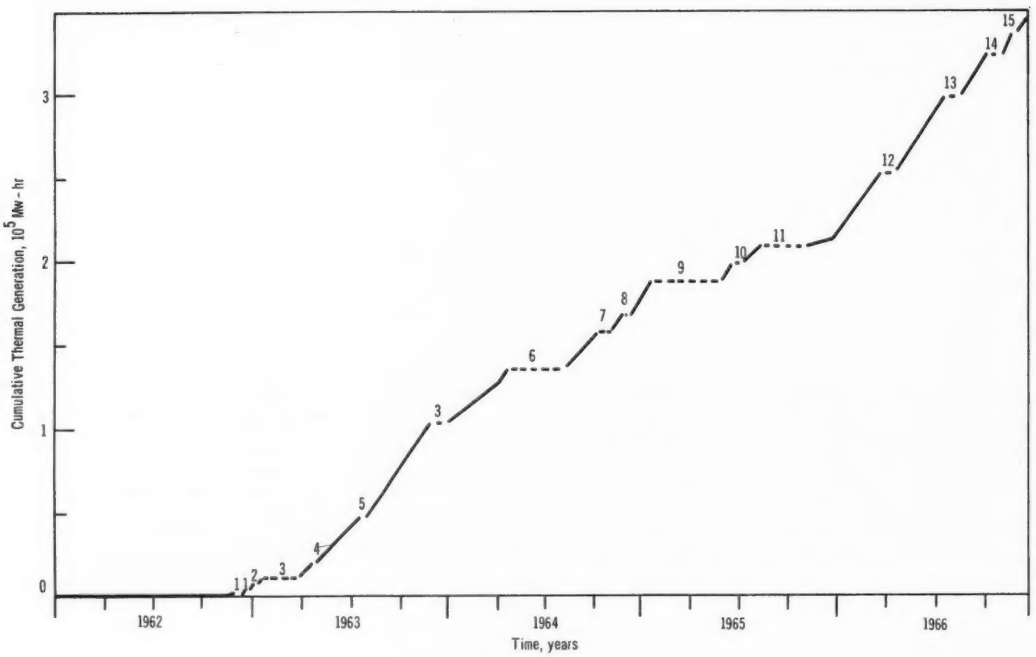

Figure 20

See legends ——→

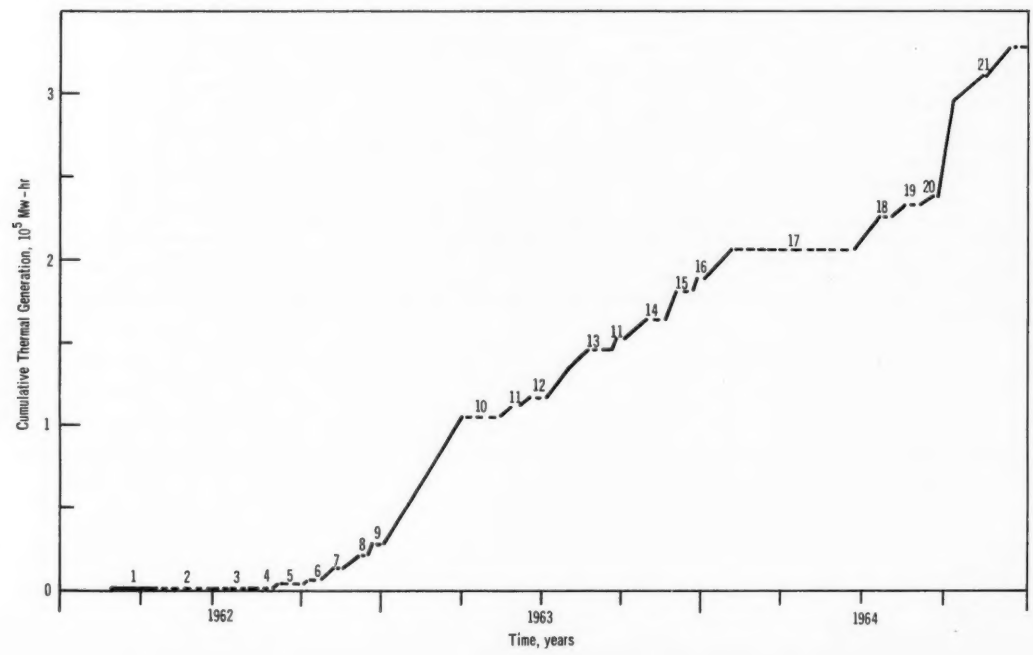

Figure 21

Fig. 20 Saxton, a 23.5-Mw(t) PWR, has produced 57,475 Mw-hr of electricity since November 1962. Major shutdowns had the following causes: 1, systems check; physics tests. 2, modify equipment. 3, replace 3 fuel subassemblies; check system. 4, test loss-of-load and natural circulation. 5, maintenance; check systems. 6, replace 2 fuel assemblies and absorber section on all 6 control rods; install 6 irradiation capsule assemblies; maintenance and physics tests. 7, replace 1 fuel assembly; maintenance and system check. 8, inspect 2 fuel subassemblies; maintenance and system check. 9, install supercritical test loop; plant maintenance and check. 10, change test fuel subassembly from periphery to center-core position. 11, replace Core 1 with Core 2 which has 9 center fuel assemblies enriched with plutonium dioxide; plant maintenance and check. 12, change and inspect test fuel subassembly; plant maintenance and check. 13, leak-test containment vessel; low-power physics tests and operator training; plant maintenance and check. 14, continue supercritical test-loop installation; plant maintenance and check. 15, pressure-relief valve maintenance and plant check.

Fig. 21 HWCTR, a 61-Mw(t) HWR, produced 333,190 thermal Mw-hr. Major shutdowns had the following causes: 1, correct safety-rod binding problems. 2, investigate cause of helium voids in moderator; correct problem. 3, modify to reduce makeup-pump discharge-piping vibration. 4, repair clutch in main pump d-c motor coupling. 5, charge test fuel assemblies; prepare for test-irradiation program. 6, repair faulty monitor-pin thermocouples. 7, replace monitor-pin thermocouples. 8, correct safety-rod seal leak; repair steam-generator leaks. 9, test fuel failure; discharge all metal test fuel similar to failed assembly; measure margin of control with new test fuel charge. 10, test fuel failure and containment modification. 11, test fuel failure. 12, remove failed test fuel element. 13, suspected fuel failure; remove boiling loop pressure tube. 14, test fuel failure; replace deionizer. 15, replace initial driver fuel charge; modify system. 16, correct feedwater control problem. 17, repair steam generator, pump seal, safety-rod guide tubes, and gas baffle support; test fuel failure and electric-power failure. (Intermittent operation on 8 days during this period.) 18, repair steam-generator leak; replace failed fuel test assembly. 19, leak-test containment building and repair steam generators. 20, repair steam-generator leak. 21, remove boronated targets from drive fuel assemblies; exchange several test fuel assemblies.

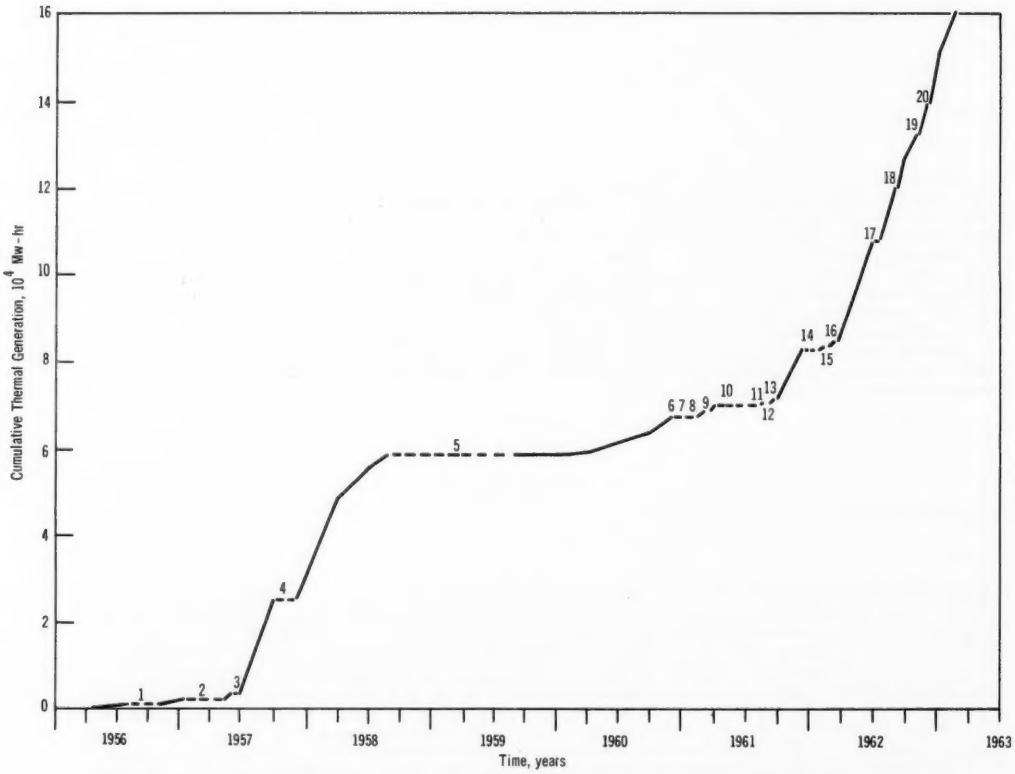

Fig. 22 SRE, a 20-Mw(t) sodium–graphite reactor, produced 37,174 Mw-hr of electricity. Major shutdowns had the following causes: 1, modify sodium-handling equipment (pumps, orifice plates, and cold traps). 2, install eddy-current brakes. 3, repair sodium pumps and other components. 4, install SIR (Seawolf prototype) steam generator. 5, fuel-element damage; cleanup; refuel; modify plant. 6, wire-wrapping fuel; repairs. 7, modify radioactive-liquid-waste system. 8, view core with optical probe. 9, view moderator can with optical probe. 10, fuel transfer; maintenance; complete core photographing. 11, repair fuel-handling machine. 12, transfer fuel element and change orifice plate. 13, transfer fuel element; repair service vault. 14, modify to eliminate helium gas bubbles. 15, modify and replace primary sodium pump. 16, repair Edison steam leak. 17, install star spreaders. 18, modify fuel element. 19, reorifice and install prototype fuel. 20, locate ruptured moderator can; modify fuel element..

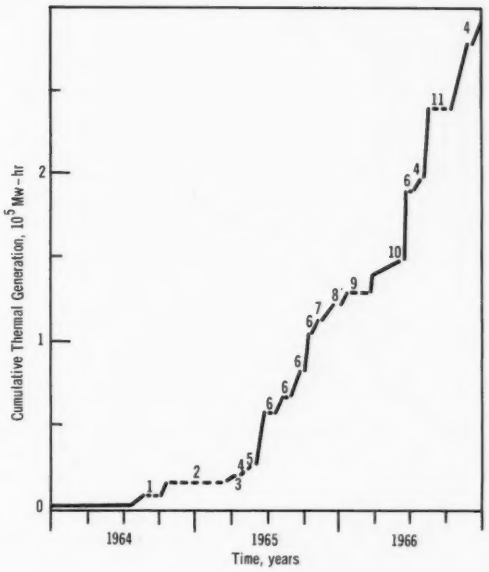

Fig. 23 EBR-2, a 62.5-Mw(t) sodium-cooled FBR, has produced 77,323 Mw-hr of electricity since August 1964. Major shutdowns had the following causes: 1, remove and inspect fuel subassembly; check and repair fuel-handling equipment. 2, repair control rod and evaporator leak; zero and low-power experiments. 3, fuel handling; repair control rods 8 and 11 gripper jaw. 4, fuel handling. 5, fuel handling; seal testing; maintenance. 6, fuel handling; fuel surveillance. 7, fuel handling; fuel surveillance; fuel unloading; machine gripper repair. 8, fuel handling; fuel surveillance; repair and leak-test equipment air lock; plant maintenance. 9, replace primary tank heaters; remove and repair fuel-handling equipment. 10, fuel handling; fuel surveillance; maintenance; leak-test reactor building. 11, fuel handling; rotating seal trough maintenance; repair turbine blading damage; modify secondary sodium trace heating system control; install oscillator rod.

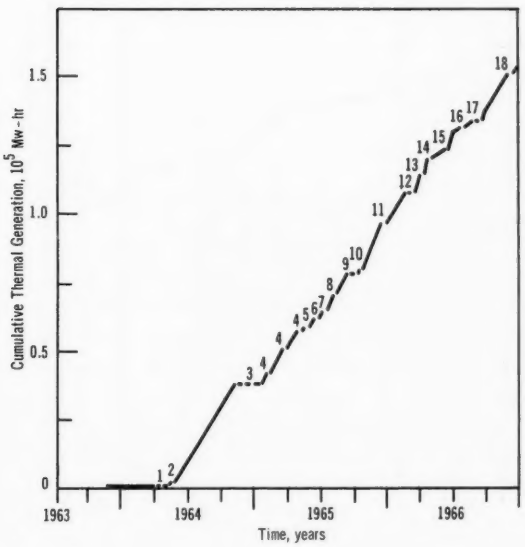

Fig. 24 EVESR, a 17-Mw(t) light-water-moderated superheater, has produced 25,199 Mw-hr of electricity since January 1965. Major shutdowns had the following causes: 1, repair leaking boiler tube; reroll tube to water drive; repair boiler hot spot. 2, repair feedwater pump bearing. 3, refuel for increased power level; connect turbine generator; routine maintenance. 4, boiler tube failure. 5, install off-gas cooler experiment. 6, repair condensate pump. 7, remove defective fuel. 8, condenser tube failure. 9, install shuttle tube, crud concentrator, autoclave, and recombiner. 10, repair ICV valve leaks; probe boiler level. 11, feedwater heater tube rupture. 12, refuel; repair control-rod seal; install larger in-core ion chamber, shuttle tube, sample autoclave, and remote control on cleanup system. 13, remove failed fuel element; repair ventilation valve; calibrate rod worth. 14, repair boiler control system and miscellaneous valves; test emergency cooling valve. 15, install dump tank eductor; repair miscellaneous valves; remove vent valve. 16, install second manufactured-defect fuel rod; install off-gas water trap and condensate storage-tank float; test control-rod friction. 17, refuel; modify safety system; repair steam valve; install white control rod and steam line hold-down. 18, install third manufactured-defect fuel rod and stack filter; repair miscellaneous leaks.

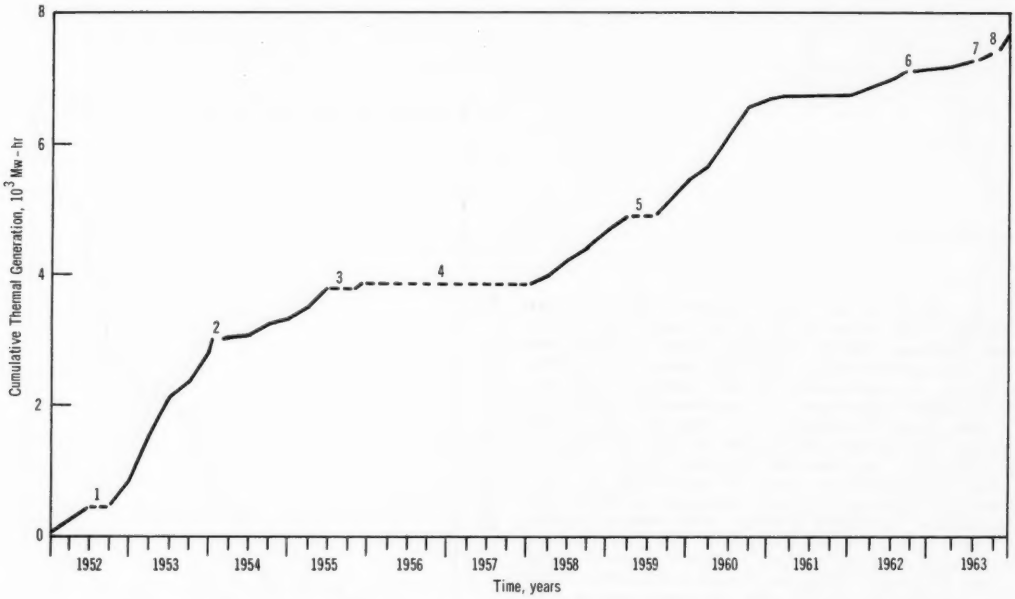

Fig. 25 EBR-1, a 1.4-Mw(t) sodium-cooled FBR, produced 579 Mw-hr of electricity. Major shutdowns had the following causes: 1, modify shielding, 2, install Mark II core. 3, low-power physics experiments. 4, system cleanup; modifications following Mark II core meltdown; install Mark III core. 5, low-power experiments. 6, installation of Mark IV core. 7, maintenance and reloading for breeding-gain measurements. 8, replace representative fuel for radiation-damage determinations.

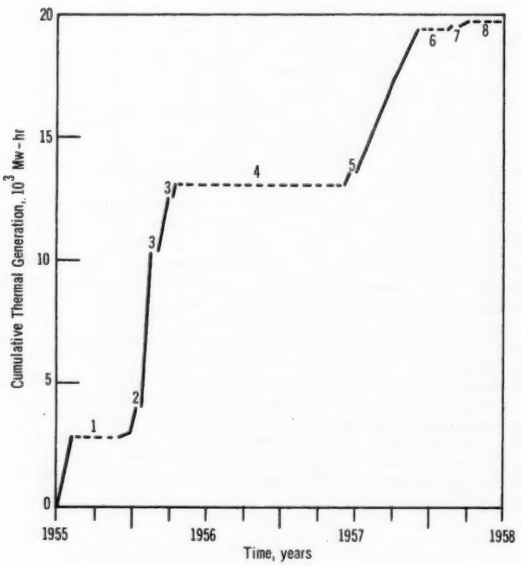

Fig. 26 BORAX-3 and -4, a 15.5-Mw(t) BWR, produced 19,750 thermal Mw-hr. Major shutdowns had the following causes: 1, plant revisions; zero-power tests. 2, plant revisions. 3, maintenance. 4, modify to BORAX-4; zero-power tests. 5, reactor-stability tests. 6, shielding modification. 7, examinations and tests of failed fuel element. 8, modify to BORAX-5.

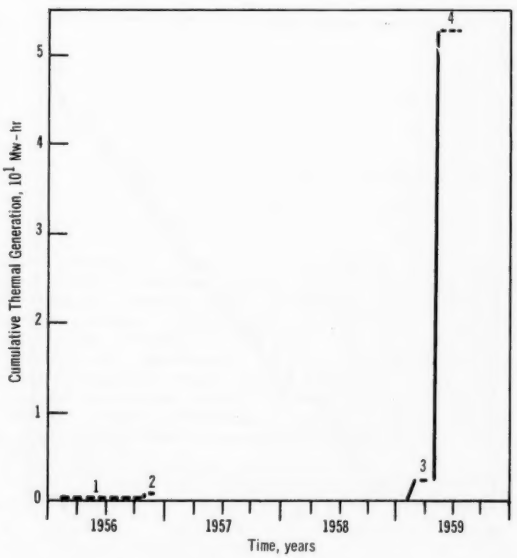

Fig. 27 LAPRE-1 and -2, two 1 to 2-Mw(t) plutonium-fueled-reactor experiments, produced ~53 thermal Mw-hr. Major shutdowns had the following causes: 1, repair LAPRE-1 gold-clad heat-exchanger tubing. 2, experiment discontinued. 3, repair LAPRE-2 primary pump; modify coolant-system surge tank. 4, experiment discontinued.

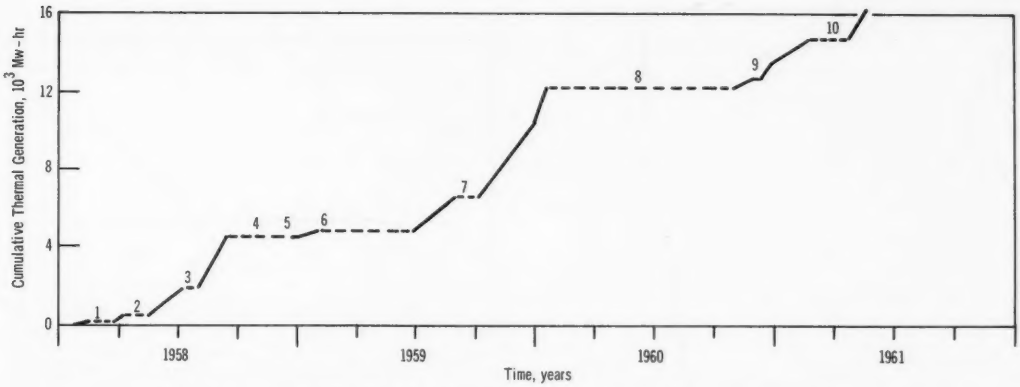

Fig. 28 HRE-2, a 5.2-Mw(t) aqueous homogeneous solution (UO_2SO_4) reactor, produced ~900 Mw-hr of electricity. Major shutdowns had the following causes: 1, zero-power operation and tests. 2, determine severity of core tank leak. 3, prepare for sustained operation with fuel in core and blanket. 4, examine core and blanket regions; zero-power operation. 5, replace pump. 6, subcritical operation, processing plant improvements, and maintenance. 7, subcritical operation; inspect core; replace fuel feed-pump head. 8, remove core diffusers; install core patches; reverse fuel-circulating-pump piping; zero-power operation. 9, replace fuel feed pump. 10, fuel leak into containment shell.

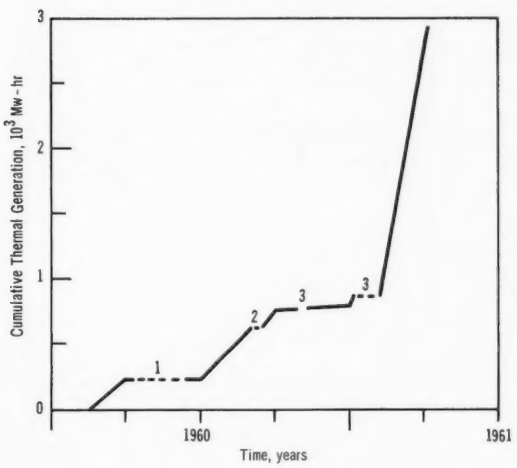

Fig. 29 GCRE, a 2.2-Mw(t) gas-cooled reactor, produced 2989 thermal Mw-hr. Major shutdowns had the following causes: 1, replace pressure vessel. 2, install redesigned fuel elements. 3, routine maintenance.

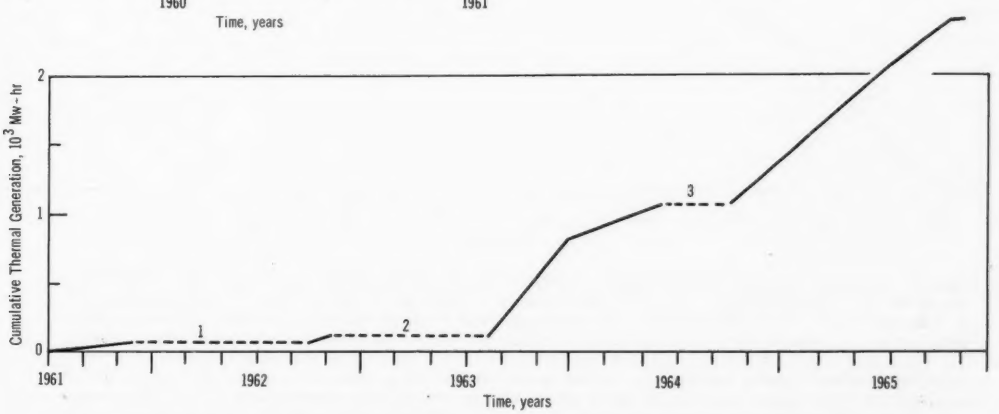

Fig. 30: LAMPRE, a 1-Mw(t) fast molten-plutonium-fueled, sodium-cooled reactor, produced 2370 thermal Mw-hr. Major shutdowns had the following causes: 1, modify shielding; repair main-loop heating transformer. 2, investigate control-element malfunction; remove Core 1. 3, remove faulty fuel capsule.

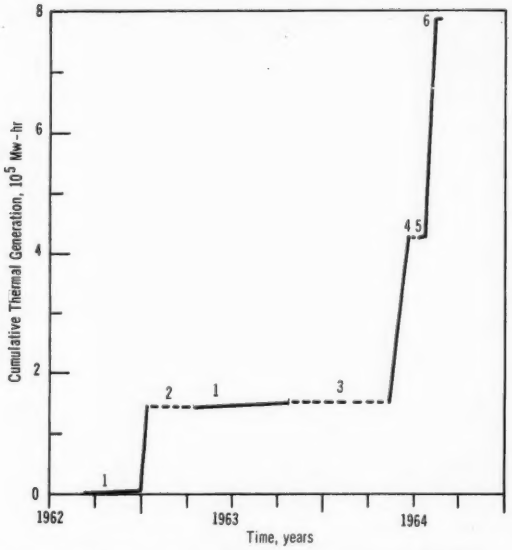

Fig. 31 BORAX-5, a 20-Mw(t) BWR, produced 563 Mw-hr of electricity and 7799 Mw-hr of heat. Major shutdowns had the following causes: 1, change from boiling to integral superheater core. 2, change to peripheral superheat core; low-power experiments. 3, install defective "boiling" fuel rods. 4, install defective superheat fuel sample. 5, termination.

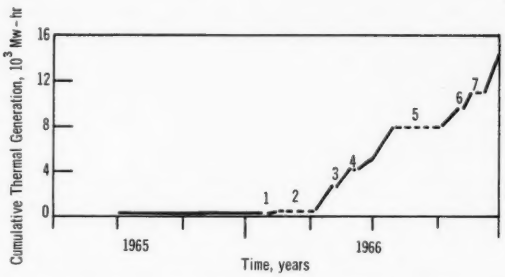

Fig. 32 MSRE, a 10-Mw(t) single-region, graphite-moderated reactor, has produced 14,033 thermal Mw-hr. Major shutdowns had the following causes: 1, remove plugged capillary; check valve and filter in off-gas system. 2, identify plugging material; install larger valves and newly designed filter in off-gas system. 3, repair electrical wiring short in fuel sample enricher. 4, leak-test reactor cell. 5, replace core sample array; replace one blower. 6, clear gas-line plug caused by salt overfill; replace second blower. 7, clear salt plug from gas line; repair air valve in reactor cell.

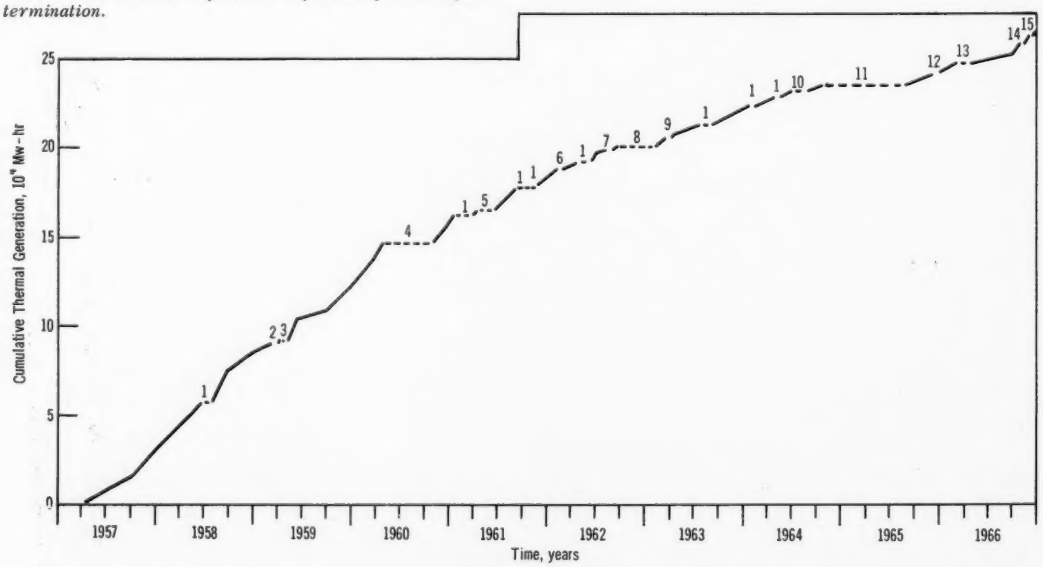

Fig. 33 SM-1, a 10-Mw(t) PWR, has produced 48,971 Mw-hr of electricity since April 1957. Major shutdowns had the following causes: 1, routine maintenance. 2, zero-power experiments. 3, core investigation. 4, rearrange core. 5, replace core. 6, determine in-plant airborne radioactivity value. 7, repair station waste pipe. 8, maintenance; turbine-control equipment tests. 9, repair control-rod-drive system. 10, maintenance and installation of nuclear instrumentation. 11, major plant modification. 12, modify vapor container manhole closing mechanism; turbine maintenance. 13, semiannual maintenance—remove 10% steam dump line; install new coaxial cable on nuclear instrumentation startup and intermediate range monitors; modify inner vapor container door; test vapor container leak rate. 14, leak-test inner vapor container liner; modify primary-coolant pump and nil ductility transition temperature protective system. 15, rebuild and reinstall water seal assemblies on shim rod number 2 and safety rod "A"; rebuild all control-rod magnetic clutch assemblies and instrument pads.

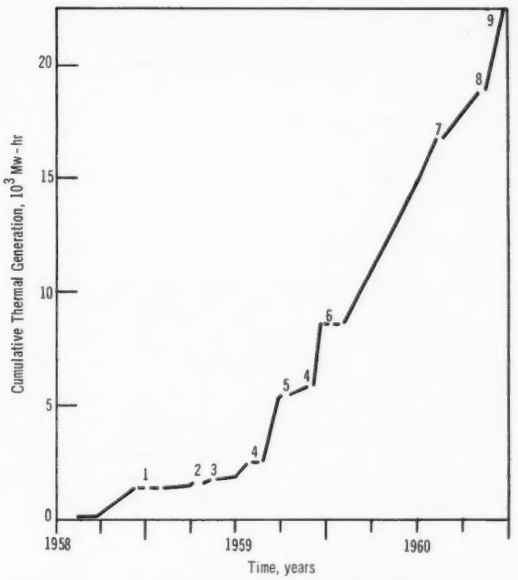

Fig. 34 SL-1, a 3-Mw(t) BWR, produced 1937 Mw-hr of electricity. Major shutdowns had the following causes: 1, modify plant. 2, replace reactor-vessel head gasket. 3, repair plugged gland air ejector. 4, maintenance and modifications. 5, remove instrumented fuel element. 6, annual maintenance. 7, remove corroded boron side plates; insert instrumented fuel element, flux wires, and test coupons. 8, maintenance. 9, maintenance (final).

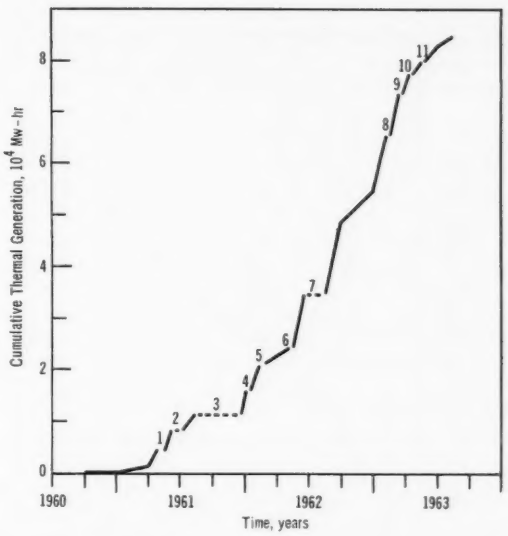

Fig. 35 PM-2A, a 10-Mw(t) PWR, produced 11,462 Mw-hr of electricity. Major shutdowns had the following causes: 1, steel filings discovered in turbine oil. 2, turbine oil pump failure. 3, turbine oil pump failure; fire in static exciter. 4, pressurizer level control circuit malfunction. 5, shim-rod clutch slippage. 6, faulty capacitor grounded generator. 7, snow tunnel arch rebuilding. 8, main steam-line leaks. 9, pressurizer cooldown. 10, routine maintenance. 11, faulty rod-drive indications.

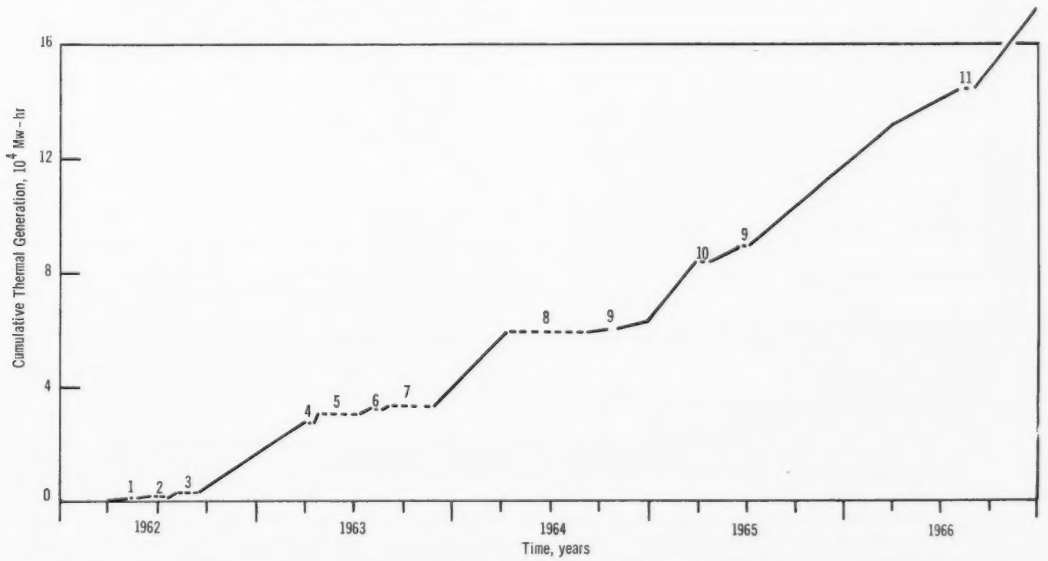

Fig. 36 PM-1, a 9.4-Mw(t) PWR, has produced 19,774 Mw-hr of electricity since April 1962. Major shutdowns had the following causes: 1, modification, maintenance, and training. 2, operations and process-control revisions. 3, modify plant. 4, repair steam leak and rod-drive system. 5, repair nuclear instrumentation and rod-drive system; repair steam leaks. 6, repair main steam stop valve; modify plant; study core physics. 7, control-rod thimble metallurgical examination; remove corrosion defects from installed thimbles. 8, maintenance; replace 403 stainless-steel thimble sections of control actuators. 9, routine maintenance. 10, replace synchro-drive motor for rod-position indicator No. 6. 11, repair leak in feedwater line; complete core change and core physics on old and new cores.

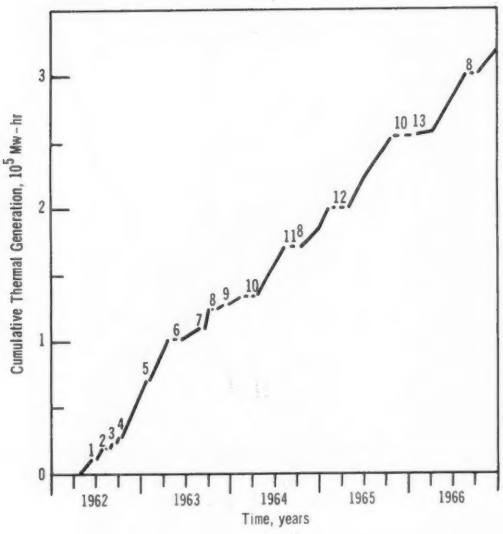

Fig. 37 SM-1A, a 20-Mw(t) PWR, has produced 37,997 Mw-hr of electricity since May 1962. Major shutdowns had the following causes: 1, repair mechanical seal pump. 2, physics test; repair control rod. 3, repair blown steam-generator gasket. 4, army IG inspection. 5, repair turbine-governor valves. 6, repair control rod. 7, replace tube bundle of primary BD cooler. 8, routine maintenance. 9, repair nuclear instrumentation; inspect PC pump No. 2. 10, core change and maintenance. 11, repair turbine steam chest; remove NRL flux-wire sheathing and associated equipment. 12, repair primary-coolant pumps. 13, rebuild rod-drive seals; install primary-coolant pump No. 1.

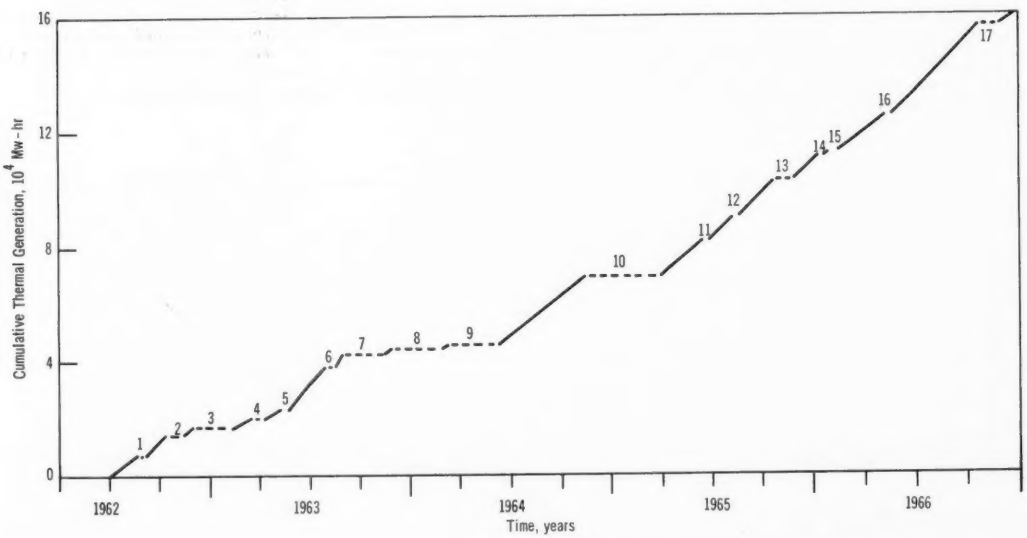

Fig. 38 PM-3A, a 9.5-Mw(t) PWR, has produced 25,836 Mw-hr of electricity since July 1962. Major shutdowns had the following causes: 1, change nuclear instrumentation cables. 2, repair hydrogen fire plant damage. 3, modify plant. 4, complete corrective actions. 5, replace demineralizer resin; repair primary-system valves. 6, routine maintenance; hydrogen test preparation. 7, replace actuator thimble. 8, replace demineralizer resin; modify plant. 9, modification and testing. 10, refueling and maintenance. 11, repair primary-system leak. 12, operator error; preventive maintenance. 13, maintenance; testing; replacement crew training. 14, remove spent core from storage; repair leaks in primary and secondary systems. 15, maintenance on decay-heat check valve and all control-rod-drive mechanisms. 16, replace nuclear instrumentation cable and connector in containment. 17, training; replace failed control rod; routine maintenance.

vessel, is to be located along the Mississippi River 35 miles northwest of Minneapolis. Full-power operation is scheduled to begin in mid-1970.

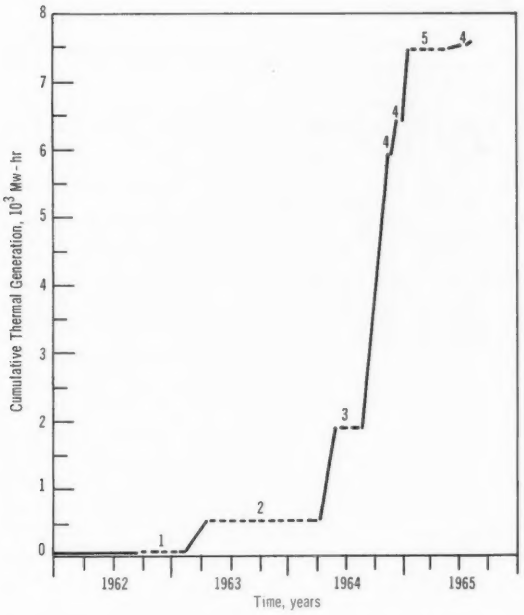

Fig. 39 ML-1, a 3.3-Mw(t) gas-cooled, light-water-moderated reactor, produced 7674 thermal Mw-hr. Major shutdowns had the following causes: 1, modify to eliminate possible coolant bypass of fuel elements. 2, repair pressure-vessel leak; improve fuel-element design and turbine-compressor set reliability. 3, core inspection; minor repair to turbine-compressor set. 4, routine maintenance and system check. 5, repair pressure-vessel leak.

Burlington Unit 1 reactor is to be furnished by Westinghouse for operation in 1971; the utilities have an option to purchase a second identical unit to be operable in 1974. The proposed site is adjacent to an existing fossil-fired station.

Browns Ferry Unit 1, as the first unit of a two-unit plant, is scheduled to operate in the fall of 1970 on the north shore of Wheeler Reservoir, about 10 miles northwest of Decatur, Ala.

Browns Ferry Unit 2 is tentatively scheduled for operation in late 1971 or early 1972 if TVA does not exercise its option to cancel the order.

Quad-Cities Unit 2 is substantially similar to Quad-Cities Unit 1, which Commonwealth Edison ordered $3\frac{1}{2}$ months earlier. Both units are to be located near the Quad Cities of Rock Island, Moline, and East Moline, Ill., and Davenport, Iowa.

Oconee Units 1 and 2 are to be built near Keowee Dam; completion of the first unit is scheduled for mid-1971; the second, a year later.

16 MORE REACTORS PLANNED

Utilities have announced their intentions to build 16 additional nuclear reactors, but by year end the companies had not yet filed applications for construction permits.

Shoreham is the site selected for this Long Island Lighting Co. plant, whose construction is scheduled to begin by late 1969 on the north shore of Long Island between Shoreham and Wading River.

Pilgrim station is planned for 5 miles east of Plymouth, Mass., on Cape Cod Bay. Start of commercial operation is scheduled for late 1971.

Bailey Point station will be about 3 miles south of Wiscasset and 35 miles northeast of Portland, Maine. Central Maine Power Co., Bangor Hydro-Electric Co., and Maine Public Service Co. will own 50% of the plant and take half its output; eight other participating New England utilities will share the balance of output and costs.

Peach Bottom Unit 2 is to be operational in 1971. An additional unit of the same 1065-Mw(e) net output is to be operational in 1973, but the site has not yet been selected.

Burlington Unit 2, a plant identical to Unit 1, would be operable in 1974 if the utilities exercise an option from Westinghouse. Burlington, N. J., is one possible site.

Fort Calhoun plant is proposed for a site on the west side of the Missouri River about 19 miles north of Omaha. The schedule calls for start of commercial operation by mid-1971.

Surry Units 1 and 2 are proposed for a site on Hog Island near Bacons Castle, across the James River from Fort Eustis. Unit 1 is scheduled to be ready for commercial operation by early 1971; Unit 2 would follow in early 1972.

Consumers Public Power District (a project name has not been selected), which is slated for completion in 1972, is proposed for the Nebraska side of the Missouri River south of Omaha. Consumers Public Power District will furnish the plant; Iowa Power and Light Co. will take half the plant output and share in the costs.

Metropolitan Water District of Southern California, Bolsa Island Nuclear Power and Desalting Plant Units 1 and 2, is a combination power and water-desalting plant proposed for location on a man-made island offshore between Huntington and Seal Beaches, Calif. One 800-Mw(e) net power plant is to be built by the Los Angeles Department of Water & Power; the other is to be built jointly by the Southern California Edison Co. and San Diego Gas & Electric Co. The Metropolitan Water District (MWD) is initially to build one 50 million gal/day desalting module; if its operation is satisfactory, MWD would then expect to add additional desalting capacity of 100 million gal/day. Initial operation of the Edison–San Diego reactor and 50 million gal/day desalting module is scheduled for 1972.

Pacific Gas & Electric Co. plant (a name has not been selected) is proposed for a site near Diablo Canyon, 12 miles southwest of San Luis Obispo. Completion is scheduled for late 1971.

Niagara Mohawk Power Corp. plant, Easton Nuclear Station, is planned for Stillwater, on the east bank of the Hudson River, about 20 miles north of Troy, N. Y. Commerical operation is scheduled for late 1971 or early 1972.

Metropolitan Edison Co. plant, Three Mile Island Station. Construction is tentatively scheduled for completion by mid-1971.

Indiana and Michigan Electric Co. plant (a name has not been selected) is planned for the southeast shore of Lake Michigan, about 11 miles southwest of Benton Harbor. Selection of a contractor was scheduled to be made about May 1967.

The assistance of Harvey I. Mueller, AEC, in compiling, updating, and reviewing the tabulated data in this article, is appreciated.

References

1. Nuclear Reactors Built, Being Built, or Planned in the United States as of June 30, 1966, USAEC Report TID-8200(14th Rev.), 1966.
2. Operating History of the U. S. Nuclear Power Reactors — 1966, in Proceedings of the Hearings Before the Joint Committee on Atomic Energy on AEC Authorizing Legislation for FY 1968, Feb. 15, 1967.
3. Harvey Mueller, U. S. Atomic Energy Commission, personal communications, May 11, 1967.
4. G. F. Bierman and W. J. Miller, Nuclear Plant Performance — Good and Getting Better, *Power Reactor Technol.*, 9(3): 110-122 (Summer 1966).
5. U. S. Atomic Energy Commission, *Major Activities in the Atomic Energy Programs, January–December 1966*, Supt. of Documents, U. S. Government Printing Office, Washington, January 1967.

An Introduction to Fuel Processing

Information on reactor fuel reprocessing, formerly published in the quarterly Technical Progress Review *Reactor Fuel Processing*, is now to be published in this new combined journal. Material on aqueous and nonaqueous reactor fuel processing and on waste disposal is presented in this issue.

Although new readers should have no difficulty in understanding the material on fuel processing without additional background information, a list of review articles has been prepared for those who may wish to explore some of the subjects further or to gain a broader perspective of the various research and development programs in reactor fuel processing and their objectives. This list was prepared by the authors of the fuel-processing material in this journal.

Aqueous Processing

1. F. L. Culler, Jr., R. E. Blanco, L. M. Ferris, E. L. Nicholson, R. H. Rainey, and J. Ullman, Proposed Aqueous Processes for Power Reactor Fuels, *Nucleonics*, 20(8): 124-127 (August 1962).
2. C. E. Stevenson, How AEC Plans to Process Power Reactor Fuels, *Nucleonics*, 18(2): 72-73 (February 1960).
3. F. L. Culler and R. E. Blanco, Advances in Aqueous Processing of Power Reactor Fuels, in *Proceedings of the Third United Nations International Conference on the Peaceful Uses of Atomic Energy, Geneva, 1964*, Vol. 10, pp. 316-327, United Nations, New York, 1965.
4. F. L. Culler and R. E. Blanco, Feed Preparation for Aqueous Separation Processes, in *Proceedings of the Second United Nations International Conference on the Peaceful Uses of Atomic Energy, Geneva, 1958*, Vol. 17, pp. 259-290, United Nations, New York, 1958.
5. V. Cooper and M. T. Walling, Aqueous Separation and Decontamination Processes, in *Proceedings of the Second United Nations International Conference on the Peaceful Uses of Atomic Energy, Geneva, 1958*, Vol. 17, pp. 291-323, United Nations, New York, 1958.
6. C. M. Slansky and J. R. McBride, The Case for Small Reprocessing Plants, *Nucleonics*, 20(9): 43-47 (September 1962).

Nonaqueous Processing

VOLATILITY PROCESSING

1. A. A. Jonke, Reprocessing of Nuclear Reactor Fuels by Processes Based on Volatilization, Fractional Distillation, and Selective Adsorption, *At. Energy Rev.*, 3(1): 3-60 (1965).
2. R. C. Vogel, W. H. Carr, G. I. Cathers, J. Fischer, L. P. Hatch, R. W. Horton, A. A. Jonke, R. P. Milford, J. J. Reilly, and G. Strickland, Fluoride Volatility Processes for Recovery of Fissionable Materials from Irradiated Reactor Fuels, in *Proceedings of the Third United Nations International Conference on the Peaceful Uses of Atomic Energy, Geneva, 1964*, Vol. 10, pp. 491-498, United Nations, New York, 1965.
3. J. Schmets, G. Camozzo, A. Francesconi, P. Godrie, R. Heremans, G. Pierini, and P. Speeckaert, Reprocessing of Nuclear Fuels by Volatilization, in *Proceedings of the Third United Nations International Conference on the Peaceful Uses of Atomic Energy, Geneva, 1964*, Vol. 10, pp. 520-529, United Nations, New York, 1965.
4. M. Bourgeois and P. Faugeras, The Processing of Irradiated Fuels by the Halogens and their Compounds, in *Proceedings of the Third United Nations International Conference on the Peaceful Uses of Atomic Energy, Geneva, 1964*, Vol. 10, pp. 483-490, United Nations, New York, 1965.

PROCESSES FOR PRODUCING URANIUM COMPOUNDS

1. C. D. Harrington and A. E. Ruehle (Eds.), *Uranium Production Technology* , D. Van Nostrand Company, Inc., Princeton, N. J., 1959.

FLUIDIZATION TECHNOLOGY IN URANIUM PROCESSING

1. *Symposium on Nuclear Plant Experience with Fluidized Beds*, Chemical Engineering Progress Symposium Series, Vol. 62, No. 65, American Institute of Chemical Engineers, New York, 1966.
2. S. H. Smiley, Gas-Solids Reactors in Uranium Processing: A Critical Review, in *Progress in*

Nuclear Energy, Technology, Engineering and Safety, Series IV, Vol. 4, pp. 191-278, Pergamon Press, Inc., New York, 1961.

PYROCHEMICAL PROCESSING

1. R. D. Pierce and L. Burris, Jr., Pyroprocessing of Reactor Fuels, in *Reactor Technology, Selected Reviews—1964*, L. E. Link (Ed.), USAEC Report TID-8540, pp. 411-476, July 1964.
2. S. Lawroski and L. Burris, Jr., Processing of Reactor Fuel Materials by Pyrometallurgical Methods, *At. Energy Rev.*, 2(3): 3-69 (October 1964).
3. P. Faugeras, Chemical Treatment of Irradiated Nuclear Fuels, *Energie Nucl.*, 7: 214-227 (June 1965).
4. L. Burris and G. A. Bennett, Salt-Transport Processes, *Reactor Fuel Process.*, 9(2): 97-100 (Spring 1966).
5. L. Burris, K. M. Harmon, G. E. Brand, E. W. Murback, and R. K. Steunenberg, Pyrometallurgical and Pyrochemical Fuel Processing, in *Proceedings of the Third United Nations International Conference on the Peaceful Uses of Atomic Energy, Geneva, 1964*, Vol. 10, pp. 501-510, United Nations, New York, 1965.
6. G. E. Benedict, W. R. Bond, G. Jansen, Jr., L. G. Morgan, and J. R. Lundquist, Status of the Salt Cycle Process for Processing Oxide Fuels, USAEC Report BNWL-SA-205, Battelle–Northwest, Sept. 3, 1965.
7. L. Burris and G. A. Bennett, Dry Processes, *Reactor Fuel Process.*, 9(1): 36-38 (Winter 1965–1966).

Waste Disposal

1. W. G. Belter and W. H. Regan, Radioactive Waste Research and Development Activities—A Report of Progress, *J. Water Pollut. Contr. Federation*, 37(3): 316-335 (March 1965).
2. J. O. Blomeke and J. T. Roberts, Waste Management, in *Annual Review of Nuclear Science*, E. Creutz et al. (Eds.), Vol. 15, pp. 151-174, Annual Reviews, Inc., Palo Alto, Calif., 1965.
3. *Radioactive Waste Disposal into the Ground*, Safety Series, No. 15, International Atomic Energy Agency, Vienna, 1966 (STI/PUB/103).
4. Known Methods Can Cope with Atomic Wastes, *Chem. Eng. News*, 44(9): 46 (Feb. 28, 1966).
5. J. R. Grover, Solidification and Long-Term Storage of Highly Radioactive Wastes, *Nucl. Eng.*, 11(120): 382-386 (May 1966).
6. W. G. Belter and D. W. Pearce, Radioactive Waste Management, in *Reactor Technology, Selected Reviews—1965*, L. E. Link (Ed.), USAEC TID-8541, pp. 149-248, January 1966.
7. *Practices in the Treatment of Low- and Intermediate-Level Radioactive Wastes*, Symposium Proceedings, Vienna, 1965, International Atomic Energy Agency, Vienna, 1966 (STI/PUB/116).

Recent Developments in Aqueous Processing

By C. E. Stevenson and D. M. Paige

Preparation for Fuel Processing

The shear–leach process for the preparation of fuel for processing is now in use at the Nuclear Fuel Services plant and has been demonstrated for newer types of fuel assemblies. The use of NaOH to declad and hydrolyze UC fuel clad with sintered aluminum product (SAP) appears advantageous. The SAP cladding may also be dissolved in H_2SO_4 containing Hg^{2+} Nitric acid containing a small amount of HF is effective in leaching the oxides of uranium and thorium from alumina fluidized beds used to oxidize graphite-base fuels, or to declad stainless-steel- or Zircaloy-clad fuels. Little tritium is released as gas in shearing and dissolving irradiated oxide fuels. Highly irradiated Pu–Al–Ni alloy may be activated with 1*M* HNO_3 containing Hg^{2+} catalyst for dissolution in more concentrated acid. Decladding of stainless-steel-clad oxides by melting of the cladding has been proposed.

MECHANICAL PROCESSING

Oak Ridge National Laboratory (ORNL) reports[1] that basic technology for the shear–leach process[2] on a full-size engineering scale is complete and that the process is now being used by Nuclear Fuel Services, Inc., in their reactor fuel-processing plant near Buffalo, N. Y.

The feasibility of shearing unirradiated fuel was tested at ORNL with three types of fuel (shown in Fig. 1). Results of the tests are summarized in Table 1. These results indicate that intact shearing is feasible if end sections are removed, the movable blade is sharp, proper clearances between the moving and fixed blade are used, and irradiation does not cause unforeseen problems.

The problem of heat generation during processing and storage of sheared fuels was studied at ORNL.[1] A computerized calculation was made of temperatures developed at various points. The results are summarized in Table 2. Since the highest calculated temperature (1586°F) was below the melting points of UO_2 (3947°F) and stainless steel (2642°F), it was concluded that heat generation is not a problem for proposed cutting and storage methods.

A study[1] of finely divided zirconium indicated a possible fire hazard from fines with particles less than 150 μ in diameter. However, since the material from sawing is mostly ZrO_2 and is diluted 7 : 1 with debris from the abrasive wheel, the only precaution suggested was to remove the smaller fines (< 150 μ) from the dissolver periodically and dissolve them in HNO_3–HF. In an experiment in which leached Zircaloy cladding and fines were dissolved, 80% of the −10-mesh fines and 5% of the bulk cladding dissolved in 2 to 3 hr.

DISSOLUTION OF FUELS CLAD WITH SAP

The SAP is of considerable interest as cladding for fuels for a heavy-water-moderated organic-

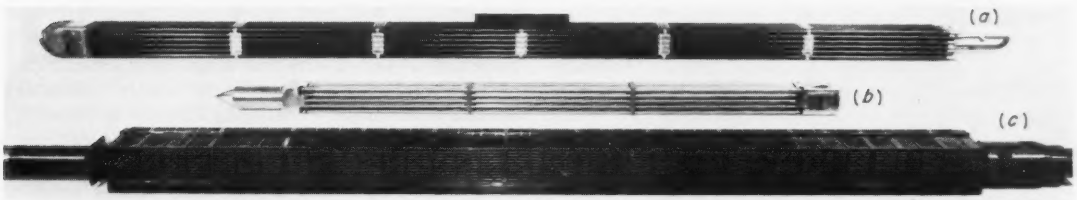

Fig. 1 Fuel assemblies used in shearing tests on second-generation power reactor fuels.[1] (a) Dresden type IV; (b) Elk River core 2; (c) Consolidated Edison core B.

Table 1 SHEARING OF SIMULATED UNIRRADIATED FUELS (BASED ON DATA IN REF. 1)

Fuel	No. of tubes	Tube material	Tube size	Filling	Grid structure	Results
Dresden type IV	36	Zircaloy-2	0.52-in. OD 0.035-in. wall 115-in. length	Porcelain	Crossed wires on 19-in. centers	Sheared to 1- to 2-in. lengths, 40–55 tons shearing force; end hardware removed by sawing
Elk River core 2	25	Stainless steel	0.452-in. OD 0.020-in. wall 60-in. length	Porcelain pellets	Leaf springs	Easily sheared to 1-in. lengths; end hardware removed
Consolidated Edison core B	231	Stainless steel	0.30-in. OD 0.010-in. wall 105-in. length	Porcelain	Leaf springs	Sheared after sharpening movable blade and reducing clearance between blades from 20 mils to 3–5 mils; some chunking noted

cooled reactor (HWOCR) because its strength at temperatures comparable with that of the reactor coolant is markedly greater than that of other aluminum-base cladding. The SAP consists of a sintered dispersion of 5 to 15% Al_2O_3 in an aluminum matrix. It was noted[3] earlier that Beone, working in Italy, had observed that the aluminum metal in SAP is dissolved relatively slowly by mercury-catalyzed HNO_3 and that dissolution of this material in mercury-catalyzed H_2SO_4 is much more effective.

At ORNL,[1] studies are being made of the dissolution of SAP-clad uranium carbide fuel, which now appears advantageous for an HWOCR. The SAP containing 6% Al_2O_3 dissolved rapidly in boiling $2M$ NaOH–$2M$ $NaNO_3$ (Ref. 4), leaving some of the Al_2O_3 as a residue; the observed rate of dissolution [~20 mg/(min)(cm^2)] is about the same as that of pure aluminum in this reagent. Uranium carbide was not dissolved in NaOH–$NaNO_3$ (the loss of uranium to the decladding solution was less than 0.1%) and was left as a residue after dissolution of the cladding. A disadvantage was noted for this decladding procedure: in the subsequent dissolution of UC in HNO_3 for solvent extraction, up to 50% of the carbon would remain in solution as soluble organic compounds. These compounds could have adverse effects on the extraction process. Accordingly, it is proposed that NaOH (without $NaNO_3$) be used for decladding to effect simultaneous hydrolysis of UC and conversion of its carbon to gaseous products. The hydrous UO_2 that is formed in this process is readily soluble in HNO_3. In preliminary experiments, decladding and hydrolysis with NaOH appeared to be feasible, but slow.

Table 2 MINIMUM, TYPICAL, AND MAXIMUM TEMPERATURES ACHIEVED BY REACTOR FUEL IN VARIOUS STEPS OF THE SHEAR–LEACH PROCESS[1]

Operation or process step		Minimum temp.,* °F	Typical temp.,† °F	Maximum temp.,‡ °F
Receiving-canal storage		68.5	71.5	75.5
Mechanical disassembly		123	150	191
Shear feed envelope		143	350	548
Storage in baskets of various internal diameters				
5 in.	Center	160	491	852
	Surface	140	324	548
7.75 in.	Center	196	720	1244
	Surface	155	453	773
10 in.	Center	232	924	1586
	Surface	171	575	979

*Burnup, 8000 Mwd/metric ton; specific power, 10 watts/g; cooled for 1080 days.
†Burnup, 20,000 Mwd/metric ton; specific power, 23 watts/g; cooled for 180 days.
‡Burnup, 50,000 Mwd/metric ton; specific power, 70 watts/g; cooled for 180 days.

Direct dissolution of cladding or sheared fuel in HNO_3 was also considered, but the low rate of dissolution of SAP in $4M$ to $13M$ HNO_3 containing $0M$ to $0.05M$ $Hg(NO_3)_2$ [average dissolution rates, 0.2 to 0.7 mg/(min)(cm^2)] is quite disadvantageous. Complete dissolution of the cladding would require long dissolution periods (20 hr or more), and the extraction feed solution would contain approximately equimolar concentrations of aluminum and uranium. Partial dissolution of the cladding would require a feed analysis for aluminum as well as a means for disposal of the residual cladding. In any case, Al_2O_3 is substantially undissolved.

Work on aluminum and SAP dissolutions was also reported by Beone.[5] The operation of a recirculating dissolver was described for the processing of aluminum or SAP tubes. In dissolution tests the tubes were filled with an inert material to simulate fuel. Aluminum tubes (12 mm in outside diameter by 1 mm in wall thickness) were dissolved in $6M$ or $7.2M$ H_2SO_4 containing $0.01M$–$0.02M$ Hg^{2+} to yield solutions containing $1M$ $Al_2(SO_4)_3$ and $1.3M$ H_2SO_4. Continuous acid feed and progressive increase in the catalyst concentration were required to overcome reduction of the catalyst. Average dissolution rates of 2.5 to 3.5 mg/(min)(cm^2) were readily obtainable. Similar tubes of SAP, containing either 4 or 7% Al_2O_3, were dissolved in NaOH at rates of 2 to 5 mg/(min)(cm^2). The dissolver was initially charged with $0.8M$ to $1M$ NaOH, and a more concentrated solution of NaOH ($9.8M$) was fed at a rate that was controlled to limit the rate of reaction. The product contained $3M$ Al^{3+} and $3M$ NaOH. When unfilled tubes were dis-

solved, shells of Al_2O_3 were left; when filled tubes were dissolved, the Al_2O_3 shells were crushed by the bumping together of the fillers.

LEACHING OF ThO_2 AND UO_2 FROM ALUMINA BEDS

Fluid-bed processes are of considerable potential utility for the preparation of reactor fuels for recovery by solvent extraction. Several applications lead to the production of beds of Al_2O_3 containing oxides of uranium, thorium, or plutonium, with or without oxides of other metals. Examples are fluid-bed oxidation of graphite-matrix, ThO_2-UO_2 particle fuels[6] and the $HF-O_2$ decladding in Al_2O_3 beds of UO_2 or UO_2-PuO_2 (Ref. 7) fuels clad with stainless steel (or Zircaloy). Ferris at ORNL has recently reported the results of leaching studies applicable to such Al_2O_3 beds.[8]

It was first established that Al_2O_3 of the type used for the inert medium in fluidized beds is relatively unattacked by HNO_3. Samples of 60-, 90-, 100-, or 120-mesh alumina were exposed to boiling 10*M* HNO_3, or to 13*M* HNO_3 containing 0.05*M* HF, for 5 hr. Samples of Alcoa T-61 and Norton abrasive material were dissolved to the extent of 0.02 to 0.50% in 10*M* HNO_3; and 0.6 to 1.1% in 13*M* $HNO_3-0.05M$ HF. Typical losses of Norton RR grain were 1 to 3%. Losses from particles of smaller size were generally higher. These losses were believed to be compatible with a leaching process.

The leaching of Al_2O_3 beds containing $ThO_2-U_3O_8$, produced by burning unirradiated prototype Peach Bottom reactor fuel (pyrolytic carbon-coated thorium–uranium dicarbide particles dispersed in graphite) at 700 to 750°C in a bed of Norton RR alumina was first examined. The bed composition was about two-thirds Al_2O_3 and one-third $ThO_2-U_3O_8$ (Th/U ratio, 4.8). When this material was leached with boiling 4*M* to 13*M* HNO_3 for 5 to 7 hr, only 8 to 15% of the thorium and 14 to 28% of the uranium was extracted. However, with 0.05*M* HF in 4*M* to 13*M* HNO_3, recovery of both elements was generally about 99% in 3 hr and was improved with longer boiling. Solutions containing about 0.6*M* Th^{4+} were obtained, and less than 2% of the Al_2O_3 was dissolved. Good recoveries were also obtained by leaching at 50 and 75°C.

Beds produced by reacting simulated Yankee Atomic fuel (UO_2 pellets clad in stainless steel) with 40% HF–60% oxygen at 600°C in a fluidized bed of Norton RR alumina were also leached. The beds contained 25% U_3O_8, 69% Al_2O_3, 13% stainless-steel oxides, and 5% fluorine. The latter element, which is readily leached by nitric acid along with the uranium, is undesirable in a solvent-extraction feed solution since Al^{3+} must be added to prevent equipment corrosion, and the volume of highly radioactive waste is correspondingly increased. Fluorine may be removed from the bed prior to leaching by pyrohydrolysis with steam, or H_2O–saturated oxygen, at atmospheric pressure and 600°C. In a 3-hr treatment of this bed material, 99% of the fluorine was removed. Leaching of the pyrohydrolyzed bed for 5 hr with 2*M* to 15*M* HNO_3, even at temperatures as low as 50°C, resulted in a uranium recovery of 99.7% or greater. Varying proportions (1 to 70–80%) of the stainless-steel elements were also leached from the bed, depending upon acid concentration and temperature.

Similar studies were made using beds produced by HF–oxygen treatment of simulated Zircaloy-clad UO_2 fuel. Again, most of the fluorine was removed by pyrohydrolysis. When the bed material was leached for 5 hr with 2*M* to 15*M* HNO_3, at least 99.6% of the uranium was dissolved along with 1 to 85% of the zirconium, depending again on acid strength and temperature. Little Al_2O_3 was dissolved in any of the tests with UO_2 fuels.

RELEASE OF TRITIUM AND KRYPTON IN SHEAR–LEACH PREPARATION OF ThO_2-UO_2 FUELS

The presence of tritium in irradiated fuels, with a fission yield of the order of 0.01%, presents a processing hazard that is somewhat difficult to evaluate. In the shear–leach process, tritium may be released as a gas or it may interchange with hydrogen in water or organic materials and thereafter accompany liquid products and wastes from processing. Since it is an isotope of the very abundant hydrogen, it is probably impractical to consider its separation or concentration. Goode of ORNL has recently effected some clarification of the fate of tritium (as well as that of krypton) in the shear–leach processing of stainless-steel-clad ThO_2-UO_2 fuels.[9,10]

Specimens of Consolidated Edison Co. reactor fuel (95% $ThO_2-5\%$ $^{235}UO_2$ pellets), irradiated to 25,600 Mwd/ton and cooled 5 years, were sheared in a hot cell under conditions where quantitative collection and analysis of the gases was possible. The tritium content was determined to be 10.7 mc per 25-g specimen. When the specimens were sheared to 0.5-in. lengths, only about 0.02 mc ^3H, or 0.2% of that present, was released to the surrounding atmosphere. Among individual tests, considerable variations were observed in the amount of ^3H released, and cutting into shorter pieces released somewhat more gas. Additional ^3H (about 0.01%) was released on overnight storage of the sheared pieces. In the same operations 0.5 to 1.0% of the ^{85}Kr present was released.

When the sheared samples were subsequently dissolved by refluxing for 6 hr in 13*M* $HNO_3-0.05M$ $HF-0.1M$ $Al(NO_3)_3$, an additional 0.2% of the ^3H was released to the gas. The remaining 99.6% of the ^3H stayed in the fuel solution, presumably as tritiated water. It was verified that, when the fuel solution was concentrated, ^3H was found in the distillate in proportion to the amount of H_2O removed.

DISSOLUTION OF Al–Pu ALLOY

The Plutonium Recycle Test Reactor (PRTR) has made use of UO_2, $PuO_2–UO_2$, and Pu–Al alloy fuels clad in Zircaloy. Dissolution studies of PRTR oxide fuel were reviewed in the Fall 1964 issue of *Reactor Fuel Processing*;[11] also discussed were studies at Savannah River on dissolution of a highly irradiated Pu–Al alloy similar to the PRTR alloy fuel. A recent report by Schulz of Battelle–Northwest[12] discusses methods developed for dissolution of the highly irradiated PRTR Pu–Al alloy fuel in HNO_3, and the methods used for processing such fuel in several campaigns in the Hanford Redox plant.

The fuel alloy is in rod form and is clad with Zircaloy-2. It is transferred for processing in type 6061 aluminum canisters. Several Al–1.8 wt.% Pu alloys of slightly different composition were involved in the program: nickel content varied from 1.3 to 2.0 wt.%, silicon from 0.03 to 1.0 wt.%, iron from 0.07 to 0.40 wt.%, and titanium from 0 to 0.15 wt.%.

For dissolution of aluminum in HNO_3 at practical rates, it is necessary to activate the metal or alloy by the addition of a small amount of $Hg(NO_3)_2$. It was observed that unirradiated Pu–Al–Ni and Pu–Al–Ni–Si alloys were activated only at HNO_3 concentrations of 4*M* or lower, irrespective of $Hg(NO_3)_2$ concentration. It was further observed that irradiation has a profound passivating effect on the behavior of Pu–Al alloys. Since the PRTR fuels were irradiated to the extent of 28 to 48% of the ^{239}Pu present, a special procedure is required for their dissolution. The activation and dissolution procedure used for irradiated PRTR fuel consisted of boiling the declad alloy initially with an activating solution [1.0*M* HNO_3–0.003*M* $Hg(NO_3)_2$], followed by addition of 12.2*M* HNO_3 to achieve a concentration of 3.0*M* to 4.0*M* HNO_3 for dissolution. The dissolver product was typically 2.1*M* HNO_3, 0.5*M* $Al(NO_3)_3$, and 0.001*M* $Pu(NO_3)_4$. In plant operation the aluminum canisters were dissolved in $NaOH–NaNO_3$, and the Zircaloy cladding was removed by boiling with 4*M* NH_4F–0.34*M* NH_4NO_3 for 6 hr.

THERMAL DECLADDING

An interesting concept for decladding stainless-steel-clad oxide fuels has recently been discussed by some Russian workers.[13] Melting of the cladding is proposed as a means of separating it from refractory-oxide pellets or powders (i.e., UO_2 or $UO_2–PuO_2$). Nonwetting of the oxides by the molten steel alloy makes this separation feasible. Sessile-drop methods were used to study the interaction of UO_2 and PuO_2 in pellet form with several stainless-steel alloys (16 Cr–15 Ni–3 Mo, 18 Cr–10 Ni, etc.). Contact angles of the molten-alloy drop ranging from 100 to 145° indicated surface tensions of the order of 1300 to 1700 dynes/cm, and nonwetting was apparent visually. Small pellets (UO_2 < 11 mm in diameter, PuO_2 < 5 mm in diameter) floated on the surface of alloy melts. The pickup of uranium by the molten alloy was only of the order of 0.01 to 0.03% for 10 to 30 min at 1450°C. The presence of simulated fission-product oxides in the UO_2 did not significantly affect uranium pickup by the stainless steel.

Tests were made in which sintered 5-mm-diameter UO_2 pellets in stainless-steel cladding were heated in a vacuum at 1400 to 1500°C in MgO, BeO, and UO_2 crucibles. Decladding was complete in 1 to 2 min, yielding steel ingots with fuel pellets on their surfaces. The pellets remained essentially intact and were readily separated from the ingots.

Separation Processes

In a new fuel-processing plant, ion exchange is proposed for use in the primary separation of plutonium from dissolved fuel. Tests have been performed in Norway of a Purex-process modification involving plutonium partitioning from solvent solution onto silica gel. In the processing of a BeO-moderated High Temperature Gas Cooled Reactor (HTGCR) fuel, the purification of beryllium by crystallization of $BeSO_4$ is proposed.

USE OF AN ION-EXCHANGE PROCESS

In the plant application of processes for separation of nuclear fuels from fission products, solvent extraction methods have received primary consideration. A recent Russian paper, however, discussed the feasibility of the primary separation of high-cross-section fission products from uranium by ion exchange.[14] In this connection it was recently reported[15] that the General Electric Company is planning a processing plant in which plutonium will be sorbed from an irradiated-fuel solution by a single-stage anion-exchange column, eluted, and then purified in a second ion-exchange stage. The effluent from the first-stage ion-exchange column will be dehydrated and calcined, and the uranium will be recovered and decontaminated from the oxides by fluorination and volatilization. This process is designated as the Aquafluor process.

PLUTONIUM PARTITION ON SILICA GEL

Kraak[16] and Hultgren[17] have described pilot-plant studies of a modification of a Purex-type process in which partition of plutonium from uranium is effected by sorption of plutonium from tributyl phosphate (TBP) solution on a column of silica gel, rather than by aqueous extraction with a reducing solution. The loaded solvent stream from the primary-extraction stage is passed through a silica-gel column which has been preconditioned with a solution of Fe^{2+}, stabilized by N_2H_4. Plutonium is reduced and sorbed on the column and is later eluted with 1*M* HNO_3. The

plutonium eluate is then fed to a plutonium extraction column for further decontamination and is concentrated by evaporation.

PROCESSING OF $BeO-PuO_2-UO_2-ThO_2$ FUEL

A proposed processing technique for the fuel from a conceptual BeO-moderated HTGCR has been discussed previously.[18,19] An extensive feasibility study of this concept has been undertaken by the Australian Atomic Energy Commission. The fuel consists of a dispersion of $PuO_2-UO_2-ThO_2$ particles in a matrix of BeO. The fuel element is a sphere about 1 in. in diameter which is coated with a layer of BeO. Because of the high cost of the moderator material, an important aspect of fuel processing is the recovery and decontamination of BeO sufficient for its reuse.

In the conceptual process the BeO-coated fuel spheres are ground in preparation for HNO_3-leaching of actinides, and the BeO residue is dissolved in H_2SO_4. An earlier flow sheet involved the recovery and purification of the beryllium by its conversion to the oxyacetate. In a more recent flow sheet,[20] the $BeSO_4$ solution is extracted with 0.05*M* Primene JMT in an aromatic diluent containing 0.5% capryl alcohol to recover residual actinides. Beryllium sulfate is crystallized from the raffinate after evaporation, and the sulfate is calcined to produce BeO for recycle.

Extraction Separation of Americium and Curium

Plans of the U. S. program for the production and separation of 3 kg of ^{244}Cm from irradiated ^{242}Pu and ^{243}Am were described previously.[21] One step of this program involves extraction of americium and curium from the $Al(NO_3)_3$ solution remaining after the dissolution of Pu–Al irradiation targets in HNO_3 and recovery of plutonium by anion exchange. Henry[22] has described the development of the extraction process. In laboratory experiments it was found that organic-to-aqueous distribution coefficients of the order of 10 to 30 for americium were obtainable with 50% TBP in a paraffinic diluent (Adakane) from low-acid solutions (0.4*M*–0.1*M* HNO_3) containing ~6*M* inextractable nitrate [i.e., from $NaNO_3$, $Ca(NO_3)_2$, $Al(NO_3)_3$]. Europium, typifying rare earths, showed distribution coefficients about twice as great as those of americium; therefore rare-earth separation from americium is not effected by the extraction. Curium extraction is intermediate between those of europium and americium. The use of a 50% TBP solution was proposed to yield a high degree of extraction in a batch operation; the presence of some diluent was thought to be necessary to effect good separation from the aqueous phase (i.e., to lower viscosity and increase density difference).

The solution from the ion-exchange step was approximately 0.7*M* Al^{3+}, and 3.8*M*–4.3*M* Na^+. This was adjusted to 6.5*M*–6.8*M* inextractable nitrate and 0.10*M*–0.35*M* HNO_3 for batch extraction with an equal volume of 50% TBP in Adakane diluent. The recovery of 91 to 95% of the curium was effected by a single extraction; this was increased to 99% by two additional extractions after readjustment to the original acidity. The Am–Cm and lanthanides were stripped from the organic phase with two half-volumes of 0.2*M* HNO_3, and the aqueous solution was washed with dodecane to remove TBP prior to concentration by evaporation. In plant-scale operations about 500 g of Am–Cm mixture was obtained from a 1500-gal batch of feed solution.

Plant and Equipment Design and Operation

An air-lift device is described for the continuous removal of undissolved material from a vertical-tube dissolver. Continuing development work on stacked-clone solvent extraction contactors is reviewed.

SOLIDS-REMOVAL DEVICES

Two interesting hydraulic-lifting devices are proposed by Larner et al.[23] for possible addition to the chop–leach dissolver mentioned in the first part of this section and in the Winter 1964–1965 issue of *Reactor Fuel Processing*.[2] Each of these devices provides a method of continuously removing undissolvable material (such as cut tubes) from a vertical-tube dissolver. With this arrangement the dissolver could be operated continuously.

Two systems are described: air lifting and pulsed-ladder lifting. The authors concluded from their tests on simulated material (Fig. 2) that the air lift would probably be the best from the standpoint of simplicity of equipment and operation. Figure 3 shows the equipment arrangement for the air-lift tests.

The air-lift loop carries the cans from a free-surface box (Fig. 4) at the base of the dissolver column to a separator at the lift head. Here the cans are deflected by a grid, which, by virtue of the air-lift principle, is situated above the liquid free surface, and cans are thus separated from the lift liquid. In an operating dissolver they would then move on to a subsequent cleaning stage; in this model they are recycled to the dissolver to allow continuous operation. The lift air is metered by rotameter and injected near the base of the lift tube. Water flow is indicated by the pressure drop across an orifice in the downcomer tube.

The flow of cans into the lift circuit from the dissolver limb is controlled by a free-surface box, the principle of which is shown in Fig. 4, together with two of the designs that were tested. The function of the box is to divert the mass horizontally so that a free surface of cans is formed, not subject to the weight of the rest of the column of material. Pulses of air injected below this free surface then cause cans to lift and become entrained in a cross flow of liquid through the attached horizontal pipe.

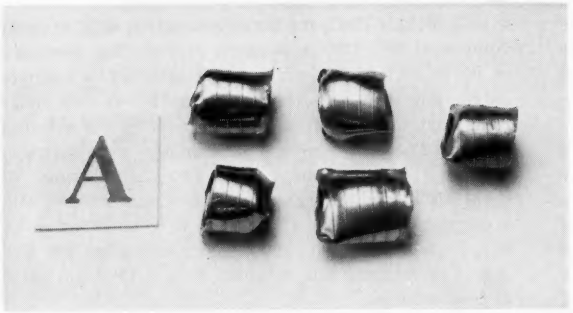

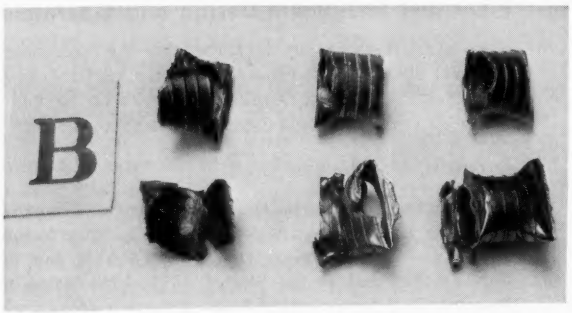

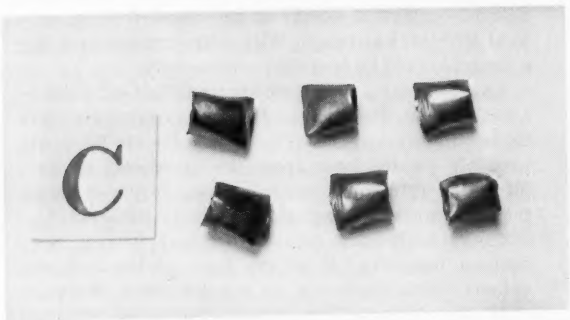

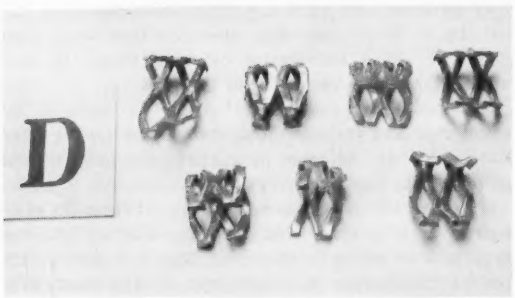

Fig. 2 Sheared material used in transport tests. (From Ref. 23, G. S. Larner, K. W. Carley-Macauly, and R. J. Moulton, Processing in Limited Geometry, Part 16. The Hydraulic Lifting of Solids from a Continuous Dissolver for Nuclear Fuel, British Report AERE-R-5104, February 1966.)

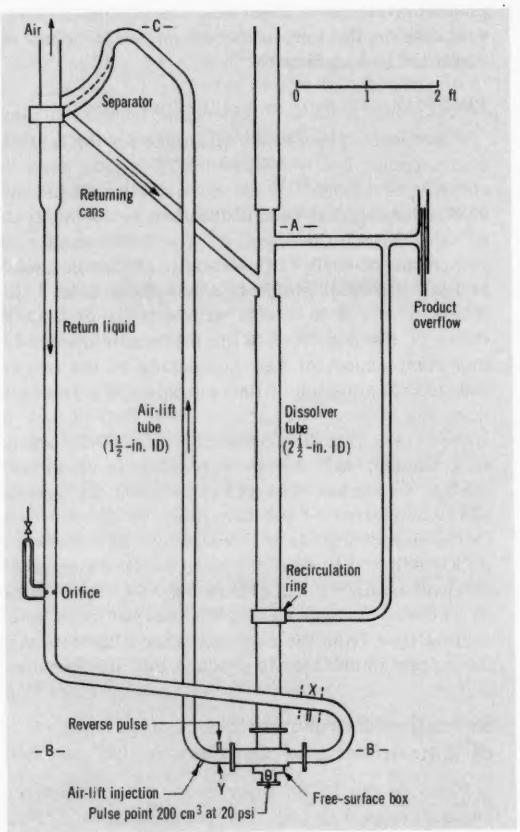

Fig. 3 Air-lift test section. (From Ref. 23, G. S. Larner, K. W. Carley-Macauly, and R. J. Moulton, Processing in Limited Geometry. Part 16. The Hydraulic Lifting of Solids from a Continuous Dissolver for Nuclear Fuel, British Report AERE-R-5104, February 1966. The subject of British and foreign patents and applications.)

Given an air-lift flow above the terminal velocity of cans, the possible throughput of the lift is large, so that the can-removal rate is completely controlled by the frequency and pressure of the pulse. For most tests, air pulses of 300 cm^3 at 20 psig were applied every half minute, dislodging 4 to 15 cans/pulse.

The pulsed ladder makes use of the ratchet principle whereby the liquid leg is pulsed and the cans are trapped on a triangular step while the liquid returns on the back stroke of the pulse.

The authors present further data (e.g., air flow rates, water flow rates, pulse frequencies) as related to can flow for both systems. Table 3 gives some of these data for the air lift.

From this study the authors conclude that such a system would be workable at practical air rates but would have to be further evaluated for individual cases. Actual designs would have to be worked out

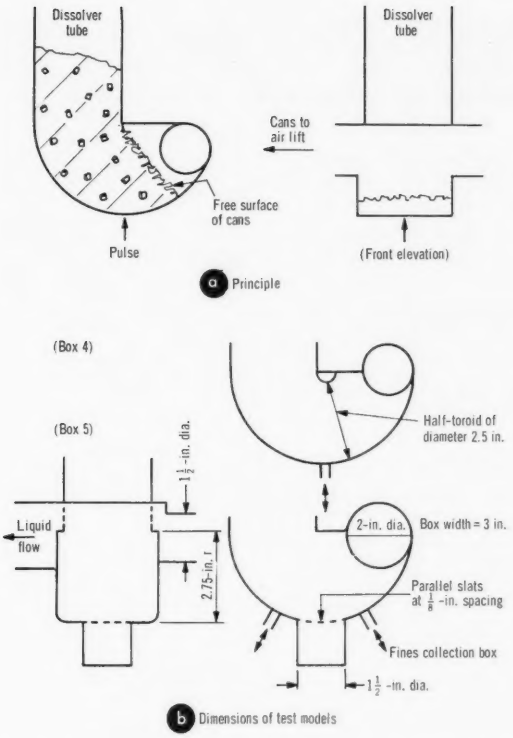

Fig. 4 Free-surface box. (From Ref. 23, G. S. Larner, K. W. Carley-Macauly, and R. J. Moulton, Processing in Limited Geometry. Part 16. The Hydraulic Lifting of Solids from a Continuous Dissolver for Nuclear Fuel, British Report AERE-R-5104, February 1966. The subject of British and foreign patents and applications.)

and tested for such items as removal of fines, transport of chopped pieces of the fuel of interest, and desired capacity of the dissolver.

STACKED-CLONE CONTACTORS

The development work on the stacked-clone solvent extraction contactors, described previously in *Reactor Fuel Processing*,[24,25] continues at ORNL. The most significant advance[1] in the past year was a demonstration that the contactor could be operated with the solvent phase as the continuous phase. Figure 5 (page 69) shows a comparison of this arrangement with that for aqueous-phase-continuous operation. The major changes required to effect this change operationally were reported to be as follows:

1. The end clone adjacent to the organic feed point must have a stronger induced flow.
2. The polishing stages for the aqueous raffinate were removed.
3. Organic-phase polishing stages were installed above the aqueous feed point (these clones are identical to extraction clones).
4. A gravity settler was required at the raffinate end.

It is stated that organic-phase-continuous operation could find application in systems where aqueous-phase viscosities are high, flow ratios (aqueous to organic) less than ½ are desired, and impurities in feed streams cause emulsions in the aqueous-continuous mode.

Data on several such runs are shown in Table 4, which also lists some new data on aqueous-continuous runs using systems with widely varying properties.

Table 3 AIR AND WATER FLOWS NEEDED TO LIFT MATERIAL IN 1½-IN.-DIAMETER AIR-LIFT TUBE[23]
(For a Single Fluid in This Tube, 1 cm/sec = 1.45 liters/min)

Material	Diameter, cm	Weight, g	Air-lift flows, liters/min				Calculated flow of water alone to suspend solid, liters/min
			Submergence*	Air flow	Water flow	Air + water	
Stainless-steel pellet	0.3	0.198			45.4 (pumped)		45
Lead pellet	0.3	0.284	0.89	59.9	48.2	108.1	57.0
Mild-steel cylinder	0.96	5.57	0.69	59.0	47.2	206.2	73.0
Mild-steel cylinder	1.28	10.32	0.89 0.69	47.6 59.0	47.2 44	94.8 103	68.2
Porcelain cylinder	1.0	3.5	0.89	9.7	35.0	44.7	43.4
Aluminum cylinder	0.95	1.96	0.89 0.81	7.9 12.3	26.8 28.5	34.7 40.8	37.0
Mild-steel tube	0.96	2.94	0.89 0.81	15.0 16.7	34.0 35.4	49.0 52.1	
Chopped can A	1.8†	1.18	0.75 0.89	14.2 (5.2)	23.6 (19.6)	37.8 (24.8)	
Chopped can B	2.3†	1.2	0.74 0.81	16.8 (10)	26.6 (18.5)	43.8 (28.5)	
Chopped can ends E	2.2†	2.3	0.75 0.81	16.2 (13)	25.7 (27)	41.9 (40)	

**AB/BC* (Fig. 3).
†Diagonal of right cylinder.

Table 4 STACKED-CLONE CONTACTOR PERFORMANCE AND FLOW-CAPACITY DATA[1]

Continuous phase	Dispersed phase	Distributing species	Density difference, g/cm³	Viscosity of continuous phase, centipoises	Viscosity of dispersed phase, centipoises	Interfacial tension, dynes/cm	Mass-transfer efficiency, %	Flow capacity, liters/min				Temp., °C
								A/O = ½	A/O = 1	A/O = 2	A/O = 3	
0.005*M* CH_3COOH	Hexone	CH_3COOH	0.198	0.89	0.56	7.1	87	3.48	4.50		6.97	25
1.7*M* $Al(NO_3)_3$, 0.2*M* acid deficient	Hexone	$UO_2(NO_3)_2$	0.474	4.17	0.56	8.1	69		1.95		2.83	30
1.0*M* $Al(NO_3)_3$, 0.2*M* acid deficient	Hexone		0.356	1.88	0.56	7.6		2.79	3.43		5.88	25
0.01*M* HNO_3	Mineral oil	C_6H_5COOH	0.121	0.84	116	53	33		2.77		3.88	30
0.01*M* HNO_3	Mineral oil	C_6H_5COOH	0.124	0.66	57	52	38				4.29	40
0.08*M* HNO_3	2-Ethyl-1-hexanol		0.171	0.84	6.6	13.4		1.21	1.43		1.96	30
0.08*M* HNO_3	*N*-Paraffins-175	C_6H_5COOH	0.254	0.84	1.34	36	65	2.23	2.64		3.79	30
0.08*M* HNO_3	*N*-Paraffins-175	C_6H_5COOH	0.258	0.66	1.10	35	57	2.80	3.32		4.57	40
0.08*M* HNO_3	Amsco		0.248	0.84	1.28	45			2.78		3.78	25
0.08*M* HNO_3	Amsco		0.254	0.66	1.07	44		2.71	3.16		4.22	40
0.08*M* HNO_3	Amsco	C_6H_5COOH	0.248	0.84	1.28	35	35	2.02	2.35		3.15	25
0.08*M* HNO_3	Amsco	C_6H_5COOH	0.254	0.66	1.07	35	31		2.92		4.01	40
0.08*M* HNO_3	Amsco		0.253	0.66	1.18	41		3.04	3.60	4.40	4.96	40
Amsco	0.08*M* HNO_3		0.251	1.18	0.66	40		6.28	5.51	4.92		40
Amsco	66 wt.% glycerol, 0.05*M* HNO_3		0.425	1.10	10.2	27		1.60	1.44	1.29	1.24	40
Amsco	1.7*M* $Al(NO_3)_3$, 0.3*M* to 0.9*M* acid deficient		0.56	1.10	3 to 4	31 to 35		2.19	2.16	2.14	2.13	40
Amsco	38 wt.% dextrose		0.409	1.10	2.35	15.6		1.87	1.82	1.78	1.76	40
Amsco	38 wt.% dextrose		0.399	1.33	3.20	12.8		1.47	1.33	1.22	1.17	25
5% TBP–Amsco	1*M* $NaNO_3$, 2.5 g of U per liter	$UO_2(NO_3)_2$	0.296	1.11	0.73	16.3	85	2.29	2.08	1.87	1.76	40
5% TBP–Amsco, 1.0 g of U per liter	1*M* $NaNO_3$		0.296	1.11	0.72	16.2		2.19	1.74	1.44	1.32	40
5% TBP–Amsco	1*M* $NaNO_3$	$UO_2(NO_3)_2$	0.297	1.11	0.72	16	67					40

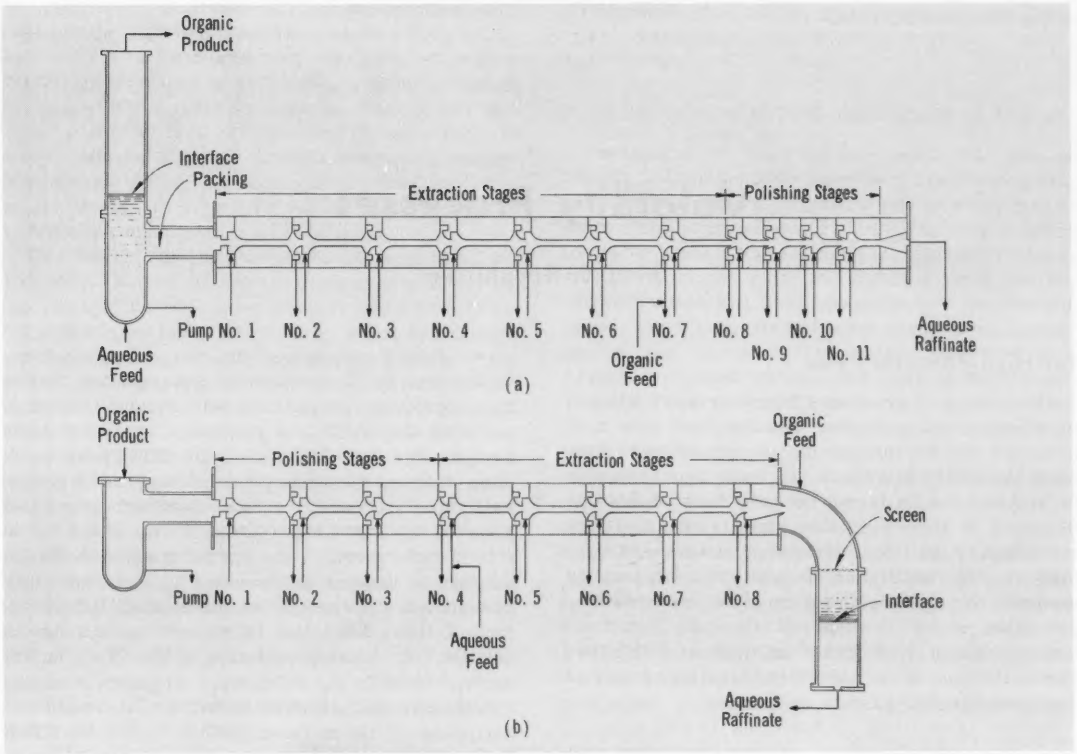

Fig. 5 (a) Normal stacked-clone contactor arrangement for aqueous-continuous operation; (b) stacked-clone contactor arrangement for organic-continuous operation.[1]

References

1. Oak Ridge National Laboratory, Chemical Technology Division Annual Progress Report for Period Ending May 31, 1966, USAEC Report ORNL-3945, September 1966.
2. *Reactor Fuel Process.*, 8(1): 8-9 (Winter 1964–1965).
3. *Reactor Fuel Process.*, 9(1): 16 (Winter 1965–1966).
4. *Reactor Fuel Process.*, 3(1): 9 (January 1960).
5. G. Beone, Dissolution of Fuel Element Jackets of Aluminum and S.A.P. in a Recirculating Dissolver, Italian Report RT/CHI(65)-1, January 1965. Translation available as USAEC Report ORNL-tr-1247.
6. *Reactor Fuel Process.*, 9(2): 69 (Spring 1966).
7. *Reactor Fuel Process.*, 9(2): 70 (Spring 1966).
8. L. M. Ferris, Acid Leaching of Products from the Fluidized-Bed Combustion of Graphite-Base Reactor Fuels and the $HF-O_2$ Disintegration of Stainless Steel- and Zirconium-Clad Oxide Fuels, USAEC Report ORNL-3876, Oak Ridge National Laboratory, November 1965.
9. J. H. Goode, Hot-Cell Evaluation of the Release of Tritium and ^{85}Kr During Processing of ThO_2-UO_2 Fuels, USAEC Report ORNL-3956, June 1966.
10. J. H. Goode, Release of Tritium and Krypton to the Atmosphere During Processing of ThO_2-UO_2 Reactor Fuel, *Trans. Amer. Nucl. Soc.*, 9: 21-22 (June 1966).
11. *Reactor Fuel Process.*, 7(4): 230-231 (Fall 1964).
12. W. W. Schulz, Aqueous Decladding and Dissolution of Plutonium Recycle Test Reactor Fuels. Part I. Plutonium–Aluminum Alloy Fuels, USAEC Report BNWL-204, Battelle–Northwest, April 1966.
13. G. P. Novoselov and A. I. Ageenkov, Thermal Method of Decladding Stainless Steel Canned Fuel Elements, presented at Fuel Processing Symposium, Mol, Belgium, September 1966.
14. *Reactor Fuel Process.*, 9(3): 152 (Summer 1966).
15. *Chem. Eng. News*, 44(33): 31 (Aug. 15, 1966).
16. W. Kraak, Reprocessing Studies of Kjeller, *EuroNuclear*, 3(2): 80-83 (February 1966).
17. A. Hultgren, Reprocessing Experiments, Work with TBP in the Silex Plant at Kjeller, *EuroNuclear*, 3(5): 227-231 (1966).
18. *Reactor Fuel Process.*, 9(4): 194-195 (Fall 1966).
19. *Reactor Fuel Process.*, 8(4): 196 (Fall 1965).
20. R. C. Cairns, M. G. Baillie, M. S. Farrell, and J. R. May, Fuel Cycle Studies for a Beryllium Oxide Moderated High Temperature Gas Cooled Reactor. Second International Thorium Fuel Cycle Symposium, Gatlinburg, Tenn., May 3–6, 1966.
21. *Reactor Fuel Process.*, 9(1): 19-21 (Winter 1965–1966).
22. H. E. Henry, Isolating Americium and Curium from $Al(NO_3)_3-NaNO_3-HNO_3$ Solutions by Batch Extraction with Tributyl Phosphate, USAEC Report DP-972, Savannah River Laboratory, August 1965.
23. G. S. Larner, K. W. Carley-Macauly, and R. J. Moulton, Processing in Limited Geometry. Part 16. The Hydraulic Lifting of Solids from a Continuous Dissolver for Nuclear Fuel, British Report AERE-R-5104, February 1966.
24. *Reactor Fuel Process.*, 8(1): 14-16 (Winter 1964–1965).
25. *Reactor Fuel Process.*, 8(4): 200-201 (Fall 1965).

Volatility Processes

By J. J. Barghusen

For High-Enriched Fuels

Various types of processes based on the volatilities of uranium and plutonium hexafluorides have been proposed for the processing of irradiated reactor fuels. Volatility processes are being applied to both highly enriched fuels and ceramic fuels of low enrichment. In these processes spent reactor fuels are converted to fluorides, and decontamination is carried out by distillation or absorption–desorption methods. A significant feature of several volatility processes under development for both high- and low-enrichment fuels is the application of fluidization techniques to the direct chemical conversion of fuel materials into gaseous compounds.

URANIUM-ALLOY FUELS

Workers in France have applied fluid-bed fluoride-volatility techniques to the recovery of uranium from highly enriched U–Zr alloy fuel and scrap materials.[1,2] The industrial-scale facility, constructed at Brignoud, for scrap-metal recovery has been described by Bourgeois and Nollet.[2] Details of this facility were presented in the Spring 1965 issue of *Reactor Fuel Processing*.[3]

A pilot plant for demonstrating the processing of irradiated U–Zr and U–Al alloy fuels is being constructed at Fontenay-aux-Roses.[1] In this process chemical separation of the alloy-fuel constituents is accomplished by selective volatilization of chlorides and fluorides. The initial processing step involves the reaction of the alloy with anhydrous hydrogen chloride in a fluidized bed of inert alumina particles at 400°C to produce volatile $AlCl_3$ or $ZrCl_4$ and nonvolatile UCl_3. Uranium is recovered as UF_6 in the second step by reaction of UCl_3 with fluorine. The UF_6 product is collected on a bed of sodium fluoride pellets and purified by selective desorption from the sodium fluoride and condensation.

GRAPHITE-BASE FUELS

Wachtel and associates[4] at Brookhaven National Laboratory (BNL) have summarized the results of engineering-scale investigations for processing graphite–uranium carbide fuels using fluid-bed fluoride-volatility techniques. These investigations involved demonstration tests with Rover Nuclear Rocket fuel (pyrolytic graphite-coated uranium dicarbide particles dispersed in a graphite matrix) and High-Temperature Gas-Cooled Reactor (HTGR) fuel (uranium–thorium dicarbide particles dispersed in graphite). The processing scheme for both fuel types involved two basic steps: (1) oxidation of the fuel in a fluid-bed reactor to convert the graphite to CO and CO_2 and to convert the uranium, thorium, and other materials to their respective oxides, and (2) fluorination of the solid oxides to recover the uranium as volatile UF_6. Final purification of the UF_6 from associated volatile fluorides was achieved by selective condensation and sorption techniques. Complete descriptions of the work at BNL on Rover and HTGR fuel materials have been previously reported.[5,6]

The use of anhydrous HCl at temperatures above 1600°C to effect recovery of uranium as a volatile chloride from carbon-coated UC_2 fuel has been briefly studied at Los Alamos Scientific Laboratory.[7] Although this work was not carried out to evaluate a reprocessing scheme, but rather to study the stability of fuel beads at high temperatures, the results of this study are nevertheless pertinent to the technology of fuel reprocessing. The results indicated that the fraction of uranium converted to a volatile chloride increased as the reaction temperature was increased from 1600 to 2100°C. In all tests uranium volatilization was less than 12%. Examination of carbon-coated UC_2 fuel particles, previously exposed to HCl at 1600 to 2100°C, showed that the reaction with HCl proceeds by diffusion of the uranium chloride through the pyrolytic carbon coating rather than by rupture of the coating.

Chloride-Volatility Processing of UO_2–PuO_2 Fuel

Warren and Ferris[8] at Oak Ridge National Laboratory (ORNL) have investigated the feasibility of processing UO_2–PuO_2 fuel containing up to 35 wt.% PuO_2 by chloride-volatility techniques. Since UO_2 reacts with chlorinating agents at a lower rate than U_3O_8, it is desirable to oxidize the fuel to U_3O_8 prior

to chlorination. A series of tests was performed to evaluate the oxidation behavior of sintered UO_2-PuO_2 fuel pellets. It was observed that sintered pellets containing less than 20 wt.% PuO_2 could be converted to $U_3O_8-PuO_2$ powder by oxidation with oxygen for 3 hr at 600°C. Pellets containing 20 wt.% PuO_2 or more could be partially oxidized; however, oxidation was always incomplete even upon extended exposure of the pellets to oxygen at 800°C. No powdering of high-PuO_2-content pellets was observed.

Chlorination studies were performed with 85% Cl_2–15% CCl_4. Within the limits of experimental error, the rates of conversion of uranium oxides to volatile chlorides in the temperature range 450 to 550°C were about the same for small, high-density UO_2-PuO_2 pellets and for $U_3O_8-PuO_2$ powder when the PuO_2 concentration was 5 wt.% or less. The efficiency of chlorination of uranium in $U_3O_8-PuO_2$ powders was not greatly affected by changes in the PuO_2 concentration from 0 to 20 wt.%. At 550°C complete conversion of uranium oxide to UCl_5 and UCl_6 required 3 to 5 hr. At temperatures above 550°C liquid oxychlorides were formed.

The amount of plutonium oxide converted to volatile $PuCl_4$ was proportional to the quantity of chlorine passed through the system. At 500 to 600°C about 10^4 moles of chlorine were required to volatilize 1 mole of $PuCl_4$. This behavior was predictable from the equilibrium constant for the reaction $PuCl_3$ (solid) + 0.5 $Cl_2 \rightleftharpoons PuCl_4$ (gas).

Owing to the high temperatures required to achieve high chlorination rates with concomitant high rates of corrosion of metallic construction materials and the large excesses of chlorine required to volatilize $PuCl_4$, Warren and Ferris[8] conclude that this process is not attractive as a method for recovering uranium and plutonium from oxide fuels.

Fluoride-Volatility Processing of UO_2–PuO_2 Fuel

In the fluoride-volatility processing of UO_2 fuels, the fuel is first declad and then pulverized to produce a powdered material that is highly reactive toward fluorination. Processes based on the use of three different fluorinating agents are being developed:

1. Reaction with fluorine wherein uranium and plutonium are both converted to volatile hexafluorides; plutonium is then separated from uranium by thermal decomposition of PuF_6 to PuF_4.

2. Reaction with BrF_5 to produce volatile UF_6 while plutonium is converted to nonvolatile PuF_4, thereby achieving a separation of uranium from plutonium; plutonium is recovered in a subsequent step as PuF_6 by reaction with fluorine.

3. Reaction with ClF_3 to achieve separation of uranium from plutonium by forming volatile UF_6 and nonvolatile PuF_4; plutonium is then recovered by reaction with fluorine.

Final purification of UF_6 may be achieved by fractional distillation or by selective sorption–desorption on a bed of NaF pellets.

DECLADDING OF STAINLESS-STEEL-CLAD UO_2 FUELS

Decladding of stainless-steel-clad UO_2 fuel is readily accomplished by reaction of the cladding with gaseous mixtures of HF and oxygen in a fluid bed of inert alumina particles at 550 to 625°C. The reaction produces rapid disintegration of the cladding by formation of powdered oxide of stainless steel. As the sintered oxide fuel becomes exposed to the reacting gases, the fuel reacts to form a powdered mixture of oxides and fluorides. Two recent reports[4,9] have reviewed process development work at Brookhaven National Laboratory (BNL) on decladding of stainless-steel-clad fuel elements in fluid beds. Much of this work has been described previously.[10,11]

Decladding studies performed at ORNL[12] have indicated that under certain conditions large lumps of U_3O_8 may be produced which may lead to caking of the fluid bed. It appears that the most significant factor affecting lump formation is the fraction of the cross-sectional area of the fluid-bed reactor occupied by the fuel elements. Under conditions in which the fuel elements initially occupied 7% of the cross-sectional area, no lumps were observed and decladding proceeded satisfactorily. In tests in which the fuel occupied 22% of the cross-sectional area, considerable bed caking resulted. Demonstration tests performed at BNL[4,9] in 3- and 4-in.-diameter reactors, with fuel charges occupying 10% of the reactor cross-sectional area, proceeded without any indications of bed caking.

FLUID-BED FLUORINATION OF UO_2-PuO_2 FUEL WITH FLUORINE

In the processing of sintered UO_2-PuO_2 fuel by fluoride-volatility techniques, the fuel is first converted to U_3O_8 and PuO_2 powder by reaction with oxygen prior to fluorination of uranium and plutonium to hexafluorides with fluorine. A series of tests was performed at Argonne National Laboratory (ANL)[13] to demonstrate the fluorination of large quantities of U_3O_8 powder in a fluid bed of inert alumina particles. In these tests in a 3-in.-diameter fluid-bed reactor, 4.4 kg of UO_2 pellets were charged into a bed containing 6.8 kg of 68- to 84-μ-diameter alumina particles. The pellets upon contact with 25 vol.% oxygen for 4 hr at 450°C produced a fluid bed containing 40 wt.% U_3O_8 powder. Fluorination of the uranium oxide fines was carried out using first 5 vol.% fluorine in nitrogen at 400°C to convert the bulk of the uranium to UF_6 and then using 90 vol.% fluorine at 550°C to complete the conversion reaction. Fluorination rates of 80 lb UF_6/(hr)(sq ft reactor cross section) were achieved for periods of 2 hr when large quantities of uranium fines were present in the fluid

bed. During both processing steps there were no indications of bed caking or sintering of uranium particles.

An alternative method for fluorinating UO_2-PuO_2 fuels, developed at ANL,[13] involves the oxidation of sintered pellet fuel in the lower portion of the fluid-bed reactor to form U_3O_8 and PuO_2 fines that are transported by the fluidizing gas to an upper zone where the fines are contacted with a separate fluorine stream. This process concept, called two-zone oxidation–fluorination, is being used in demonstration tests with UO_2-PuO_2 fuel materials in an engineering-scale alpha facility.[13] Results of the first test in the facility were described in the Fall 1966 issue of *Reactor Fuel Processing*.[14]

Prusakov,[15] in a paper presented at the 36th International Congress on Industrial Chemistry, described the results of experiments with UO_2 fuels employing the two-zone oxidation–fluorination technique. Since the rate of fluorination to UF_6 depends in part upon the rate of transport of U_3O_8 fines into the upper zone, any irregularities in the rate of U_3O_8 transport lead to marked variations in UF_6 production rates. This behavior was avoided by a modification of the process to provide oxidation and fluorination in separate fluid-bed reactors. The sintered UO_2 pellets were oxidized in a fluid-bed reactor, and the U_3O_8 product was continuously conveyed to the fluorinator by means of a pneumatic pulse feeder. Close control of the U_3O_8 feed rate was maintained by regulating the frequency of the pulses.

Demonstration of fluorination of U_3O_8 fines was carried out[15] at 500°C using 24 vol.% fluorine in nitrogen. Uranium hexafluoride production rates were relatively constant at 3500 g UF_6/(hr)(dm^2) [72 lb UF_6/(hr)(sq ft)] throughout the 5.8-hr test. Fluorine efficiency in this test was approximately 90%. It is suggested[15] that, owing to the high fluorine efficiency and the fact that PuF_6 does not exist at high temperature in the absence of fluorine, it may be possible to separate uranium from plutonium by fluorinating U_3O_8 with fluorine in this manner and then recover plutonium separately in a second fluorination step.

FLUORINATION WITH CHLORINE TRIFLUORIDE

Workers at Centre d'Étude de l'Énergie Nucléaire (CEN) at Mol, Belgium, are developing a fluorination process for the recovery of uranium and plutonium from UO_2 fuel based on the selective fluorination of uranium to volatile UF_6 by the use of ClF_3. Schmets et al.[16] have summarized the chemical aspects of the use of chlorine fluorides in volatility processing. A comprehensive study was made to determine the behavior of plutonium during fluorination with chlorine fluorides. In laboratory experiments it was observed that PuF_4 reacts with ClF_3 (30 to 70 vol.% in argon) in the temperature range 225 to 500°C to form volatile PuF_6. An activation energy of 17.5 kcal/mole was calculated from rate data at temperatures below 375°C. In comparison of these data with data using fluorine, it appears that ClF_3 may be a more active agent than fluorine for producing PuF_6 from PuF_4. The reaction between PuF_4 and ClF_3 apparently proceeds by dissociation of ClF_3 at the solid surface to produce ClF and fluorine atoms.

To simulate process conditions and to calculate the potential of ClF as a selective fluorinating agent for uranium, workers studied the reactions between PuF_4 and the following: ClF, gaseous mixtures of ClF_3–chlorine, and ClF_3–ClF. Mixtures of chlorine or ClF with ClF_3 decrease the dissociation of ClF_3 and thus decrease the fluorine concentration in the mixture, thereby reducing the volatilization of PuF_6. It was observed that no reaction occurs between PuF_4 and ClF at temperatures between 200 and 550°C. As the chlorine-to-ClF_3 mole ratio is increased from 0 to 1, there is a marked decrease in the rate of PuF_6 volatilization at 400°C. Plutonium hexafluoride volatility is not completely suppressed in 50 vol.% ClF – 50 vol.% ClF_3; the rate of PuF_6 volatilization in this mixture is equal to that obtained with pure ClF_3 at a temperature 50°C lower.

In studies of the reaction of powdered UO_2 and ClF_3, it was observed that, up to 300°C, the rate of reaction is rather insensitive to temperature and is proportional to the partial pressure of ClF_3. The effects of gas concentration and temperature on the reaction rate are shown in Fig. 1.

The rates of reaction between several uranium compounds and gaseous mixtures containing chlorine and ClF_3 were measured at 400°C. The mole ratio of chlorine to ClF_3 was varied from 0 to 3. It was observed that, as the ratio Cl_2/ClF_3 increased from 0 to 1, the rate of reaction of the gaseous mixture with UF_4, UO_2, and U_3O_8 decreased markedly. Further increase in the ratio to 3.0 did not affect the rate of reaction. The rate of reaction of UO_2F_2 with mixtures of chlorine and ClF_3 was unaffected by changes in composition of the mixture between mole ratios of 0 and 3.

It has been reported previously[17,18] that UO_2 pellets react readily with ClF_3. At low temperatures (~100°C) an induction period is observed,[16] which apparently is related to the pellet density — the higher the density, the longer the induction period. This phenomenon is not observed at 300°C. For fluid-bed reactors it was observed that the reaction proceeds mainly at the inlet to the reactor; therefore it is necessary to inject fluorine at several elevations within the oxide pellet bed in order to achieve high fluorination rates. The rate of reaction of ClF_3 with sintered UO_2 is directly proportional to the concentration of ClF_3 and the linear gas velocity. If fluorine is mixed with ClF_3, an increase in reaction rate and fluorine utilization is observed. Chlorine monofluoride acts as an inert gas; no significant change in reaction rate is observed when ClF is added to ClF_3.

When chlorine is added to ClF_3, the rate of reaction decreases owing to formation of ClF. Chlorine monofluoride does not react readily with sintered bodies of UO_2 at temperatures up to 450°C, and it is necessary to pulverize the oxide pellets prior to fluorination with ClF.

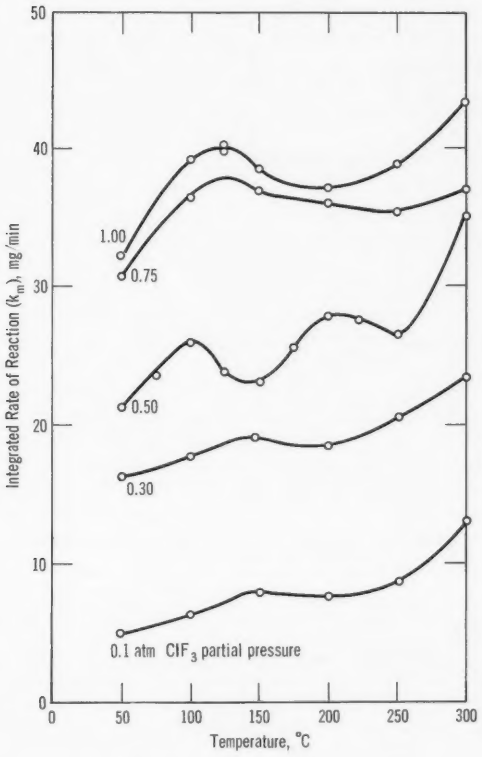

Fig. 1 Rate of reaction[16] of UO_2 with ClF_3.

The processing of sintered UO_2 pellets with ClF_3 has been demonstrated in a fluid-bed reactor using a pellet-bed depth of 1 m. In this test 25 vol.% ClF_3 in nitrogen was introduced into the reactor at 6 cm/sec at a temperature of 100°C. Reaction rates of 3.8 kg UO_2/(hr)(dm^2) [98.8 lb UF_6/(hr)(sq ft)] were sustained, with an average fluorine utilization of 81% during the period of up to 85% conversion.

One processing cycle under investigation at CEN involves oxidation of sintered fuel to U_3O_8 followed by hydrofluorination to a powdered mixture of UO_2F_2 and UF_4. The reaction of this powdered mixture toward ClF_3 and mixtures of chlorine and ClF_3 has been studied.[16] The rate of reaction with ClF_3 increases with an increase in temperature between 150 and 200°C and with an increase in ClF_3 concentration. In a fluid-bed reactor, at 200°C with 14 vol.% ClF_3 in nitrogen, rates of reaction with UO_2F_2 and UF_4 equivalent to 3.6 kg UO_2/(hr)(dm^2) [93.6 lb UF_6/(hr)(sq ft)] were achieved. The reaction of UO_2F_2 and UF_4 with an equimolar mixture of ClF_3 and chlorine showed a maximum at 300°C. A linear relation was observed between the rate of reaction and the concentration of reaction species for equimolar mixtures of ClF_3 and chlorine. It was expected that equimolar mixtures of chlorine and ClF_3 would behave like ClF. This was not observed; the relative reaction rates corresponding to ClF = 1.0 were 1.65 for ClF_3–chlorine and 1.83 for ClF_3.

A proposed flow sheet for the reprocessing of fast reactor fuels by application of the chlorine fluoride process is shown in Fig. 2. In the flow sheet, blanket-fuel pins (stainless-steel clad) are chemically declad by reaction with a mixture of HF and oxygen. The blanket fuel is then contacted with a mixture of ClF and ClF_3; the concentration of ClF_3 is maintained at a low level to minimize PuF_6 volatilization. The reagents are recycled and fluorine is introduced in the gas loop to regenerate ClF and ClF_3. The gas stream is periodically purged to eliminate oxygen produced in the reaction. The UF_6 is selectively sorbed on a bed of sodium fluoride, then desorbed, and finally purified by distillation.

Core fuel elements are processed by decladding and pulverization by either oxygen or a mixture of oxygen and HF. The fuel is then contacted directly with fluorine to produce simultaneously UF_6 and PuF_6. If desired, uranium could be recovered separately as UF_6 by fluorination with ClF.

FLUORINATION OF UO_2–PuO_2 WITH BrF_5

Recent studies at ANL have concerned the use of BrF_5 to selectively convert uranium in UO_2–PuO_2 fuel to volatile UF_6 while plutonium is converted to nonvolatile PuF_4. The process flow sheet for Zircaloy-clad UO_2–PuO_2 fuel[19] is shown in Fig. 3. The process involves four steps: (1) the oxide fuel is declad by reaction of the Zircaloy cladding with HCl to form volatile $ZrCl_4$ that is subsequently converted to solid ZrO_2; (2) the oxide pellets that remain unaffected by the decladding step are contacted with oxygen at 450°C to form a mixture of U_3O_8 and PuO_2 fines (~20 μ in diameter); (3) the oxide fines are contacted with BrF_5 at 300°C (Fluorination I) to form UF_6 that is volatilized from the fluid-bed reactor and collected in a condenser together with excess BrF_5, volatile fission-product fluorides, and with the reaction product, elemental bromine; and (4) plutonium is fluorinated to volatile PuF_6 (Fluorination II) by reaction with fluorine at 300 to 550°C. Final purification of the UF_6 product is effected by fractional distillation techniques. Plutonium is recovered by thermal decomposition of PuF_6 to solid PuF_4.

In the application of the BrF_5 process to the recovery of uranium and plutonium from spent fuel, it

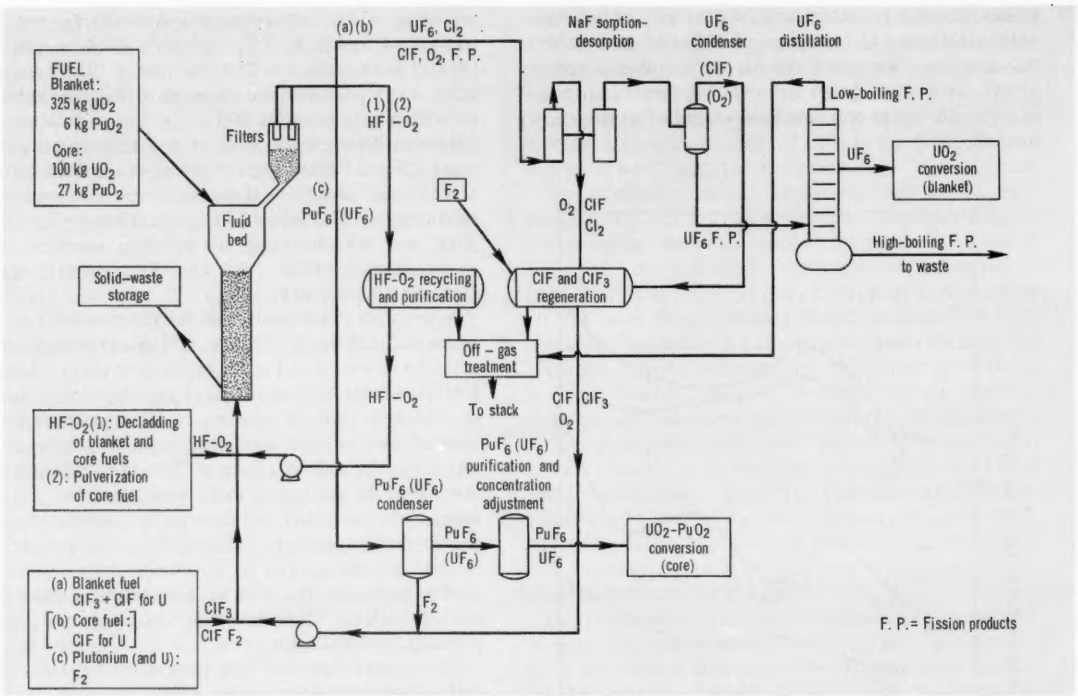

Fig. 2 Flow sheet[16] for recovery of uranium and plutonium from fast reactor fuels using chlorine fluorides.

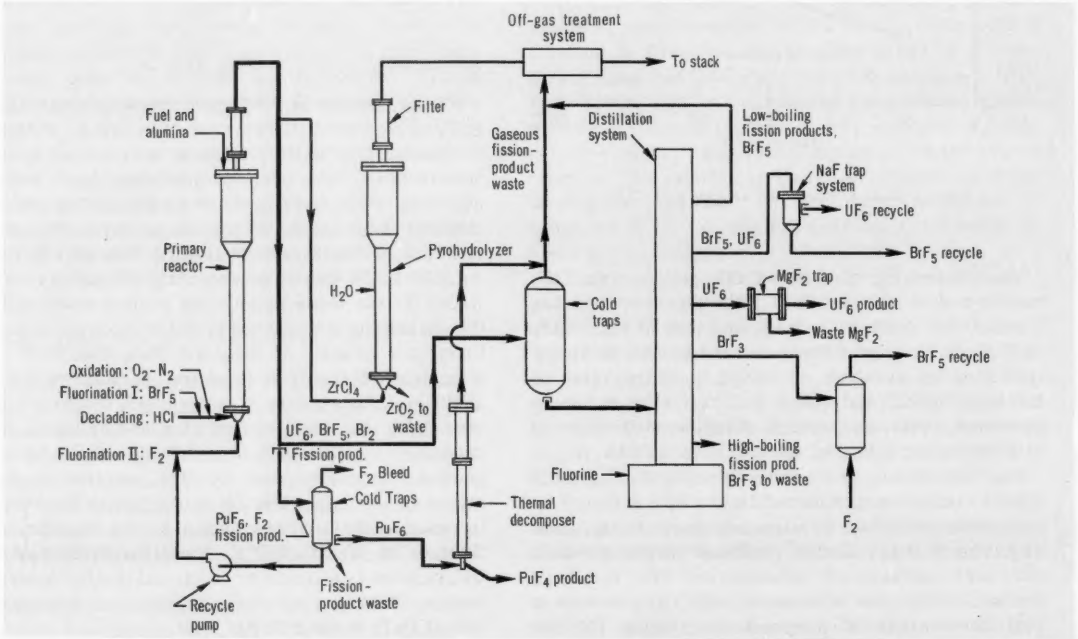

Fig. 3 Flow sheet for reprocessing of UO_2 fuel material using bromine pentafluoride.[19]

is necessary to consider the recycle of BrF_5. Two different schemes for BrF_5 recycle are being considered. In the first scheme, presented in part in Fig. 3, the liquid mixture containing bromine, BrF_5, fission-product fluorides, and UF_6 is contacted with fluorine at 30°C. Under these conditions bromine is rapidly and completely converted to BrF_3. At slightly higher temperatures some BrF_5 will be formed. The fluorinated mixture is then distilled to separate the UF_6 from the interhalogens and fission-product fluorides. The BrF_3 fraction is then fluorinated to BrF_5 with fluorine at 400°C prior to recycle.

The second scheme involves fluorination of the bromine to BrF_3 in the upper portion of the primary fluid-bed reactor and completion of the regeneration of BrF_5 in a separate gas-phase fluorination reactor. By dividing the refluorination (to form BrF_5) between the fluid-bed reactor and the separate gas-phase reactor, the size and cooling requirements of the separate gas-phase reactor can be substantially reduced without impairing the performance of the overall process. The gas-phase reactor is supplied with fluorine in slight excess of the stoichiometric requirement and is operated at about 400°C.

Laboratory experiments have been performed to study the reactions of BrF_5 with various uranium compounds. During this study the kinetics of the reactions between BrF_5 and UF_4, UO_2F_2, U_3O_8, UO_3, and UO_2 were measured. A summary[20] of the data appears in Table 1 in the form of constants for the equations representing the temperature and BrF_5 partial-pressure dependence of the rates of reaction.

Table 1 EQUATIONS FOR ESTIMATING THE RATES OF REACTION OF BrF_5 WITH URANIUM COMPOUNDS[20]

(Rate Equation: $\log k = n \log P - (A/T) + B$, Where P Is in torrs and k Is in min^{-1})

	UF_4	UO_2F_2	U_3O_8	UO_2	UO_3
n	0.38	0.71	0.90	0.84	1.05
A	3690	1810	2000	1630	1680
B	4.286	0	−0.220	−0.270	−0.767
Activation energy, kcal/mole	16.9	8.3	9.2	7.5	7.7

Demonstration tests on the $O_2-BrF_5-F_2$ process cycle are being carried out in a 2-in.-diameter fluid-bed reactor with UO_2-PuO_2 fuel containing simulated fission products. A series of tests was performed to determine the effect of the BrF_5 fluorination temperature on plutonium recovery in the subsequent fluorination step.[21–23] In these tests 650 g of sintered pellets and 1100 g of alumina containing 0.6 g of cesium fluoride (CsF) were charged to the fluid-bed reactor. The pellets were pulverized with 20 vol.% oxygen for 4 hr at 450°C. The oxide fines were reacted with 10 vol.% BrF_5 in nitrogen for 2 hr. The temperature levels of the BrF_5 fluorination step in the series of three tests were 200, 300, and 400°C. Plutonium fluorination was carried out with 90 vol.% fluorine for 3 hr at 300°C, for 5 hr while the temperature of the reactor was increased from 300 to 550°C, and for 3 hr at 550°C.

The plutonium concentrations in the alumina beds after fluorination were: 0.009 wt.% for BrF_5 fluorination at 200°C, 0.007 wt.% for BrF_5 fluorination at 300°C, and 0.012 wt.% for BrF_5 fluorination at 400°C. On the basis of these data, it appears that the BrF_5 fluorination temperature does affect the extent of plutonium removal, and the best temperature for the BrF_5 fluorination step is 300°C.

Engineering-scale studies in a 3-in.-diameter fluid-bed reactor have indicated[24] that large quantities of U_3O_8 powder can be fluorinated to UF_6 at high rates with 12 vol.% BrF_5 at 250 to 275°C. In one test 4.4 kg of UO_2, after oxidation to U_3O_8 powder, was completely fluorinated to UF_6 in 3 hr. The average rate of UF_6 production in this test was 86 lb UF_6/(hr)(sq ft reactor cross section). Since the bulk of the uranium was fluorinated during the first 2 hr, rates approaching 130 lb UF_6/(hr)(sq ft) were achieved for short periods. No external heat was supplied to the reactor during fluorination, and the reactor was cooled by natural air convection. The average BrF_5 utilization during the 3 hr of fluorination was 60%.

Experiments have been performed at ANL to determine the behavior of neptunium during the $O_2-BrF_5-F_2$ process. It has been shown[23] that NpF_4 reacts with BrF_5 to form volatile NpF_6 at rates significantly lower (by factors of about 10^{-2}) than rates measured for the UF_4-BrF_5 reaction. Demonstration tests with UO_2-PuO_2 fuel spiked with NpO_2 have confirmed[24] that neptunium volatilizes along with UF_6 in the BrF_5 fluorination step.

PILOT-PLANT DESIGN STUDIES

In connection with the plan of the U. S. Atomic Energy Commission to construct a hot engineering-scale pilot plant at ORNL to demonstrate the separation of plutonium and uranium from low-enrichment fuels, workers at ORNL have been concerned with the design of the major equipment items required in the pilot-plant facility. Details of the ORNL studies have been published in an annual report.[12]

Among the process studies being made at ORNL is the development of methods for continuous in-line monitoring of process gas streams.[12,25] Evaluations of gas chromatography and of infrared and ultraviolet spectrophotometry are being made.

Conceptual plant studies and evaluation of plant-scale component designs, such as compressors, are being performed at the Oak Ridge Gaseous Diffusion Plant (ORGDP) in connection with the construction of the hot pilot plant at ORNL. A summary of the scope of the studies at ORGDP is presented in a recent paper.[26]

CORROSION IN FLUORIDE-VOLATILITY PROCESSES

Owing to the high temperatures and the highly reactive nature of the principal reagents used in the fluid-bed volatility processes, corrosion of equipment and piping must be carefully considered in the design of processing plants. A survey of corrosion data related to fluoride-volatility processes indicated that, upon exposure to process conditions, nickel may exhibit intergranular modifications. Subsequent studies[12] showed that similar modifications in Nickel-200 and Nickel-201 were produced by exposing coupons to alumina, a material that might be used for the fluid bed. Different types of alumina produced varying degrees of modifications, usually in proportion to their sulfur content. Sulfur was identified by chemical spot tests and microprobe analysis in the affected areas of the nickel coupons. Nickel coupons exposed to a relatively pure grade of alumina showed a significant loss of ductility. Attempts to solve the problem will be made by alloying the nickel, seeking sulfur-free raw materials, or developing purification methods. Modifying the nickel will probably be most effective because of the presence of sulfur-related fission products in the process.

An investigation has been carried out at ANL[13] to determine the rates of corrosion of Nickel-200, Monel, and Inconel by some volatile fission-product fluorides, namely, GeF_4, AsF_5, SeF_6, MoF_6, and TeF_6, either individually or in the presence of fluorine. Data were obtained at 500°C for exposures up to 29.5 hr. The corrosion rates of nickel and Monel when exposed to the fluorides alone or in the presence of fluorine excluding TeF_6 were low (< 0.008 mil/hr), whereas Inconel exhibited corrosion rates up to 0.284 mil/hr. The corrosion of nickel and Monel by TeF_6 is quite rapid, with rates up to 0.608 mil/hr. The rate of corrosion of Inconel by TeF_6 was 0.030 mil/hr. Essentially no corrosion of nickel or Monel was observed in a TeF_6 and fluorine environment. Very little intergranular penetration of nickel and Monel by TeF_6 was observed. High concentrations of TeF_6 appear to cause severe surface corrosion of nickel and Monel; however, the partial pressure of TeF_6 in the fluid-bed reactor under process conditions should be considerably less than 1 mm Hg.

A survey of the corrosion of several metals by gases containing fluorine has been published by Vincent.[27] In particular, this article discusses the corrosion of steel and nickel by UF_6. The reactions of UF_6 with metals are considered to be a special case of dry oxidation. In a comprehensive study of the corrosion of copper by ClF_3, Vincent[28] observed that the kinetics of the reaction was of the same order of magnitude as the copper–fluorine reaction. At 1 atm the reaction occurs by the formation of CuF_2 and CuCl. The presence of the latter product indicates that ClF_3 does not act simply as a fluorinating agent.

In a study of the fluorination of metallic nickel by fluorine at 540 to 810°C, Luk'yanychev, Astakhov, and Nikolaev[29] observed that the kinetics of the reaction is determined by a diffusion mechanism. Over the temperature interval 540 to 600°C, the activation energy of the reaction is 59 kcal/mole, whereas, at temperatures between 720 and 810°C, the activation energy is 18.5 kcal/mole. The difference in the values of the activation energy is attributed to a change in crystal structure of the nickel fluoride film, not to a change in the composition of the film. The decrease in activation energy at high temperatures is evidently due to enhancement of the diffusion process of the reacting substances as a result of the growth of NiF_2 crystals.

SAFETY ASPECTS AND ENVIRONMENTAL CONTAMINATION CONTROL

High-efficiency cleaning systems for treating the environmental air in plutonium-handling facilities are required since the permissible concentrations for plutonium in air are extremely low (3×10^{-8} mg $^{239}Pu/m^3$ air). Special considerations must be taken for facilities in which PuF_6 is handled owing to the high volatility of PuF_6. Kessie and Ramaswami[30] have evaluated the factors that affect the filtration of plutonium particulate matter obtained by the hydrolysis of PuF_6 with moisture in the environmental air. Details of this study were presented in the Winter 1965–1966 issue of *Reactor Fuel Processing*.[31]

In connection with the design of the ORNL fluoride-volatility pilot plant for processing irradiated fuel materials, Miles[32] has prepared a survey of the criteria required for the design of equipment to ensure safety in handling of plutonium within the facility. The quantity of plutonium to be handled per run will vary from 200 to 1250 g, whereas the in-plant inventory may reach 10 kg.

The off-gas streams from the fluoride-volatility processing of reactor fuel materials represent materials that require further treatment before discharge to the environment. Workers at ANL[33,34] are developing methods for the disposal of waste fluorine from process gas streams using fluidization techniques. Activated alumina has been shown to be a highly effective agent for removing fluorine from process gas streams. The reaction between fluorine and alumina is characterized by an initial period during which the fluorine concentration in the off-gas from the fluid-bed reactor remains at a relatively constant value, less than 50 ppm, and by a breakthrough period in which the fluorine concentration increases rapidly to greater than 50 ppm. It was observed that: (1) increasing the bed temperature from 300 to 400°C, increasing the ratio of bed depth to diameter from 3 to 6, and decreasing the alumina particle size from 28–48 mesh to 48–100 mesh were all effective in increasing the capacity of activated

alumina for fluorine and (2) changing the fluidizing gas velocity (1.25 to 1.65 times the minimum fluidizing velocity) and changing the fluorine concentration in the gas stream (from 5 to 75 vol.% in nitrogen) had no effect on the capacity of the bed. In the course of this work, fluorine capacities as high as 0.8 g F_2/g activated alumina were achieved. The theoretical capacity (complete conversion to aluminum fluoride) is 0.95 g F_2/g activated alumina.

Several reports related to safety procedures in handling of fluorinating agents[35] and in the handling and storage of UF_6 (Refs. 36–38) are available.

BINARY PHASE DIAGRAMS INVOLVING URANIUM HEXAFLUORIDE

Vapor–liquid equilibrium data have been obtained[39] for the system UF_6–PuF_6 in the composition range 1 to 48 mole % PuF_6 at 73 to 89°C. Results indicate that the activity coefficients of both UF_6 and PuF_6 are close to unity, and the mixtures behave ideally in the concentration range studied. Fractional distillation columns for the distillation of UF_6-rich mixtures can be designed assuming ideal behavior of UF_6–PuF_6 solutions.

Trevorrow and associates[40] at ANL have published data on the condensed-phase equilibria for the system MoF_6–UF_6. The data were obtained by thermal analysis and X-ray diffraction techniques. The temperature–composition phase diagram (Fig. 4) is characteristic of a binary system forming solid solutions, a minimum-melting mixture (22 mole % UF_6 at 13.7°C), and having a solid miscibility gap. The diagram shows that the maximum solid solubility of the smaller MoF_6 molecule in the UF_6 lattice is about 30 mole % MoF_6, whereas the maximum solubility of UF_6 in the MoF_6 lattice is 12 to 18 mole % UF_6. The temperature of the solid-state transformation of MoF_6 increases from about −5°C in mixtures with UF_6, indicating that the solid solubility of UF_6 is greater in the low-temperature form of MoF_6 than in the high-temperature form. This solid-solubility relation can be expected in view of the crystal structure of the pure components. The X-ray diffraction pattern of the high-temperature form of pure MoF_6 can be indexed as a body-centered cubic structure, and the X-ray pattern of the low-temperature form can be indexed as an orthorhombic structure similar to the orthorhombic structure of UF_6.

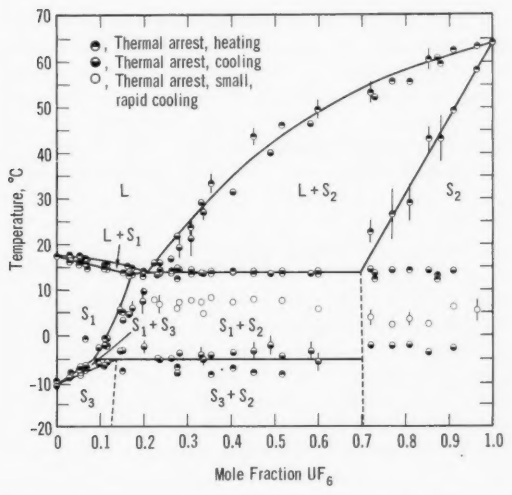

Fig. 4 Phase equilibria[40] in the condensed system UF_6–MoF_6.

References

1. Jean Sauteron, *Les Combustibles Nucléaires*, Hermann, Paris, 1965, pp. 394-400.
2. M. Bourgeois and P. Nollet, Étude du Traitement Chimique des Combustibles Uranium-Zirconium par Voie Sèche, *Energie Nucl.*, 8(3): 165-174 (May 1966).
3. *Reactor Fuel Process.*, 8(2): 88-90 (Spring 1965).
4. S. J. Wachtel, J. J. Reilly, C. B. Bartlett, R. Johnson, and E. Wirsing, Jr., Reprocessing of Nuclear Fuels by Volatility Separations in Fluidized Beds, USAEC Report BNL-973, Brookhaven National Laboratory, March 1966.
5. *Reactor Fuel Process.*, 9(2): 84-85 (Spring 1966).
6. *Reactor Fuel Process.*, 8(2): 90-91 (Spring 1965).
7. M. E. Smith, J. H. Cappis, and G. R. Waterbury, Leaching of Uranium by Hydrogen Chloride from Pyrolytic-Carbon-Coated Uranium Dicarbide Beads, USAEC Report LA-3488, Los Alamos Scientific Laboratory, Feb. 1, 1966.
8. K. S. Warren and L. M. Ferris, Oxidation and Chlorination of UO_2–PuO_2, USAEC Report ORNL-3977, Oak Ridge National Laboratory, July 1966.
9. C. B. Bartlett, E. Wirsing, Jr., S. J. Wachtel, R. Johnson, J. J. Reilly, and L. P. Hatch, Fluidized Bed Reprocessing of Stainless Steel Clad UO_2 Powder Reactor Fuels, USAEC Report BNL-968, Brookhaven National Laboratory, November 1965.
10. *Reactor Fuel Process.*, 9(1): 26-27 (Winter 1965–1966).
11. *Reactor Fuel Process.*, 9(4): 206-208 (Fall 1966).
12. Oak Ridge National Laboratory, Chemical Technology Division Annual Progress Report for Period Ending May 31, 1966, USAEC Report ORNL-3945, September 1966.
13. Argonne National Laboratory, Chemical Engineering Division Semiannual Report July–December 1965, USAEC Report ANL-7125, May 1966.
14. *Reactor Fuel Process.*, 9(4): 208-209 (Fall 1966).
15. V. N. Prusakov, V. K. Ezhov, O. G. Lebedev, and V. K. Popov, Some Aspects of Nuclear Fuel Reprocessing by Fluorination Method, paper presented at the 36th International Congress on Industrial Chemistry, Brussels, Sept. 10–21, 1966.
16. J. Schmets et al., The Use of Chlorine Fluorides for the Reprocessing of Spent Nuclear Fuels, paper presented at the National Meeting of the American Chemical Society, New York, Sept. 12–16, 1966.
17. *Reactor Fuel Process.*, 9(4): 209-210 (Fall 1966).
18. *Reactor Fuel Process.*, 9(3): 159 (Summer 1966).
19. J. J. Barghusen, M. J. Steindler, D. Ramaswami, and A. A. Jonke, The Use of Bromine Pentafluoride in the Reprocessing of Low Enrichment Nuclear Reactor Fuels, paper presented at the National Meeting of the American Chemical Society, New York, Sept. 12–16, 1966.
20. R. M. Adams and A. Glassner (Comps.), Reactor Devel-

opment Program Progress Report, August 1966, USAEC Report ANL-7249, pp. 57-58, Argonne National Laboratory, Sept. 23, 1966.
21. R. M. Adams and A. Glassner (Comps.), Reactor Development Program Progress Report, February 1966, USAEC Report ANL-7176, pp. 64-65, Argonne National Laboratory, Mar. 23, 1966.
22. R. M. Adams and A. Glassner (Comps.), Reactor Development Program Progress Report, April 1966, USAEC Report ANL-7204, p. 63, Argonne National Laboratory, May 31, 1966.
23. R. M. Adams and A. Glassner (Comps.), Reactor Development Program Progress Report, July 1966, USAEC Report ANL-7245, pp. 45-46, Argonne National Laboratory, Aug. 26, 1966.
24. R. M. Adams and A. Glassner (Comps.), Reactor Development Program Progress Report, September 1966, USAEC Report ANL-7255, pp. 58-59, Argonne National Laboratory, Oct. 26, 1966.
25. M. E. Whatley, P. A. Haas, R. W. Horton, A. D. Ryon, J. C. Sudduth, and C. D. Watson, Unit Operations Section Quarterly Progress Report, January–March 1966, Chemical Technology Section, USAEC Report ORNL-3995, Oak Ridge National Laboratory, September 1966.
26. S. H. Smiley, J. H. Pashley, and D. C. Brater, Fluid-Bed Volatility Component, Engineering Feasibility, and Scale-up Studies at the Oak Ridge Gaseous Diffusion Plant, USAEC Report K-L-6091, Oak Ridge Gaseous Diffusion Plant, 1966.
27. L. M. Vincent, Corrosion Due to Gases Containing Fluorine. The Special Case of Dry Oxidation, *Genie Chim.*, 95(4): 611-621 (April 1966).
28. L. Vincent, Corrosion of Copper by Chlorine Trifluoride, French Report CEA-R-2790, Jan. 16, 1965.
29. Yu. A. Luk'yanychev, I. I. Astakhov, and N. S. Nikolaev, Mechanism of the Formation of Fluoride Films on Nickel and Their Properties, *Bull. Acad. Sci. USSR, Div. Chem. Sci. (English Transl.)*, (No. 4): 577-581 (April 1965).
30. R. W. Kessie and D. Ramaswami, Removal of Plutonium Hexafluoride from Cell Exhaust Air by Hydrolysis and Filtration, USAEC Report ANL-7066, Argonne National Laboratory, December 1965.
31. *Reactor Fuel Process.*, 9(1): 29-31 (Winter 1965–1966).
32. F. W. Miles, Plutonium-Related Safety Aspects in Designing the Fluidized-Bed Volatility Pilot Plant, USAEC Report ORNL-TM-1593, Oak Ridge National Laboratory, November 1966.
33. R. M. Adams and A. Glassner (Comps.), Reactor Development Program Progress Report, August 1966, USAEC Report ANL-7249, p. 60, Argonne National Laboratory, Sept. 23, 1966.
34. R. M. Adams and A. Glassner (Comps.), Reactor Development Program Progress Report, September 1966, USAEC Report ANL-7255, p. 89, Argonne National Laboratory, Oct. 26, 1966.
35. D. R. Cloyd and W. J. Murphy, Technology Survey, Handling Hazardous Materials, Report NASA-SP-5032, Chap. 3, Liquid Fluorine, pp. 43-54 and Chap. 4, Chlorine Trifluoride, pp. 55-62, September 1965.
36. E. L. Keller (Comp. and Ed.), Uranium Hexafluoride Handling Procedures and Container Criteria, USAEC Report ORO-651, 1966.
37. W. R. Pedigo, V. A. Smith, S. Bernstein, W. J. Hammer, and J. L. Myers, Testing of Ten-Ton Uranium Hexafluoride Cylinders, USAEC Report KY-500, Paducah Gaseous Diffusion Plant, Oct. 22, 1965.
38. *Chem. Eng. News*, 44(24): 79 (June 13, 1966).
39. D. V. Steidl, L. E. Trevorrow, and M. J. Steindler, Laboratory Investigations in Support of Fluid-Bed Fluoride Volatility Processes. Part XI. Vapor–Liquid Equilibria in the System Uranium Hexafluoride–Plutonium Hexafluoride, USAEC Report ANL-7186, Argonne National Laboratory, April 1966.
40. L. E. Trevorrow, M. J. Steindler, D. V. Steidl, and J. T. Savage, Laboratory Investigations in Support of Fluid-Bed Fluoride Volatility Processes. Part XIII. Condensed Phase Equilibria in the System Molybdenum Hexafluoride–Uranium Hexafluoride, USAEC Report ANL-7240, Argonne National Laboratory, August 1966.

Compact Pyrochemical Processes

By T. R. Johnson

Pyrochemical processes are a class of nonaqueous procedures for the recovery and purification of both ceramic (oxide and carbide) and metallic reactor fuels. These processes make extensive use of molten metals and salts as media in which separations are effected. The liquid metals are typically alloys of magnesium with copper, cadmium, or zinc, and the salts are usually mixtures of magnesium chloride and chlorides of alkali and alkaline-earth metals. In other pyrochemical processes certain types of fuel are treated in the absence of a solvent.

Because pyrochemical processes have certain technological and economic features that should be particularly beneficial in fast reactor fuel cycles, much of the developmental effort is directed toward the recovery of fast breeder fuels. Among these features are (1) the ability to accommodate short-cooled, high-burnup fuels with a consequent reduction in out-of-reactor fuel inventories, (2) small process volumes that require a minimum of shielded space, (3) less restrictive criticality limits because of the absence of neutron-moderating materials, (4) compact, solid-waste streams, and (5) adaptability to small, on-site plants for one or a few reactors. In the case of metal fuels, expensive alloying agents can be recovered. Since these processes do not provide complete fission-product removal, all handling operations including fuel refabrication are performed remotely.

Salt-Transport Processes

Fuel-recovery processes that incorporate a salt-transport step[1] for removal of fission products are being investigated at Argonne National Laboratory (ANL). In the salt-transport step, fissile and fertile constituents of the fuel are transferred selectively from one liquid-metal solution (donor solvent) to other metal solutions (acceptor solvents), while fission products remain in the donor solvent. A molten-salt phase containing magnesium chloride serves as the carrier for the transfer of solutes between the liquid-metal solutions.

The selective transport of the valuable fuel constituents takes place as a result of differences in distribution coefficients and solubilities of the fuel constituents in the metal donor alloy : salt solvent : metal acceptor alloy systems. The various salt/metal systems under consideration and the advantages of each were discussed in the Spring 1966 issue of *Reactor Fuel Processing*.[1] The metal donor alloy : salt solvent : metal acceptor alloy systems that seem promising for the transport of uranium and/or plutonium away from noble-metal fission products and fuel-cladding elements are Cu–5 wt.% Mg : $MgCl_2$: Zn–Mg; Cu–33 wt.% Mg : $MgCl_2$–NaCl–KCl : Zn–Mg; Cd–Mg : $MgCl_2$–NaCl–KCl : Zn–Mg; and Cd–Zn–Mg : $MgCl_2$–NaCl–KCl : Zn–Mg.

Salt-transport processes utilize simple, compact equipment. Volumes of the process solutions are small since not all the uranium or plutonium is in solution at any one time. The processes show promise of providing good fission-product removals and high recoveries of uranium and plutonium.

REFERENCE FLOW SHEET

The reference flow sheet[2] (Fig. 1) of the salt-transport process that is currently under investigation at ANL differs slightly from that described in the Spring 1966 issue of *Reactor Fuel Processing*.[1] After the fuel is separated from its cladding by dissolution in zinc, the fuel is fed to a reduction–partition step. The alkali, alkaline-earth, and rare-earth fission products are extracted into the salt phase; uranium, plutonium, and the remaining non-volatile fission products are reduced by a Cu–33 wt.% Mg alloy and appear in the metal phase. Uranium is insoluble and plutonium is soluble in this metal phase. Plutonium is then separated from the remaining fission products and uranium by a salt-transport step. The Cu–Mg donor alloy and a Zn–Mg acceptor alloy are placed in mutual contact with a $MgCl_2$-based carrier salt, and plutonium is transferred to the Zn–Mg alloy. The uranium and the fission products remain in the copper alloy. In

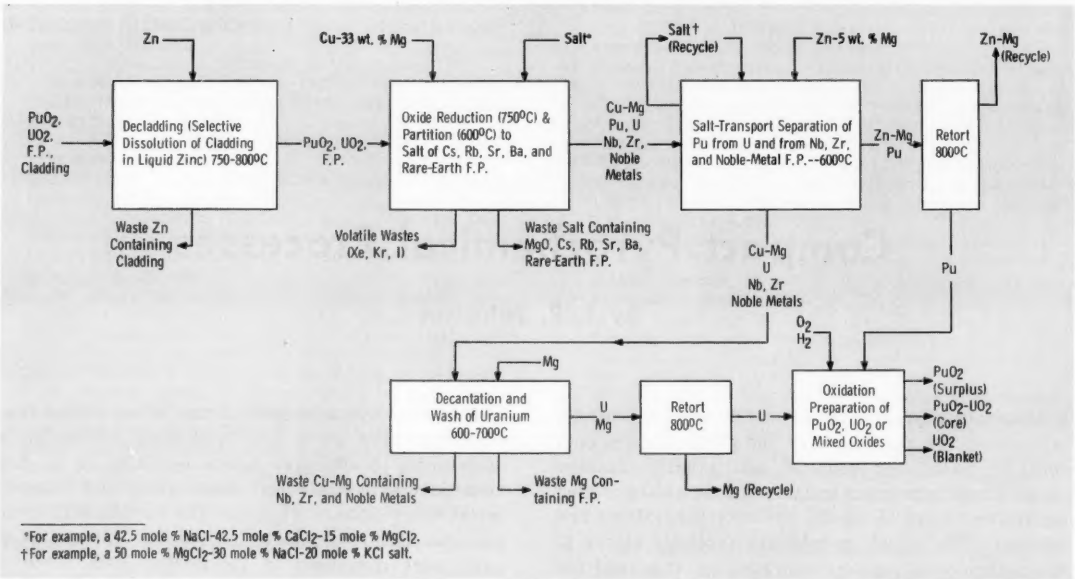
Zn
Cu-33 wt. % Mg
Salt*
Salt† (Recycle)
Zn-5 wt. % Mg
Zn-Mg (Recycle)
PuO2, UO2, F.P., Cladding
Decladding (Selective Dissolution of Cladding in Liquid Zinc) 750-800°C
PuO2, UO2, F.P.
Oxide Reduction (750°C) & Partition (600°C) to Salt of Cs, Rb, Sr, Ba, and Rare-Earth F.P.
Cu-Mg Pu, U Nb, Zr, Noble Metals
Salt-Transport Separation of Pu from U and from Nb, Zr, and Noble-Metal F.P.--600°C
Zn-Mg Pu
Retort 800°C
Waste Zn Containing Cladding
Volatile Wastes (Xe, Kr, I)
Waste Salt Containing MgO, Cs, Rb, Sr, Ba, Rare-Earth F.P.
Cu-Mg U Nb, Zr Noble Metals
Pu
O2 H2
Mg
Decantation and Wash of Uranium 600-700°C
U Mg
Retort 800°C
U
Oxidation Preparation of PuO2, UO2 or Mixed Oxides
PuO2 (Surplus)
PuO2-UO2 (Core)
UO2 (Blanket)
Waste Cu-Mg Containing Nb, Zr, and Noble Metals
Waste Mg Containing F.P.
Mg (Recycle)

*For example, a 42.5 mole % NaCl-42.5 mole % $CaCl_2$-15 mole % $MgCl_2$.
†For example, a 50 mole % $MgCl_2$-30 mole % NaCl-20 mole % KCl salt.

Fig. 1 Reference pyrochemical-process flow sheet for fast breeder reactor oxide core and blanket fuel[2] (cladding material: stainless steel).

this new process it is not necessary to transfer large volumes of salt to recover and purify uranium. Uranium is isolated by decantation of the salt and metal supernatant and washing away the remaining copper alloy and fission products with magnesium. The final uranium and plutonium products are recovered from residual solvent metals by vacuum retorting. The Cu–Mg alloys have been chosen for the reduction–partition and the salt-transport steps because these alloys provide large separation factors between actinides and rare earths.

OXIDE-REDUCTION STEP

To understand the mechanism of the oxide reduction in Cu–Mg–halide salt systems, the chemical interactions of UO_2, U_3O_8, and PuO_2 with various molten salts are being studied[3] by measuring the amount of uranium or plutonium that dissolves in the salt at 800°C. Four salt compositions were investigated: 100% $MgCl_2$, 50 mole % $MgCl_2$–30 mole % NaCl–20 mole % KCl, 50 mole % $MgCl_2$–50 mole % $CaCl_2$, and 59 mole % LiCl–41 mole % KCl. The amount of plutonium that dissolved in the salts containing $MgCl_2$ was greater than 1 wt.% and was several hundred times greater than the amount of uranium dissolved from UO_2. The solubilities of uranium or plutonium in the LiCl–KCl mixture were 0.005 wt.% and 0.12 wt.%, respectively. The addition of 5 mole % MgF_2 to the salts increased the concentration of plutonium and decreased the concentration of uranium. When U_3O_8 was contacted with these salts, a soluble phase was formed initially that slowly decomposed to insoluble UO_2.

SALT-TRANSPORT STEP

A salt-transport experiment in which plutonium was separated from uranium was reported.[2] Plutonium was selectively transferred at 600°C from a liquid Cu–33 wt.% Mg donor alloy containing a U–20 wt.% Pu alloy through molten $MgCl_2$–NaCl–KCl to a Zn–10 wt.% Mg acceptor alloy. After 48 hr of gentle agitation, 99.5% of the plutonium had been transported to the acceptor alloy and only 1.9% of the uranium had been transported.

In a separate experiment the distribution coefficients of uranium between the $MgCl_2$–NaCl–KCl carrier salt and Zn–Mg alloys at various temperatures were determined[2] to predict the behavior of uranium in the plutonium-transport step. In a Zn–Mg alloy the uranium distribution coefficients first decreased to a minimum value from their value in pure zinc and then increased to their value in pure magnesium. The minimum values for the distribution coefficients (wt.% U in salt/wt.% U in metal) ranged from 1.3×10^{-4} at 600°C and 25 wt.% magnesium to 3.3×10^{-4} at 800°C and 11 wt.% magnesium. From these results it is believed that satisfactory concentration of plutonium from the reactor core and blanket can be achieved in the reference process.

An experiment[4] was conducted to investigate the feasibility of an engineering-scale salt-transport process for the partition of uranium from various

refractory and noble-metal fission-product elements. The separation of uranium by salt transport was included in an earlier flow sheet; this flow sheet and the equipment and procedure for the experiment were described in the Spring 1966 issue of *Reactor Fuel Processing*.[1] The feed was prepared by adding uranium metal (2 kg) and representative fission products (zirconium, palladium, and niobium) to a Cu–5 wt.% Mg donor alloy. The uranium was transferred to a molten Mg–35 wt.% Zn acceptor alloy by alternately contacting the two metal alloys with a charge of $MgCl_2$. Prior to each salt transfer, the salt and metal phases were mixed for 4 to 5 min and then were allowed to separate by settling. In the experiment, 99% of the uranium was transported to the Mg–Zn acceptor alloy. The precipitated uranium product was first washed with Mg–30 wt.% Zn alloy and then dissolved in a Zn–13 wt.% Mg solution. Analyses of the U–Zn–Mg product solution showed the following removals of fission-product elements: zirconium, 99.7%; palladium, 99.99%; niobium, >99.999%.

In the recovery of plutonium that has been bred in the uranium blanket of a fast breeder reactor, a relatively small amount of plutonium must be separated from a large amount of uranium. In a laboratory-scale salt-transport experiment[4] at 700°C, plutonium was separated from 300 g of U–3 wt.% Pu alloy that simulated the blanket in a fast breeder reactor. A Mg–20 wt.% Cd alloy was used as the donor solvent, 50 mole % $MgCl_2$–30 mole % NaCl–20 mole % KCl was the salt carrier, and a Zn–6 wt.% Mg alloy was the acceptor solvent. For donor solvents, Mg–Cd alloys are alternatives to the Cu–Mg alloys. When the experiment was terminated, about 89% of the plutonium had been transported from the liquid donor alloy through the molten ternary salt to the acceptor alloy; however, the rate of plutonium transfer was still significant at the time that the experiment was terminated. The plutonium-to-uranium ratio in the feed alloy was 0.029, whereas in the acceptor alloy the ratio was 15.5. Extrapolation of the experimental data indicates that the plutonium-to-uranium ratio would be about 11.5 when the plutonium transfer reaches the theoretical limit of 98.5% in this system.

Because a Cd–Zn alloy is also being considered as an alternative to the Cu–Mg alloy for the donor solvent, the low-zinc portion of the U–Cd–Zn system was investigated[5] to obtain information about the solubility of uranium in the liquid phase. The peritectic decomposition temperature of UCd_{11} increased from 472 ± 2°C to 485 ± 2°C as the zinc concentration was increased from 0.0 to 2.0 wt.%. With increasing zinc concentrations the solubility of uranium increased at temperatures above the decomposition temperature and the solubility decreased below this transition temperature. The retrograde solubility of alpha uranium found in the U–Cd system continues in the ternary system up to at least 2 wt.% zinc.

DECANTATION AND WASH STEP

In the reference flow sheet, the fission products remaining after the extraction step are removed from the uranium by decanting the supernatant Cu–Mg alloy and washing the precipitated uranium with magnesium. For effective washing of the uranium, the fission products must be soluble in magnesium that contains up to 60 wt.% copper. At 800°C the solubility[5] of zirconium varied from 3.9 wt.% in a Cu–Mg alloy containing 37.5 wt.% magnesium to 2.7 wt.% in an alloy containing 49.1 wt.% magnesium. These values indicate that it will be possible to separate zirconium from uranium by taking advantage of solubility differences; for example, the solubility of uranium in a Cu–Mg alloy containing 49 wt.% magnesium is about 0.007 wt.% at 800°C.

Salt-Transport Studies with Thorium

The chemistry of thorium in liquid-metal–molten-salt systems is of interest in the development of recovery processes for thorium-based reactor fuels. In recent work,[4] thorium distribution coefficients were determined for the following systems: (1) 50 mole % $MgCl_2$–30 mole % NaCl–20 mole % KCl and Zn–10 wt.% Mg alloy and (2) the same ternary salt and Cu–8 wt.% Mg alloy. In both systems thorium distributed strongly in favor of the metal phase. At 800°C the distribution coefficients (wt.% Th in salt/wt.% Th in alloy) were $\sim 10^{-4}$ for the Zn–Mg/ternary-salt system and $\sim 10^{-3}$ for the Cu–Mg/ternary-salt system.

MATERIALS EVALUATION

In recently reported[2] corrosion work supporting the pyrochemical-process studies at ANL, specimens of molybdenum and TZM alloy (Mo–0.5 wt.% Ti–0.08 wt.% Zr) were exposed for 200 hr to a Cu–Mg–U/chloride-salt system or to a Zn–Mg–U/chloride-salt system at temperatures up to 850°C. When the salt phase was the $MgCl_2$–NaCl–KCl ternary eutectic, molybdenum exhibited a pitting-type attack with penetrations up to 0.25 mm at 700°C. Both materials showed good corrosion resistance (penetrations of <0.1 mm) at 850°C and 750°C in tests where the salt was pure magnesium chloride.

Salt-Cycle Process

The electrodeposition of uranium and plutonium oxides from a molten-salt bath, commonly referred to as the salt-cycle process,[6] has received extensive study at Hanford as a close-coupled reprocessing scheme for reactor fuels. Hot-cell demonstrations with both unirradiated and irradiated mixed plutonium

and uranium oxides have produced reactor-grade PuO_2-UO_2 as a solid solution on an engineering scale. An economic evaluation[7] was made of the potential of the salt-cycle process as a commercial producer of reactor-grade fuel oxides. The fixed-capital requirements and the feed, conversion, and production costs were estimated for a glove-box facility to convert natural UO_2 and fully decontaminated PuO_2 into reactor-grade mixed-oxide fuel material ready for vibratory compaction into fuel rods. The plant was designed to meet the fuel requirements of a 1000- Mw(e) reactor with plutonium enrichments of up to 5 wt.%.

In the conceptual plant the cycle begins with the loading of the UO_2 into a molten equimolar LiCl–KCl salt bath that receives radiant heat from an inductively heated susceptor. (Two related reports[8,9] that were released recently describe the electrolytic heating of salt baths that are contained within a frozen wall.) The UO_2 is dissolved in 22 hr using a chlorine-gas sparge. Next the PuO_2 is introduced into the salt pot, and the melt is sparged with HCl gas for 14 hr. A portion of this time is required for drying the molten salt. Since the melt must be dry for this electrolysis, a dry atmosphere is maintained in the glove box by a Molecular-Sieve air-drying system. Following the dissolution steps, two graphite anodes and a pyrolytic graphite-coated cathode are introduced into the melt. The melt is then electrolyzed at 1.5 volts with a current of 800 amp while sparging with oxygen and chlorine for 32 hr. All the gases evolved from the molten salt are passed from the glove box through absolute filters and a caustic scrubber. Upon completion of the electrolysis, a 200-lb deposit is removed from the salt bath and after being allowed to cool, the PuO_2-UO_2 is stripped from the cathode with a hydraulic press. The stripped PuO_2-UO_2 is then washed to remove the adhering chlorides. Upon completion of the washing step, the oxide is dried at 300°C with a mixture of argon and hydrogen gas. The dry oxide is crushed and screened to a specified particle size.

FIXED-CAPITAL INVESTMENT

A fixed-capital investment of about $1 million was estimated[7] from the plant layout and process-equipment requirements. The operating costs are shown in Table 1 for various product enrichments. It was estimated that an inventory of 1 month would be required.

Table 1 OPERATING COSTS AS A FUNCTION OF WEIGHT PERCENT PLUTONIUM (DOLLARS PER KILOGRAM OF PuO_2-UO_2)

Pu, wt.%	Feed cost	Conversion cost	Inventory charges	Product cost
5	$439	$21.50	$8.00	$468
3	269	18.90	4.60	293
1	100	16.30	1.80	118

EBR-II Fuel Cycle Facility and Operations

The fuel cycle[10,11] for the second Experimental Breeder Reactor (EBR-II) involves mechanical decanning of discharged fuel, partial decontamination of the fuel by melt refining, re-forming the fuel pins by injection casting, and remote refabrication of fuel elements. Most of these operations are done in the Argon Cell of the Fuel Cycle Facility. This facility is presently operating[4] routinely and is reprocessing and returning fuel to the reactor. The operating experience with the argon purification system for the Argon Cell has been summarized in a recent article.[12] The argon purification system for this cell consists of a filter, a centrifugal compressor, a cooling coil to remove the heat of compression, a palladium catalyst bed to remove oxygen from the gas by combining it with added hydrogen, and a Molecular-Sieve dryer to remove water. Continuous operation of this system can maintain an atmosphere that contains about 8 ppm oxygen and 5 ppm water at the cell inleakage rate[5] of 0.24 cu ft (STP) of air per hour. Normally the oxygen and water concentrations are maintained in the range of 20 to 60 ppm to minimize difficulties in the handling of sodium and to decrease the wear of motor brushes and bearings. Nitrogen concentration is maintained at about 5% by the argon additions that are required through normal operations. Carbon dioxide, which results from the radiolytic decomposition of organic materials, is removed periodically on freshly regenerated type 5A Molecular Sieves. Since the introduction of irradiated fuel into the Argon Cell in September 1964, the various systems have continued to function very satisfactorily.

Skull-Reclamation Process

The skull-reclamation process is being developed at ANL specifically to recover and purify the uranium-bearing residue or skull that is left in the crucible following the melt refining of enriched-uranium-alloy fuel pins discharged from the EBR-II reactor. The uranium in the skull amounts to 5 to 10% of the original charge. Although the skull-reclamation process for EBR-II fuel does not recover plutonium, much of the chemistry and technology being accumulated in the course of this process development is applicable to advanced pyrochemical processing concepts that are capable of recovering plutonium. The skull-reclamation process has been tested with nonirradiated uranium in remotely operated plant-scale equipment (~4 kg of uranium per batch) comprising a reduction furnace and a retorting furnace. The steps in this process were described in the Fall 1965 issue of *Reactor Fuel Processing*.[13]

Work has continued on the final operation in the skull-reclamation process, the retorting or solvent

evaporation step. In this step the product uranium is separated from a Zn–12 wt.% Mg–12 wt.% U ingot that is cast from the final product solution transferred out of the reduction furnace. The retorting procedure consists of distilling the zinc and magnesium under vacuum (~10 torrs) at 650 to 750°C, after which the uranium is melted (~1200°C) to form a button. Nine additional plant-scale retorting runs[4] were completed using two large-size (8 in. in outside diameter by 17 in. high) beryllia crucibles. One of the crucibles, which had been used in two earlier runs, was used in three distillations, and the other crucible, which was new, was used in the other six runs. Satisfactory results were achieved in all experiments. These experiments complete the developmental work on the skull-reclamation process.

Preparation of Metals by Reduction of Their Compounds

Additional information has been published on the electrowinning of plutonium metal from molten halide salts. Previously reported processes for electrowinning[14] or electrorefining[15] employed molten chloride salts and operated best with a feed of pure $PuCl_3$ or $PuCl_3$ containing some oxygen. The design, method of fabrication, properties, and operating behavior have been reported[16] for four continuous-electrowinning and two batch-electrorefining cells. Cells and agitators were made of a ceramic material having a composition of 6 mole % Mg_2TiO_4 and 94 mole % MgO. At the cell operating temperatures around 800°C, the low-viscosity chloride melts did not penetrate or corrode this ceramic material. The chlorine released during electrowinning did attack the cell, and this corrosion limited the useful lifetime of the cell. Reduction of the oxide-titanate material by liquid plutonium caused some magnesium contamination of the plutonium product. However, the product was not contaminated by titanium because titanium volatilized as the tetrachloride.

The mechanism of reducing $PuCl_3$ to the metal in the LiCl–KCl eutectic has been studied[17] with chronopotentiometric techniques. A trivalent plutonium complex underwent direct reduction to the metal by a one-step, three-electron transfer. At temperatures of 500 and 600°C, an equilibrium apparently existed between two complex ionic species, and the rate-controlling step was the rate of transforming one complex to the other.

Porter and Symonds[18] have described techniques for electrowinning molten plutonium metal in fused-fluoride electrolytes using a feed of PuO_2. Electrolytes containing about 50 wt.% LiF, 20 wt.% BaF_2, and 30 wt.% PuF_3 gave the best cell performance. Each cell consisted of a tantalum crucible, which functioned as the cathode and contained the fluids, and a graphite anode. The best anode designs were those which promoted agitation of the melt by the rising anode gases. Laboratory-scale cells (2.6 in. in inside diameter by 5.5 in. high) that operated at 1000°C at a current of 100 amp were capable of producing plutonium metal at a rate of 40 g/hr. Utilization of PuO_2 was essentially 100%, and current efficiencies were 10 to 20%. The purity of the electrolytically produced metal was comparable to that produced by bomb reduction with the exception that the product usually contained about 3500 ppm tantalum, which was derived from the cell.

Low-melting thorium alloys were prepared[19] by electrolysis of thorium dioxide dissolved in fluoride melts. Experiments were performed at 950 to 1250°C using electrolytes that contained ThF_4 and various alkali and alkaline-earth fluorides. Thorium was deposited on a nickel or iron cathode and formed a molten alloy that dripped off and collected on the bottom of the cell or in a tungsten cup. Thorium and a second metal (Ni, Fe, Cr, or Mn) were codeposited on a tungsten cathode by electroreduction of the two metal oxides. Also, dendritic deposits of thorium metal were formed by reduction of ThO_2 in a fused-fluoride system at 1075 to 1200°C. The thorium was recovered and arc-melted into a button that contained less than 0.2 wt.% total impurities of which Al, C, Cu, Fe, O, and Si were the major constituents.

A German patent[20] was issued on a method for the preparation of Al–U alloys. The alloys were prepared by the reduction of uranium hexafluoride with an excess of molten aluminum metal. The surface of the aluminum metal was covered by a molten mixture of NaCl, KCl, and NaF. The gaseous uranium hexafluoride was introduced below the surface of the liquid metal at a temperature of 850°C.

Low-temperature pyrochemical processes have been previously used to prepare uranium, plutonium, and thorium metal by the reduction of their oxides.[21–23] A recent laboratory experiment has shown that this method can be extended to the reduction of neptunium oxide.[24] About 2.3 g of NpO_2, suspended in molten 50 mole % $MgCl_2$–30 mole % NaCl–20 mole % KCl, was reacted with liquid Zn–10 wt.% Mg alloy at 800°C. After 2 hr of agitation, about 99.8% of the neptunium oxide was reduced. The Zn–Mg–Np alloy was then retorted to remove the zinc and magnesium, after which the neptunium was consolidated by arc melting.

Miscellaneous

Patents[25,26] have been granted to Vogg and Baehr for improvements on the techniques of separating fuel materials in alkali–nitrate melts. The general methods were reported in the Fall 1966 issue of *Reactor Fuel Processing*.[27] Uranium, when digested with an oxidizing nitrate melt, was precipitated and could be separated by filtration from the melt in which molybdenum and other fission products remained dissolved. Uranium could be separated from

plutonium or thorium by controlling the alkalinity of the melt during the digestion process.

Speeckaert and Dumont at Centre d'Étude de l'Énergie Nucléaire, Mol, Belgium, have reported[28,29] experiments in which PuO_2 was precipitated from a medium of molten chloride salts containing PuF_4 by addition of KNO_3. In these preliminary experiments the oxide was recovered by dissolving the salt mass in water and filtering. Over 99% of the plutonium was recovered, but it was contaminated with LiF, which is insoluble in water. Filtration of the molten salts should eliminate LiF from the product because this fluoride is soluble in the molten salt.

References

1. *Reactor Fuel Process.*, 9(2): 97-100 (Spring 1966).
2. R. M. Adams and A. Glassner (Comps.), Reactor Development Program Progress Report, September 1966, USAEC Report ANL-7255, pp. 30-34, Argonne National Laboratory, Oct. 26, 1966.
3. D. Wenz, Argonne National Laboratory, personal communication.
4. R. M. Adams and A. Glassner (Comps.), Reactor Development Program Progress Report, July 1966, USAEC Report ANL-7245, pp. 11-14, Argonne National Laboratory, Aug. 26, 1966.
5. R. M. Adams and A. Glassner (Comps.), Reactor Development Program Progress Report, August 1966, USAEC Report ANL-7249, pp. 8-10, Argonne National Laboratory, Sept. 23, 1966.
6. *Reactor Fuel Process.*, 9(2): 101 (Spring 1966).
7. W. R. Bond, A Preliminary Economic Study of the Preparation of Reactor Grade PuO_2-UO_2 by the Salt Cycle Process, USAEC Report HW-83984, General Electric Company, Sept. 9, 1964.
8. D. C. Brandt, Alternating-Current Heating of Molten Salts, USAEC Report HW-75468, General Electric Company, Nov. 28, 1962.
9. J. E. Morrissey, Preliminary Study on the Application of a Frozen Wall and Electrolytic Heating to Molten Salt Baths, USAEC Report HW-72572, General Electric Company, Feb. 2, 1962.
10. *Reactor Fuel Process.*, 7(4): 250-254 (Fall 1964).
11. J. C. Hesson, M. J. Feldman, and L. Burris, Jr., Description and Proposed Operation of the Fuel Cycle Facility for the Second Experimental Breeder Reactor (EBR-II), USAEC Report ANL-6605, Argonne National Laboratory, April 1963.
12. W. F. Holcomb, D. M. Paige, and L. F. Coleman, Operating Experience with the EBR-II Fuel Cycle Facility Inert Atmosphere Cell, *Nucl. Appl.*, 2(3): 254-255 (June 1966).
13. *Reactor Fuel Process.*, 8(4): 216 (Fall 1965).
14. M. H. Curtis, Continuous Electrowinning of Plutonium Metal, USAEC Report RL-SEP-30, General Electric Company, April 1964.
15. L. J. Mullins and J. A. Leary, Fused-Salt Electrofining of Molten Plutonium and Its Alloys by the Lamex Process, *Ind. Eng. Chem., Process Design Develop.*, 4(4): 394 (October 1965).
16. R. S. Rosenfels, Ceramic Cells and Accessories for Electrowinning and Electrorefining of Plutonium Metal, USAEC Report RL-SEP-824, General Electric Company, Dec. 17, 1965.
17. D. A. Nissen, Electrochemistry of Plutonium (III) in Molten Alkali Chlorides, *J. Inorg. Nucl. Chem.*, 28(8): 1740 (1966).
18. J. A. Porter and A. E. Symonds, Jr., Electrowinning Plutonium Metal, USAEC Report DP-1021, Savannah River Laboratory, February 1966.
19. D. G. Kesterke, D. C. Fleck, and T. A. Henrie, Fused-Fluoride Electrowinning of Thorium-Base Alloys, Report BM-RI-6789, Bureau of Mines, 1966.
20. D. A. Zappi, Method for the Preparation of Aluminum-Uranium Alloys, German Patent No. 1,212,304, to Comisión Nacional de Energía Atómica (Argentina), Mar. 10, 1966 (filed Aug. 19, 1963).
21. J. B. Knighton and R. K. Steunenberg, Preparation of Metals by Magnesium-Zinc Reduction. Part I. Reduction of Uranium Oxides, USAEC Report ANL-7057, Argonne National Laboratory, June 1965.
22. A. V. Hariharan, J. B. Knighton, and R. K. Steunenberg, Preparation of Metals by Magnesium-Zinc Reduction. Part II. Reduction of Thorium Oxide, USAEC Report ANL-7058, Argonne National Laboratory, June 1965.
23. J. B. Knighton and R. K. Steunenberg, Preparation of Metals by Magnesium-Zinc Reduction. Part III. Reduction of Plutonium Dioxide, USAEC Report ANL-7059, Argonne National Laboratory, June 1965.
24. R. M. Adams and A. Glassner (Comps.), Reactor Development Program Progress Report, June 1966, USAEC Report ANL-7230, p. 31, Argonne National Laboratory, July 27, 1966.
25. H. Vogg and W. Baehr, Method for Reprocessing of Irradiated Nuclear Fuel, German Patent No. 1,209,564, to Gesellschaft für Kernforschung mbH, Jan. 27, 1966 (filed Aug. 8, 1964).
26. H. Vogg and W. Baehr, Method for the Separation of Nuclear Fuel Materials, German Patent No. 1,209,745, to Gesellschaft für Kernforschung mbH, Jan. 27, 1966 (filed Aug. 8, 1964).
27. *Reactor Fuel Process.*, 9(4): 222 (Fall 1966).
28. Centre d'Étude de l'Énergie Nucléaire, Reprocessing of Irradiated Fuels, Quarterly Report No. 22, July 1-September 30, 1965, USAEC Report EURAEC-1601, 1966.
29. Centre d'Étude de l'Énergie Nucléaire, Reprocessing of Irradiated Fuels, Quarterly Report No. 23, October 1-December 31, 1965, USAEC Report EURAEC-1646, 1966.

Progress in Waste-Disposal Research and Development

By Phillip Fineman

Treatment of Low-Level-Activity Wastes

ION EXCHANGE

Oak Ridge National Laboratory (ORNL) has developed a water-recycle process (Fig. 1) for the treatment of low-level-activity aqueous wastes (LLW).[1,2] The process is based on demineralization of all raw water entering a nuclear installation and recycle of used water after it has been decontaminated and demineralized. Treatment of the LLW consists in the following steps: (1) a flocculation–clarification step using zeta-potential-controlled* additions of coagulant and coagulant aid, (2) a demineralization step to treat the clarified effluent from the previous step, and (3) a second sorption step using activated carbon for additional removal of radioactive species, such as ruthenium and cobalt.

Three laboratory tests (runs 6, 12, and 13) of the process were completed using actual ORNL plant LLW; in runs 6 and 13, the *p*H of the LLW was its usual value (7 to 8), and in run 12 it was lower (4.9) than usual because of an unusually large increase in the nitrate-ion concentration (Table 1). In runs 6 and 12, treatment of the LLW followed the process steps shown in the flow sheet. In run 13 the treatment was modified by the addition of a second activated-carbon column that was placed between the cation and anion exchangers. In all runs the cation exchanger was Dowex 50, the anion exchanger was Dowex 1, and the activated carbon (both columns) was a granular bituminous-coal-based product.

The overall decontamination values for individual nuclides and total rare earths are shown in Table 1. The high overall decontamination factors achieved in run 6 were not generally maintained in runs 12 and 13. The ^{60}Co values were particularly low in the two latter runs for the following reasons. In run 12 the low *p*H of the LLW prevented proper flocculation from taking place in the clarifier, and in run 13 the activated-carbon column between the two ion exchangers is believed to have altered the ionic form of the ^{60}Co species present in the cation-column effluent (*p*H, 2.5 to 3.0). These results indicate that, to maintain high ^{60}Co decontamination factors, the *p*H of the LLW should be in the range of 7 to 8 and the use of the activated-carbon column should come only after the demineralization step.

*Zeta potential keeps particles in suspension and hinders or prevents their agglomeration.

Tank Storage of High-Level-Activity Wastes

SAFETY ANALYSIS OF TANK STORAGE

ORNL has undertaken a safety analysis of tank storage of high-level-activity wastes.[3] In the analysis the wastes are stored as alkaline or acid solutions in tanks that are similar in design to those in use at Savannah River Laboratory. The tanks each have a capacity of about 1 million gal and are equipped with submerged cooling coils. When the tanks are newly filled, the wastes in each will contain between 4 and 7 billion curies of fission-product activity.

Two incidents are postulated, both of which are based on loss of cooling of the tank contents and on the atmosphere constituting the major exposure pathway. In the first incident it is assumed that a temporary loss of cooling has occurred, that in this period the wastes self-heat to boiling, and that they boil for 10 hr with both the condenser and filter out of service. The fission-product activity released to the atmosphere from a tank filled with acid wastes would amount to 720,000 curies (ruthenium, 300 curies/min; fission products, 10^3 curies/min), and from a tank containing alkaline wastes it would be 180,000 curies (fission products, 300 curies/min).

In the second incident it is assumed that a permanent loss of cooling has resulted from an explosion of radiolytic hydrogen in the tank. Radiolytic hydrogen is produced in the wastes at such rates that, if the ventilation system fails, the lower explosive limit of 4 vol.% hydrogen in air would be reached in $1\frac{1}{2}$ to 3 hr and the quantities accumulated could explode with a force sufficient to rupture the tank and the concrete encasement. In this event, if no effective remedial action were taken, atmospheric releases of a major magnitude would be encountered over the ensuing 168 to 300 hr. The fission-product activity released to the atmosphere from a tank containing acid wastes would amount to 1.1×10^9 curies (over

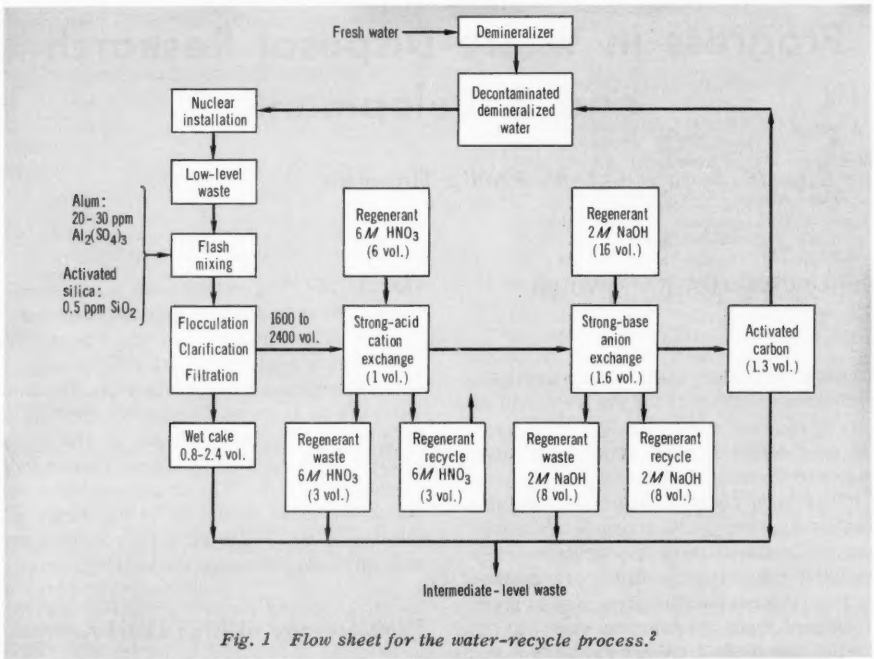
Fresh water
Demineralizer
Decontaminated demineralized water
Nuclear installation
Low-level waste
Alum: 20-30 ppm $Al_2(SO_4)_3$
Activated silica: 0.5 ppm SiO_2
Flash mixing
Flocculation Clarification Filtration
1600 to 2400 vol.
Regenerant 6 M HNO_3 (6 vol.)
Strong-acid cation exchange (1 vol.)
Regenerant 2 M NaOH (16 vol.)
Strong-base anion exchange (1.6 vol.)
Activated carbon (1.3 vol.)
Wet cake 0.8-2.4 vol.
Regenerant waste 6 M HNO_3 (3 vol.)
Regenerant recycle 6 M HNO_3 (3 vol.)
Regenerant waste 2 M NaOH (8 vol.)
Regenerant recycle 2 M NaOH (8 vol.)
Intermediate-level waste

Fig. 1 Flow sheet for the water-recycle process.[2]

Table 1 OVERALL DECONTAMINATION FACTORS OBTAINED IN LABORATORY TESTS OF THE WATER-RECYCLE PROCESS USING ORNL LOW-LEVEL-ACTIVITY PLANT WASTE (LLW)[2]

	Properties of feeds (LLW) used			
Run	pH	Specific conductance, μmho/cm	Total hardness, ppm $CaCO_3$	Nitrate, ppm NO_3^-
6	7.4	280	130	15
12	4.9	427	123	264
13	8.0	316	123	10

Treatment of LLW consisted in the following steps:
Runs 6 and 12—Alum-activated silica flocculation–clarification, cation–anion exchange, and activated-carbon sorption
Run 13—Alum-activated silica flocculation–clarification, cation exchange, activated-carbon sorption, anion exchange, and activated-carbon sorption

	Decontamination factors obtained for the indicated nuclides and total rare earths								
Run	^{137}Cs	^{90}Sr	^{60}Co	^{106}Ru	^{144}Ce	Total rare earths	^{125}Sb	^{95}Zr–^{95}Nb	^{131}I
6	2600	6300	12,000	610	330	11,000	300	160	430
12	1000	5500	350	500	110	5,200	250	75	50
13	3000	3000	100	500	70	2,000	250	40	>30*

*Decontaminated to background.

a 168-hr period); from a tank holding alkaline wastes, the activity was estimated to be 1.5×10^8 curies (over a 300-hr period).

Estimates were made of the radiation exposures to neighboring populations at various distances downwind from the two types of incidents. In Figs. 2 to 5 are shown the results for tanks filled with acid wastes. Figures 2 and 3 present the gamma-exposure rate at ground level for nighttime conditions of dry weather and rainfall as a function of the distance downwind from the acid-waste tank. The ground-level exposure rates for the incident following the permanent loss of cooling (Fig. 3) are about 5000 times higher than the rates following the temporary loss of cooling. Figures 4 and 5 give ground-level concentrations as a function of the distance downwind from the acid-waste tank. They also show the resulting exposure to the lungs from inhaling the fission products over the duration of the incident; these dose equivalents are the result of integration over the first year. The ground-level concentrations and dosages to the lungs shown for the incident following permanent loss of cooling (Fig. 5) are about 1000 times higher than those following temporary loss of cooling.

For the case of tanks filled with alkaline wastes, the results for the two incidents were estimated to be one-fifth to one-half those for acid wastes.

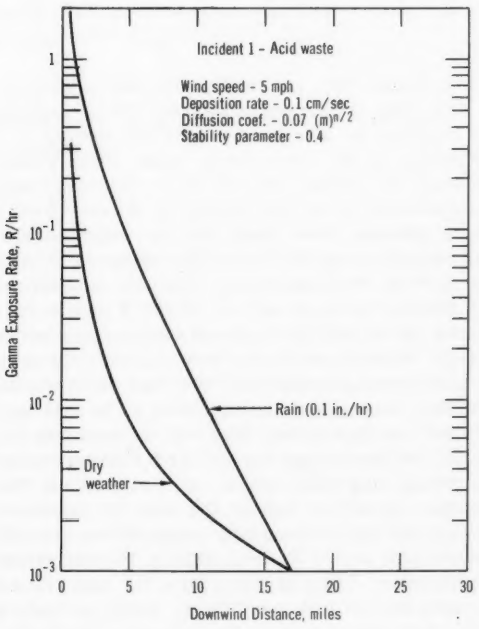

Fig. 2 Ground-level exposure rate as a function of distance downwind from an acid-waste tank following temporary loss of cooling.[3]

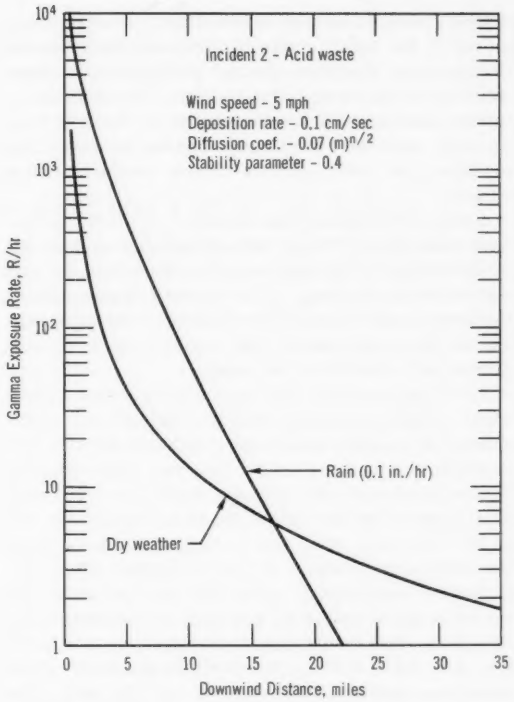

Fig. 3 Ground-level exposure rate as a function of distance downwind from an acid-waste tank following permanent loss of cooling.[3]

Another source of radiation exposure to the surrounding population is the direct radiation that would result from the passing radioactive cloud. However, this exposure was determined to be only a few percent of that found for the other two sources and may be considered to be of negligible importance.

Temperatures of Buried Waste-Storage Tanks and of the Soil Near Leaks in the Tank

Storage systems for high-level-activity waste solutions and sludges are designed to assure means of dissipating fission-product heat under all normal operating conditions. If leakage of heat-generating wastes from a storage tank occurs, the designed means of heat dissipation are compromised, and the thermal conditions that may occur outside the basic tank structure must be considered.

After a tank failure has been detected, an obvious action would be to remove the waste from the suspect tank. However, for alkaline wastes a major fraction of the heat-generating fission products (Sr, Ce, Zr–Nb, and Ru) resides in a precipitated sludge layer that is dependent upon vaporization of liquid for heat dissipation; cesium and a small fraction of the ru-

thenium remain in the supernatant. Arbitrary removal of the liquid cover to eliminate the source of leakage may result in greater problems than those associated with the initial leakage. The problem is further complicated by the ability of the soil surrounding the tank to sorb[4] fission products and to filter out the dispersed fission-product-bearing solids.

Jansen, Willingham, and DeMier,[5] at Pacific Northwest Laboratory (PNL), have presented an analysis of the temperatures that might be attained in the tank and in the surrounding soil as a result of pumping out the supernatant from a buried sludge-containing tank and of the temperatures that would occur in the soil because of a leak from the tank.

The temperatures and heat losses around intact waste tanks containing boiling solutions and heat-generating sludge layers are compared for dry (low thermal conductivity) soil and wet (high thermal conductivity) soil. In all cases most of the conducted heat flows from the top of the tank, through the soil layer above the tank, and to the atmosphere. When the tank temperature is held constant by reflux boiling of supernatant, more heat is dissipated into surrounding soil that is wet than is dissipated into dry soil. The temperature distribution throughout the soil–tank system is nearly independent of the moisture content of the soil if all the soil in the system has the same thermal conductivity; however,

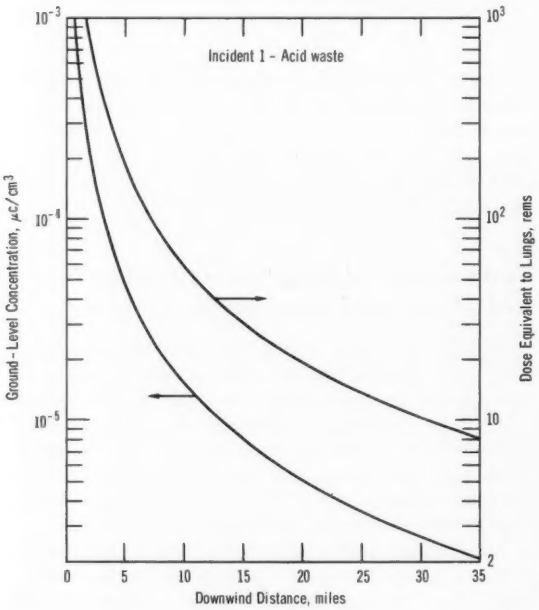

Fig. 4 Ground-level concentration as a function of distance downwind from an acid-waste tank following temporary loss of cooling. The dose equivalents to the lungs are the result of integration over the first year.[3]

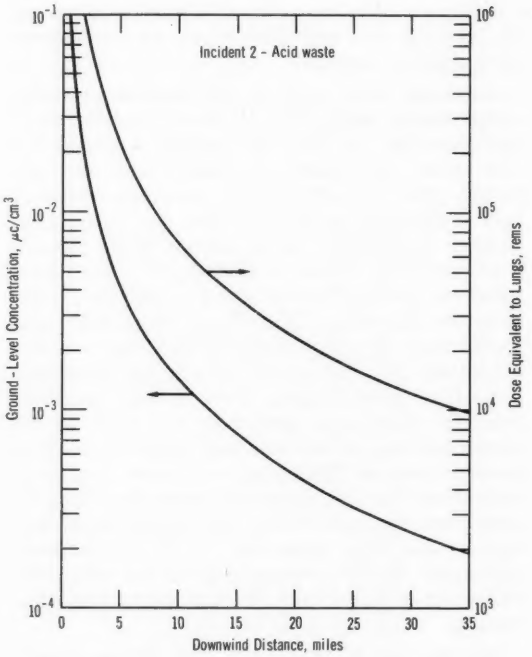

Fig. 5 Ground-level concentration and dosage to the lungs as a function of distance downwind from an acid-waste tank following permanent loss of cooling. The dose equivalents to the lungs are the result of integration over the first year.[3]

if a localized wet region appears only adjacent to the tank wall, higher temperatures will be found in this region of the soil than in nearby dry areas.

Removal of all liquid from waste tanks without removing the sludge can result in extremely high temperatures. If the supernatant is removed from a typical alkaline-waste tank and the only means of heat removal from the radioactive sludge is conduction through the surrounding dry soil, equilibrium tank temperatures as high as 25,000°F can be calculated. Of course, the tank will collapse long before thermal equilibrium is reached and radically alter the heat-transfer conditions. The rate of rise in the adiabatic temperature is estimated to be less than 20°F/hr, so that a long time will be needed to approach the equilibrium temperature. Passing cooling air through the tank offers little relief from this condition. At a flow rate of 100 cfm, the calculated exit-air and equilibrium tank temperatures are still greater than 10,000°F. Even after a 10-year period of radioactive decay of the sludge, the temperature can still be as high as 2000°F. Spraying the dry sludge with water to keep its surface at the boiling point of water can keep the bottom of the tank below 500°F, provided the cake is sufficiently thin and the sludge thermal conductivity is high.

Leaks of alkaline supernatant containing only cesium and small amounts of ruthenium cannot cause dangerously high soil temperatures. In a 50,000-gal hemispherical leak of typical acid supernatant, the maximum rise in temperature at the concrete–soil interface is only 35°F and the maximum rise in the soil temperature at a distance of 8 ft from the tank wall is 524°F. Even the flashing off of the water in the supernatant at the leak point will not cause high temperatures because large quantities of inert salts dilute the fission products.

The leakage of even small volumes (less than 1000 gal) of alkaline sludge that might be slurried in the supernatant or of acid solutions containing highly adsorbable zirconium and cerium could cause high temperatures at the concrete–soil interface because of the localized high concentrations of fission products at the leak point.

The authors have provided temperature-rise maps for hemispherical leaks, varying from 100 to 100,000 gal, for wet and dry soil, and for various types of fission products. These maps may prove useful in analyzing temperature records to determine the size and location of a leak. Accurate records are essential for such analyses since the temperature rises are superimposed on a previously existing temperature gradient around intact tanks. A computer program is provided for calculating temperature-rise maps around hemispherical leaks and hemispheroidal leaks of varying shapes. Higher temperatures are reached in prolate–hemispheroidal leaks than in hemispherical leaks of equal volume.

Conversion of High-Level-Activity Wastes to Solids

FLUID-BED CALCINATION

High-level-activity aqueous waste is being converted to granular solids in a fluid-bed calciner at the Idaho Chemical Processing Plant (ICPP).[6] In 5 months (to September 1966) of operation since the start of the second radioactive-waste-processing campaign in the Waste Calcining Facility (WCF), some 230,000 gal of waste solutions have been processed. Various kinds of plant wastes were successfully processed in the WCF; these included aluminum nitrate wastes containing high concentrations of nitric acid, sodium ion, or ammonium ion.[7] The average volume reduction has amounted to about 11. Operation of the WCF has been generally quite satisfactory despite the several problems that were encountered, in particular those of feed control,[7,8] leakage of one of the two NaK* expansion tanks,[7] and buildup of pressure in the final off-gas filters.[9] All the problems were solved satisfactorily.

Decontamination of the off-gas from the calciner continued to be satisfactory[7]; release rates for ^{106}Ru and ^{90}Sr remained significantly below the established limits for permissible occupational exposure.[11]

Radiant-Spray Calciner and Melter

A spray-solidification process for high-level-activity wastes is being developed at PNL.[12] It is one of three selected solidification processes that are being tested on an engineering scale in a demonstration program at PNL.† The spray solidification of wastes is carried out by means of a radiant-heat spray calciner coupled to a continuous melter. In this system the liquid waste is first converted in the spray calciner to a powder or calcine that is then discharged to the melter where it is melted. The molten calcine or glassy solid flows from the melter into a final receiver where the molten material is solidified for storage.

In recent laboratory work at PNL[14] in support of this process, data were obtained on the properties of melts formed by combining first-cycle Purex wastes (PW-1)‡ with sodium and phosphate additives. Of the melts prepared in the system PW-1 waste–Na_2O–P_2O_5, glasses were formed from melts having ratios of metallic cation (M) to phosphorus (P) of less than 1.5. Microcrystalline products containing some glassy portions when rapidly quenched resulted from melts having an M-to-P ratio between 1.5 and 2.3. All-microcrystalline products were obtained from melts having an M-to-P ratio greater than 2.3.

Two modes of melter operation are being considered. In the first no reagents are charged to the melter to lower the temperature of the melt; the melt, which has a relatively high temperature (up to 1200°C), requires a storage receiver fabricated of stainless steel. A suitable melt (m.p. 900°C) can be produced using PW-1 (100 gal/metric ton of uranium) which is made 1.60*M* in phosphate and 0.75*M* in sodium.

In the second mode, reagents (such as $NaPO_3$) are charged to the melter to produce a low-temperature, fluid melt (750°C or less). At these relatively low temperatures, receivers of mild carbon steel could be used. Low-temperature (720°C) melts were pro-

*The fluidized bed is heated by means of a liquid-metal (NaK) heat-transfer system. The expansion tanks are a part of this system.[10]

†The other two solidification processes are the ORNL pot-calcination and rising-level glass processes and the BNL phosphate process.[12] The three processes will be tested in a multipurpose facility, known as the Waste Solidification Engineering Prototypes (WSEP). Their demonstration in the WSEP will allow a comparison of the technical, economic, and safety aspects of each process. Operation of the WSEP with radioactive solutions has begun.[13]

‡PW-1 wastes are high in nitric acid (5*M*), are free of sulfate ion, and contain added iron from a dissolvable container used to transport chopped fuel.

duced from PW-1 (100 gal/metric ton of U) containing varying amounts of phosphate (4.6*M* to 7.5*M*) and sodium (5.4*M* to 7.2*M*); the melts would just flow at this temperature. The solid products from these melts were 5 to 10 times more soluble in water than the higher melting-temperature products described in the preceding paragraph. The lower melting-temperature products contained only 20 wt.% waste oxides, as compared with the 45 to 50 wt.% waste oxides contained in the higher melting-temperature melts. Corrosion rates of mild-steel specimens exposed to some of these candidate melts ranged from 25 to 45 mils/day at 720°C.

Conversion to Glass

At Harwell a process known as FINGAL (Fixation in Glass of Active Liquor) has been under development for converting to a glass product the highly radioactive nitric acid wastes that will arise from the reprocessing of fuel from the U. K. nuclear power program.[15] In the processing of the acid wastes, three stainless-steel cylindrical vessels connected in series are used. The process is carried out as follows. The wastes, together with glass-forming reagents (silica and borax), are pumped into the first (process) vessel, which is maintained at 1050°C. Feed to this vessel is continued until it is about three-fourths full of molten-glass product. The process off-gas is passed through a small primary filter in the second vessel and a large secondary filter in the third vessel; both vessels are held at 250°C. The filters are packed with granular ferric oxide for sorption of volatilized ruthenium. Most of the entrained particulate material carried out of the process vessel is removed by the primary filter. The off-gas from the secondary filter is passed successively through a condenser, an NO_2 adsorber, and a sodium hydroxide scrubber for removal of the acid vapors, after which it is passed through an absolute filter before discharge to the atmosphere. The process is maintained at subatmospheric pressure. When the process cycle is completed, the vessel containing the glass product is removed from the furnace and sent to storage. For the new process cycle, the vessel containing the spent primary filter is moved to the first position to serve as the process vessel,* and a new vessel with a new primary filter is installed in the second position.

Grover and associates,[16] at Harwell, have summarized the results of 72 pilot-plant runs, 8 of which were carried out with radioactive solutions containing a total of 30,000 curies of radioactive fission products. In the final radioactive run, 52.3 liters of fission-product solution (containing 14,500 curies) was converted to 42 kg of glass product. The decontamination factor to the condensate for ruthenium varied from 10^4 to 10^8 and for other fission products was 10^{10}. For all activity, including ruthenium, the overall decontamination factor to the effluent gas from the absolute filter ranged from 10^{14} to 10^{16}.

With completion of the radioactive runs, the authors believe that the FINGAL process is ready for commercial exploitation. They also point out that previously obtained scale-up data[17] show that the possible wastes arising from a U. K. nuclear power program of 20,000 MW(e) could be processed in a full-scale waste-treatment plant consisting of two or three lines of 12-in.-diameter vessels working in parallel.[16]

Fission-Product Recovery

LEACHING OF WCF CALCINE TO RECOVER STRONTIUM AND CESIUM

In early work undertaken at the ICPP to study the recovery of fission products from fluid-bed calcined wastes, one technique under consideration was the leaching[18] of the calcine. Considerable development work had also been done on a pulsed-multistage countercurrent column for leaching fission products from calcine.[19–21]

In recent laboratory work at Idaho Nuclear Corporation, actual calcine† from the WCF, which is primarily amorphous alumina, was leached[22] with distilled water at 25°C or 80 to 90°C or with dilute (0.25*M* to 0.5*M*) nitric acid at 25°C. Leaching was performed in an apparatus that was designed to pass liquid through the calcine continuously and, at the same time, minimize attrition of the solids.

After 7 weeks of continuous leaching with distilled water at 25°C, greater than 95% of the cesium, 33% of the strontium, and less than 0.01% of the aluminum were found to have dissolved from the calcine. Most of the leaching of the cesium and strontium occurred in the first 2 or 3 days. On the basis of initial leaching rates, the rates for cerium and ruthenium were estimated to be the same as that for aluminum from the calcine. In the distilled water tests at 80 to 90°C, only the aluminum leaching rate was determined. The rate was found not to be a great deal higher than that at 25°C; the total amount of aluminum leached in 7 weeks was less than 0.03%. This amount of leached aluminum is considered to be sufficiently low so that practical recovery of cesium and strontium appears feasible at the higher temperature.

*While the temperature of the furnace is being increased at the beginning of the new cycle, a heat-sensitive link at 400 to 450°C releases the spent filter. The filter drops to the bottom of the vessel and becomes a part of the next charge of glass.

†Each gram of calcine contained the following principal amounts (millicuries) of fission products: ^{144}Ce, 26; ^{137}Cs, 10.5; ^{90}Sr, 7.6; and ^{106}Ru, 1.4.

After 6 weeks of leaching with dilute HNO_3 at 25°C, the calcine disintegrated and more than 99% of the alumina dissolved; nearly 90% dissolved in the first 2 days. The author concludes that the use of dilute nitric acid would not seem practical for the selective recovery of fission products from the amorphous calcine currently being produced in the WCF.

General

CORROSION IN WASTE PROCESSING

During the past 10 years, high-level-activity alkaline wastes from the separations area at Savannah River have been stored in underground double-wall carbon steel tanks of 750,000- and 1,000,000-gal capacity. In this period the inner vessels in 4 of the 16 tanks in use have developed side-wall leaks. It was reported in the Summer 1966 issue of *Reactor Fuel Processing*[23] that stress cracking was the most probable cause for the leaks. Costas, Holzworth, and Rion,[24] at Savannah River, have reported on the laboratory corrosion-test program that was carreid out to determine the cause of cracking failure in the plant tanks. The results of the laboratory tests were as follows: (1) simulated alkaline wastes (aqueous solutions of ~30% $NaNO_3$ at *p*H 11 to 12) could cause stress-corrosion cracking of large, welded, carbon-steel specimens, (2) the cracks induced in the laboratory were similar to those observed in the plant tanks, and (3) full stress relief, which prevented stress cracking of the specimens in the test solutions, should be considered for future tanks of this type.

RECOVERY OF ALUMINUM NITRATE FROM REDOX ACID WASTE

In the Redox solvent extraction process for the recovery of plutonium, aluminum nitrate nonahydrate (ANN) is employed for the salting agent and methyl isobutyl ketone (hexone) is used for the organic extraction agent. The recovery of the ANN from Redox nitric acid wastes and the reuse of ANN would be desirable since its recovery would make possible the reduction of plant waste volumes. Crystallization of the ANN from a concentrated nitric acid solution offers a practical means for separating the ANN from fission products. In the Spring 1966 issue of *Reactor Fuel Processing*,[25] it was reported that a countercurrent crystallization system had been developed which permits multiple stages of crystallization without requiring the separation of crystals and supernatant following each stage and which also is capable of achieving high decontamination factors. Parts 1 and 3 of a report that describes the development of the crystallization system have been published.[26,27] Part 1 presents the analog-computer and the iterative-analog-computer programs used for investigating the process variables.[26] The results from both computer programs checked satisfactorily with laboratory data. Part 3 discusses the development of a rigorous mathematical model of the system.[27]

Selected Current Literature

The proceedings of the American Nuclear Society national topical meeting on the large-scale production and application of radioisotopes have become available. This meeting was held Mar. 21–23, 1966, at Augusta, Ga.[28] Of the papers published in the proceedings, the following pertain to the recovery and packaging of fission products from reactor-fuel-processing waste solutions and to the conversion of specific fission products to salts and source compounds:

1. Processing and Source Preparation of Separated Fission Products—S. J. Beard and P. W. Smith, General Electric Company, Richland; J. S. Cochran, Isochem Inc., Richland.
2. Fission Product Recovery Research at Battelle–Northwest—R. L. Moore, Pacific Northwest Laboratory.
3. Recovery and Purification of Promethium-147—J. T. Lowe, Savannah River Laboratory.
4. Preparation of Megacurie Quantities of Cesium-137 Salts and Source Compounds at Oak Ridge National Laboratory—R. E. Lewis and C. L. Ottinger, Oak Ridge National Laboratory.
5. "ELAN"—Installation for the Recovery and Packaging of Cesium-137 in France—A. Raggenbrass, J. M. Courouble, J. Lefevre, J. Fradin, and C. Perebaskine, Saclay, France.

A five-part series of journal articles on the development of radioactive waste disposal by hydraulic fracturing[29] at ORNL is being published. The series will describe fully the work carried out—from the initial concept to its final application as a practical method for radioactive-waste disposal. The titles of these papers are as follows:

Part I. General Concept and First Field Experiments

Part II. Mechanics of Fracture Formation and Design of Observation and Monitoring Wells

Part III. Chemical Development Waste-Cement Mixes

Part IV. Design of ORNL's Shale-Fracturing Plant

Part V. First Injections of Actual Wastes

Parts I and II have been published.[30,31]

The proceedings have been published of a symposium on practices in the treatment of low-level- and intermediate-level-activity liquid and solid wastes. The symposium[32,33] was held in Vienna from Dec. 6–10, 1965. The meeting was jointly sponsored by the International Atomic Energy Agency and the European Nuclear Energy Agency. Fifty-one papers

were presented and covered the following aspects of the treatment of these wastes: (1) general management in the treatment of low-level- and intermediate-level-activity liquid and solid wastes, (2) operating experience with existing facilities, (3) treatment of solid wastes, (4) special techniques for the treatment of liquid and solid wastes, and (5) recent research and development activities in the United States, Europe, Russia, India, and the Republic of South Africa.

References

1. *Reactor Fuel Process.*, 9(2): 110-111 (Spring 1966).
2. R. E. Blanco and F. L. Parker, Waste Treatment and Disposal Semiannual Progress Report, July–December 1965, USAEC Report ORNL-TM-1465, pp. 26-30, Oak Ridge National Laboratory, June 1966.
3. *Ibid*, pp. 35-41.
4. *Reactor Fuel Process.*, 8(4): 221 (Fall 1965).
5. G. Jansen, Jr., W. E. Willingham, and W. V. DeMier, Buried Radioactive Waste Storage Tank Temperatures and Soil Temperatures near Leaks, USAEC Report BNWL-181, Pacific Northwest Laboratory, March 1966.
6. *Reactor Fuel Process.*, 9(4): 232 (Fall 1960).
7. J. A. Buckham, Idaho Nuclear Corporation, unpublished, Sept. 2, 1966.
8. J. A. Buckham, Phillips Petroleum Company, unpublished, June 30, 1966.
9. J. A. Buckham, Idaho Nuclear Corporation, unpublished, Aug. 4, 1966.
10. R. E. Commander, G. E. Lohse, D. E. Black, and E. D. Cooper, Operation of the Waste Calcining Facility with Highly Radioactive Aqueous Waste. Report of the First Processing Campaign, USAEC Report IDO-14662, Phillips Petroleum Company, June 1966.
11. Maximum Permissible Body Burdens and Maximum Permissible Concentrations of Radionuclides in Air and Water for Occupational Exposure, National Bureau of Standards Handbook 69, June 1959.
12. *Reactor Fuel Process.*, 9(4): 230 (Fall 1966).
13. *Nucleonics*, 24(9): 28-29 (September 1966).
14. A. M. Platt (Ed.), Fixation of Radioactive Residues, Quarterly Progress Report, January–March 1966, USAEC Report BNWL-267, pp. 5-6, Pacific Northwest Laboratory, May 1966.
15. *Reactor Fuel Process.*, 8(2): 115-116 (Spring 1965).
16. J. R. Grover, W. H. Hardwick, R. Gaylor, and M. H. Delve, The FINGAL Process, British Report AERE-R-5188, March 1966.
17. M. N. Elliot and J. R. Grover, Scale-Up of FINGAL Glassmaking Process, *Chem. Process Eng.*, 47(3): 105 (March 1966).
18. E. S. Grimmett, Recovery of Fission Products from Calcined First Cycle Solvent Extraction Wastes, USAEC Report IDO-14408, Phillips Petroleum Company, June 26, 1956.
19. C. E. Stevenson, Idaho Chemical Processing Plant Technical Progress Report for April–June 1959, USAEC Report IDO-14494, p. 64, Phillips Petroleum Company, March 1960.
20. J. I. Stevens (Ed.), Idaho Chemical Processing Plant Technical Progress Report, Radioactive Waste Disposal Projects, January–March 1960, USAEC Report IDO-14530, p. 20, Phillips Petroleum Company, Sept. 9, 1960.
21. J. R. Bower (Ed.), Chemical Processing Technology Quarterly Progress Report, April–June 1960, USAEC Report IDO-14534, p. 44, Phillips Petroleum Company, Dec. 5, 1960.
22. B. E. Paige, Leachability of Alumina Calcine Produced in the Idaho Waste Calcining Facility, USAEC Report IN-1011, Idaho Nuclear Corporation, July 1966.
23. *Reactor Fuel Process.*, 9(3): 174 (Summer 1966).
24. L. P. Costas, M. L. Holzworth, and W. C. Rion, Stress Corrosion Cracking of Carbon Steel in Simulated Waste Solutions, USAEC Report DP-1023, Savannah River Laboratory, June 1966.
25. *Reactor Fuel Process.*, 9(2): 118 (Spring 1966).
26. W. L. Godfrey and R. D. Benham, Recovery of Aluminum Nitrate Nonahydrate from Redox Acid Waste. Part 1: Computer Study, USAEC Report HW-82771 (Pt. 1), Hanford Atomic Products Operation, July 1964.
27. W. L. Godfrey, R. Y. Dean, and J. C. Stouffer, Recovery of Aluminum Nitrate Nonahydrate from Redox Acid Waste. Part 3. Mathematical Description, USAEC Report HW-82771(Pt. 3), Hanford Atomic Products Operation, December 1965.
28. Large Scale Production and Applications of Radioisotopes, Proceedings of the American Nuclear Society, National Topical Meeting, March 21–23, 1966, Augusta, Ga., Vols. I and II, USAEC Report DP-1066, Savannah River Laboratory, May 1966.
29. *Reactor Fuel Process.*, 9(2): 116-117 (Spring 1966).
30. W. De Laguna, Disposal of Radioactive Wastes by Hydraulic Fracturing. Part I. General Concept and First Field Experiments, *Nucl. Eng. Design*, 3: 338-352 (1966).
31. W. De Laguna, Disposal of Radioactive Wastes by Hydraulic Fracturing. Part II. Mechanics of Fracture Formation and Design of Observation and Monitoring Wells, *Nucl. Eng. Design*, 3: 432-438 (1966).
32. *Reactor Fuel Process.*, 9(4): 225-227 (Fall 1966).
33. *Practices in the Treatment of Low- and Intermediate-Level Radioactive Wastes*, Symposium Proceedings, Vienna, 1965, International Atomic Energy Agency and the European Nuclear Energy Agency, Vienna, 1966 (STI/PUB/116).

LEGAL NOTICE

This journal was prepared under the sponsorship of the U. S. Atomic Energy Commission. Neither the United States, nor the Commission, nor any person acting on behalf of the Commission:

A. Makes any warranty or representation, expressed or implied, with respect to the accuracy, completeness, or usefulness of the information contained in this journal, or that the use of any information, apparatus, method, or process disclosed in this journal may not infringe privately owned rights; or

B. Assumes any liabilities with respect to the use of, or for damages resulting from the use of any information, apparatus, method, or process disclosed in this journal.

As used in the above, "person acting on behalf of the Commission" includes any employee or contractor of the Commission, or employee of such contractor, to the extent that such employee or contractor of the Commission, or employee of such contractor prepares, disseminates, or provides access to, any information pursuant to his employment or contract with the Commission, or his employment with such contractor.

NUCLEAR SCIENCE ABSTRACTS

The U. S. Atomic Energy Commission, Division of Technical Information, publishes *Nuclear Science Abstracts* (*NSA*), a semimonthly journal containing abstracts of the literature of nuclear science and engineering.

NSA covers (1) research reports of the U. S. Atomic Energy Commission and its contractors; (2) research reports of government agencies, universities, and industrial research organizations on a worldwide basis; and (3) translations, patents, books, and articles appearing in technical and scientific journals.

Complete indexes covering subject, author, source, and report number are included in each issue. These are cumulated quarterly, semiannually, and annually providing a detailed and convenient key to the literature.

Availability of *NSA*

SALE *NSA* is available on subscription from the Superintendent of Documents, U. S. Government Printing Office, Washington, D. C., 20402, at $30.00 per year for the semimonthly abstract issues and $22.00 per year for the four cumulated-index issues. Subscriptions are postpaid within the United States, Canada, Mexico, and all Central and South American countries, except Argentina, Brazil, Guyana, French Guiana, Surinam, and British Honduras. Subscribers in these Central and South American countries, and in all other countries throughout the world, should remit $37.00 per year for subscriptions to semimonthly abstract issues and $25.00 per year for the four cumulated-index issues.

EXCHANGE *NSA* is also available on an exchange basis to universities, research institutions, industrial firms, and publishers of scientific information. Inquiries should be directed to the Division of Technical Information Extension, U. S. Atomic Energy Commission, P. O. Box 62, Oak Ridge, Tennessee, 37830.

TECHNICAL PROGRESS REVIEWS may be purchased from Superintendent of Documents, U. S. Government Printing Office, Washington, D. C., 20402. *Nuclear Safety* at $3.00 per year for each subscription or $1.00 per issue; each of the other journals at $2.50 per year or $0.70 per issue. The use of the coupon below will facilitate the handling of your order.

POSTAGE AND REMITTANCE: Postpaid within the United States, Canada, Mexico, and all Central and South American countries except Argentina, Brazil, Guyana, French Guiana, Surinam, and British Honduras. For these Central and South American countries and all other countries, add $0.75 for each annual subscription or $0.20 for a single issue. Payment should be by check, money order, or document coupons, and MUST accompany order. Remittances from foreign countries should be made by international money order or draft on an American bank payable to the Superintendent of Documents or by UNESCO book coupons.

order form

SUPERINTENDENT OF DOCUMENTS
U. S. GOVERNMENT PRINTING OFFICE
WASHINGTON, D. C., 20402

Enclosed:
document coupons ☐ check ☐ money order ☐

Charge to Superintendent of Documents No. _____

Please send a one-year subscription to

☐ ISOTOPES AND RADIATION TECHNOLOGY

☐ POWER REACTOR TECHNOLOGY

☐ REACTOR MATERIALS

(Each subscription $2.50 per year; $0.70 per issue.)

☐ NUCLEAR SAFETY

(Each subscription $3.00 per year; $1.00 per issue.)

SUPERINTENDENT OF DOCUMENTS
U. S. GOVERNMENT PRINTING OFFICE
WASHINGTON, D. C., 20402

(Print clearly)

_____
Name

_____
Street

_____
City, State, ZIP Code